

Editor-in-Chief B.E.Paton

Editorial board:

Yu.S.Borisov	V.F.Khorunov
A.Ya.Ishchenko	I.V.Krivtsun
B.V.Khitrovskaya	L.M.Lobanov
V.I.Kirian	A.A.Mazur
S.I.Kuchuk	Yatsenko
Yu.N.Lankin	I.K.Pokhodnya
V.N.Lipodaev	V.D.Poznyakov
V.I.Makhnenko	K.A.Yushchenko
O.K.Nazarenko	A.T.Zelnichenko
I.A.Ryabtsev	

International editorial council:

N.P.Alyoshin	(Russia)
U.Diltay	(Germany)
Guan Qiao	(China)
D. von Hofe	(Germany)
V.I.Lysak	(Russia)
N.I.Nikiforov	(Russia)
B.E.Paton	(Ukraine)
Ya.Pilarczyk	(Poland)
P.Seyffarth	(Germany)
G.A.Turichin	(Russia)
Zhang Yanmin	(China)
A.S.Zubchenko	(Russia)

Promotion group:

V.N.Lipodaev, V.I.Lokteva
A.T.Zelnichenko (exec. director)

Translators:

A.A.Fomin, O.S.Kurochko,
I.N.Kutianova, T.K.Vasilenko
PE «Melnik A.M.»

Editor

N.A.Dmitrieva
Electron galley:
I.S.Batasheva, T.Yu.Snegiryova

Address:

E.O. Paton Electric Welding Institute,
International Association «Welding»,
11, Bozhenko str., 03680, Kyiv, Ukraine

Tel.: (38044) 287 67 57
Fax: (38044) 528 04 86

E-mail: journal@paton.kiev.ua
http://www.nas.gov.ua/pwj

State Registration Certificate
KV 4790 of 09.01.2001

Subscriptions:

\$324, 12 issues per year,
postage and packaging included.
Back issues available.

All rights reserved.

This publication and each of the articles
contained herein are protected by copyright.
Permission to reproduce material contained in
this journal must be obtained in writing from
the Publisher.
Copies of individual articles may be obtained
from the Publisher.

CONTENTS

SCIENTIFIC AND TECHNICAL

<i>Makhnenko V.I. and Romanova I.Yu.</i> Calculation prediction of fatigue life of freight car side frame under alternating cyclic loads	2
<i>Falchenko Yu.V., Muravejnik A.N., Kharchenko G.K., Fedorchuk V.E. and Gordan G.N.</i> Pressure welding of micro-dispersed composite material AMg5 + 27 % Al ₂ O ₃ with application of rapidly solidified interlayer of eutectic alloy Al + 33 % Cu	7
<i>Tsybulkin G.A.</i> Evaluation of quality of the arc self-adjustment process	11
<i>Chernaya T.I., Tsaryuk A.K., Siora A.V., Shelyagin V.D. and Khaskin V.Yu.</i> Laser welding of root welds of thick joints of heat-resistant steel	14
<i>Dolinenko V.V., Skuba T.G., Kolyada V.A. and Shapovalov E.V.</i> Optimal control of formation of weld reinforcement	17

INDUSTRIAL

<i>Kuchuk-Yatsenko S.I., Nejlo Yu.S., Gavrish V.S. and Gushchin R.V.</i> Prospects of increasing energy characteristics of flash butt welding (Review)	23
<i>Rudenko P.M. and Gavrish V.S.</i> Portable system of monitoring and control of resistance spot welding process	27
<i>Zhudra A.P., Krivchikov S.Yu. and Petrov V.V.</i> Technology for wide-layer hard-facing of crankshafts	32
<i>Royanov V.A. and Korostashevsky P.V.</i> Determination of additional resistances to sheet panel displacement over dead roller table of assembly and welding lines	36

BRIEF INFORMATION

News	41
------------	----

NEWS

XIII Republican Scientific-Technical Conference of Kazakhstan Welders	42
Problems of Life and Safe Operation of Structures, Constructions and Machines (Final Scientific Conference at the E.O. Paton Electric Welding Institute of the NAS of Ukraine)	43

INFORMATION

Loyalty Program of Fronius Ukraina Ltd. in crisis period and its results	47
Developed at PWI	6, 31, 48



CALCULATION PREDICTION OF FATIGUE LIFE OF FREIGHT CAR SIDE FRAME UNDER ALTERNATING CYCLIC LOADS

V.I. MAKHNENKO and I.Yu. ROMANOVA

E.O. Paton Electric Welding Institute, NASU, Kiev, Ukraine

An example of calculation prediction of fatigue crack growth in a side frame of freight cars at a preset range of random cyclic loads is considered. Relationship between exceeding design conditions of operation of the car and probable cause of its fracture was studied.

Keywords: *fatigue crack, random cyclic loading, side frame, freight car, casting defect, calculation prediction of fatigue life*

In connection with increased scope of railway freight traffic, more attention is given to the «viability» of various parts and components of load-carrying elements of freight cars. Experience of operation of structures developed in Ukraine and Russia is indicative of insufficient cyclic strength of individual components, which results in failure of cars which have not yet completed their design life period [1].

Let us consider a real case of failure of a cast side frame of a freight car (Kabakly Station, West-Siberian Railway, RF, 2009), designed in keeping with [2] and manufactured at OJSC «Azovmash» (Mariupol, Ukraine). Fracture occurred as a result of fatigue crack growth from a technological defect.

Initial information on the fractured side frame is as follows: material is steel of 20GFL type; car run to fracture $L = 108,482$ km; design average technical speed of car movement $\bar{v} = 22.4$ m/s; average daily run of a loaded car $L_d = 210$ km/d; effective frequency of car vertical oscillations $f_e = 2.23$ Hz; coefficient of run in the loaded condition $K = 0.6$; average daily number of cycles under load $N_d = (L_d/\bar{v})10^3 f_e = 20,906$ cycle/d; number of cycles under load during run L to fracture $N = (LK\bar{v})10^3 f_e = 6.48 \cdot 10^6$ cycles; current evaluating repairs were performed at $N_{rep} = N - N_d \cdot 9.5 \cdot 30K = 2.91 \cdot 10^6$ cycles.

Figure 1 shows fracture of a failed frame, and arrows indicate sites of fatigue fracture initiation [3]. According to this work, the site of initiation of a primary fatigue crack (#1 in Figure 1) was a casting defect — surface blowhole, having the length of 2.6 mm, depth of 1.8 mm in the fracture section and located at 31 mm distance from the surface of the outer vertical wall of the side frame. The defect was not detected by NDT means. Site of initiation of secondary fatigue cracks were casting blowholes located at 66, 104 and 125 mm distance from the surface of outer vertical wall and having the dimensions of 2.0×1.5 mm (#2), 4.3×2.3 mm (#4) and 4.0×1.3 mm (#5) in the fracture section. In addition, there is a

surface defect of 3.0×2.0 mm size (#3 in Figure 1), not specified by the drawing of the technological stiffener, which in [3] is regarded as the site of secondary fatigue cracks formation.

Thus, five sites of fatigue fracture are located in the fracture section on the surface with the maximum operating longitudinal stresses, which sufficiently conservatively can be described by semi-elliptical cracks of $2ca$ size, where $2c$ is the crack length along the free surface, and a is the crack depth.

Table 1 gives the initial dimensions of such defects and shows the distance from defect centers to the free vertical surface, as well as the distance between the edges of adjacent defects (L_{n-1} on the left, L_{n+1} on the right), in the initial condition and characteristic parameter b of interaction with adjacent defects:

$$b = c + \min \begin{cases} L_{n-1, n} \\ L_{n+1, n} \end{cases}$$

or the free edge (vertical free surface). In [13] it is noted that the described casting contamination defects were evaluated in terms of their admissibility (inadmissibility) based on the principles (approaches) of fracture mechanics of cracked solids, described for the case considered in [4]. From this assessment it follows that the described casting defects are inadmissible, as under the design operation conditions during three years they grow by the fatigue mechanism to dimensions, at which their progressive growth begins, leading to fracture after approximately 2.9 months of service. Unfortunately, absence of such substantiation after the assessment performed in [3], in view of the design conditions of frame loading, gives rise to some doubts as to determination of the main cause for its fracture, so that PWI conducted a study, the essence of which is as follows.

For the above described defects (Table 1) their loading by the spectrum of random cyclic loads described in [2] was considered for average speed of train movement $\bar{v} = 22.4$ m/s at static stresses in the defect zone in the range from $\sigma_{st} = 105.2$ MPa (#1) to $\sigma_{st} = 93.2$ MPa (#2–5), which is in good agreement with the data of [4], where values of the above characteristics are equal to 80–90 MPa.

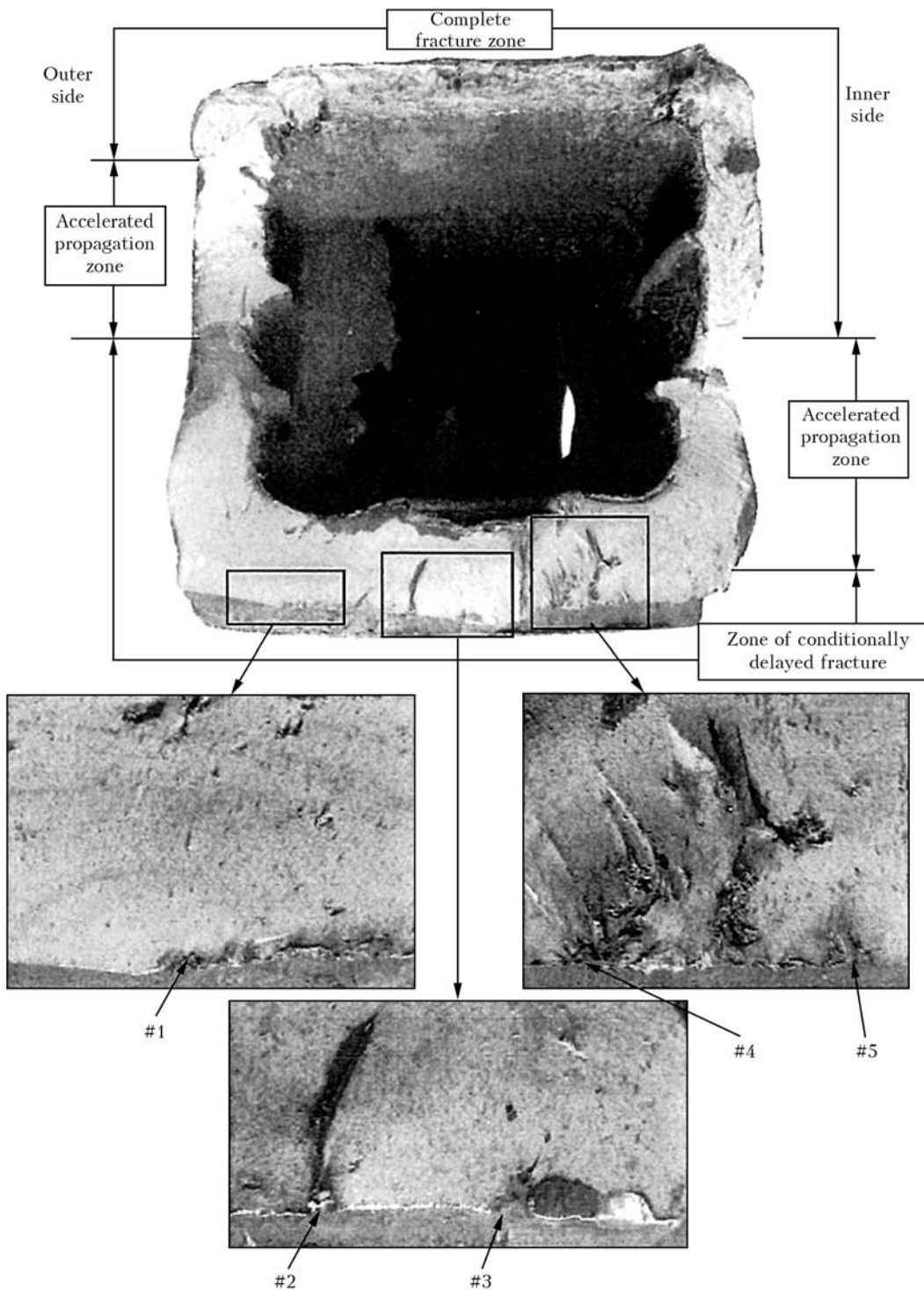


Figure 1. Fracture of side frame of freight car (#1-5 – sites of fatigue crack initiation)

Calculation of dynamic index K_{dyn} , depending on variation of movement speed v is performed according to [2] at static deflection of spring suspension $f_{st} = 0.049$ m (Table 2).

Amplitude of dynamic (cyclic) stresses was determined from the expression

$$\sigma_a = \sigma_{st} K_{dyn} \quad (1)$$

depending on the train movement speed v_i , the value of which is determined within the ranges indicated in Table 2 at probability P_i in the basic loading cycle

N_b , i.e. N_i for the i -th element of loading spectrum in the following form:

$$N_i = N_b P_i, \quad (2)$$

It is assumed that in each element of the spectrum $\sigma_{max} = \sigma_{st}$, i.e. coefficient of asymmetry R_i for the i -th element of the loading spectrum is equal to

$$R_i = (1-2)K_{dyni}. \quad (3)$$

The rate of growth of the initial crack dimensions $l = a, c$ at the specified load is determined by the



Table 1. Initial dimensions of defect and distance from defect centers to free vertical surface according to [3]

Defect #	Defect parameter, mm					
	2c	a	L ₁	L _{n-1}	L _{n+1}	b
1	2.6	1.8	31	29.7	22.7	24.0
2	2.0	1.5	66	22.7	22.5	23.5
3	3.0	2.0	86	22.5	14.4	15.9
4	4.3	2.3	104	14.4	16.6	15.5
5	4.0	1.3	125	16.6	23.0	18.6

diagram of cyclic crack resistance of steel, a section of which for the considered material of the side frame is given in Figure 2, i.e. it is determined by the range of values of stress intensity factors ΔK_I and loading asymmetry R .

For a broad class of medium-carbon steels such a diagram only slightly depends on the material composition and its microstructure, and various dependencies are used for conservative estimates. According to recommendations of [5], it is rational to apply the following dependence:

$$\frac{dl}{dN} = \frac{C_0 \Delta K_I^m}{(1-R) - \frac{\Delta K_I}{K_c}} \text{ at } \Delta K_I > \frac{\Delta K_{th}(R)}{\gamma_m};$$

$$\frac{dl}{dN} = 0 \text{ at } \Delta K_I < \frac{\Delta K_{th}(R)}{\gamma_m},$$

(4)

where $C_0 = 5 \cdot 10^{-13} \text{ mm}/(\text{MPa} \cdot \text{mm}^{1/2})$; $m = 3$; ΔK_{th} is the threshold value of the range of stress intensity factor dependent on R :

$$\Delta K_{th} = (190-144)R, \tag{5}$$

but not less than 62 MPa·mm^{1/2}; K_c is the material fracture toughness (taken at the temperature of -30 °C) equal to 2065 MPa; γ_m is the safety factor according to [5] equal to 1.25 for primary crack #1 and 1.20 for secondary cracks #2-5.

Table 2. Dynamic indices K_{dyn} for design condition of freight car side frame loading

i	v _i , m/s	K _{dyni}	P _i
1	6.25	0.063	0.03
2	13.75	0.138	0.07
3	16.25	0.159	0.09
4	18.75	0.177	0.12
5	21.25	0.196	0.16
6	23.75	0.214	0.19
7	26.25	0.232	0.16
8	28.75	0.250	0.10
9	31.25	0.269	0.06
10	33.75	0.287	0.02

Dependence (4), compared to the data in Figure 2, gives somewhat higher values of the growth rate, which is quite acceptable for conservative estimates.

Parameter ΔK_I is determined for a semi-elliptical crack, according to [5], in the following form:

$$\Delta K_I = 2\sigma_a \sqrt{\frac{\pi a}{Q}} F, \tag{6}$$

where Q and F are calculated by the following dependencies:

$$F = \left[M_1 + M_2 \left(\frac{a}{\delta} \right)^2 + M_3 \left(\frac{a}{\delta} \right)^4 \right] g f_{wf} b,$$

where δ is the wall thickness in the defect zone (taken to be $\delta = 25 \text{ mm}$).

At $a < c$

$$Q = 1 + 1.464 \left(\frac{a}{c} \right)^{1.65}; \quad M_1 = 1.13 - 0.09 \left(\frac{a}{c} \right);$$

$$M_2 = -0.54 + \frac{0.89}{0.2 + \frac{a}{c}};$$

Table 3. Calculation of ΔK and safety factor γ_m for primary crack #1 (according Table 1)

v _i , m/s	K _{dyni}	ΔK_{th} , MPa·mm ^{1/2}	$\Delta\sigma$, MPa	$\Delta K_I(a)$	$\gamma_m(a)$	$\Delta K_I(c)$	$\gamma_m(c)$
6.25	0.063	64.1	13.25	17.2	3.73	22.3	2.88
13.75	0.138	85.7	29.03	37.7	2.27	48.8	1.75
16.25	0.159	91.8	33.45	43.4	2.11	56.3	1.63
18.75	0.177	97.0	37.24	48.3	2.00	62.6	1.55
21.25	0.196	102.4	41.24	53.5	1.91	69.3	1.48
23.75	0.214	107.6	45.02	58.4	1.84	75.7	1.42
26.25	0.232	112.8	48.81	63.3	1.78	82.1	1.37
28.75	0.250	118.0	52.60	68.3	1.73	88.5	1.33
31.25	0.269	123.5	56.60	73.4	1.68	95.2	1.29
33.75	0.287	128.6	60.40	78.4	1.64	101.5	1.27



$$M_3 = 0.5 - \frac{1}{0.65 + \frac{a}{c}} + 14 \left(1 - \frac{a}{c}\right)^{24}$$

For parameter a , $g = 1$, $f_b = 1$.
For parameter c

$$g = 1 + \left[0.1 + 0.35 \left(\frac{a}{\delta}\right)^2\right], \quad f_b = \sqrt{a/c}.$$

At $a > c$

$$Q = 1 + 1.464 \left(\frac{c}{a}\right)^{1.65}; \quad M_1 = \left(1 + 0.04 \frac{c}{a}\right) \sqrt{\frac{c}{a}};$$

$$M_2 = 0.2 \left(\frac{c}{a}\right)^4; \quad M_3 = -0.11 \left(\frac{c}{a}\right)^4.$$

For parameter a , $g = 1$, $f_b = \sqrt{c/a}$.

For parameter c , $g = 1 + \left[0.1 + 0.35 \left(\frac{a}{\delta}\right)^2 \left(\frac{c}{a}\right)\right], \quad f_b = 1.$

The rest as for $a/c < 1$.

Dependencies (1)–(6) were used to trace the development of defects (cracks) considered in Table 1 at the design spectrum of train movement speed at $N_b = 6.47 \cdot 10^6$ cycles, i.e. on the base of the real run

dI/dN , m/cycle

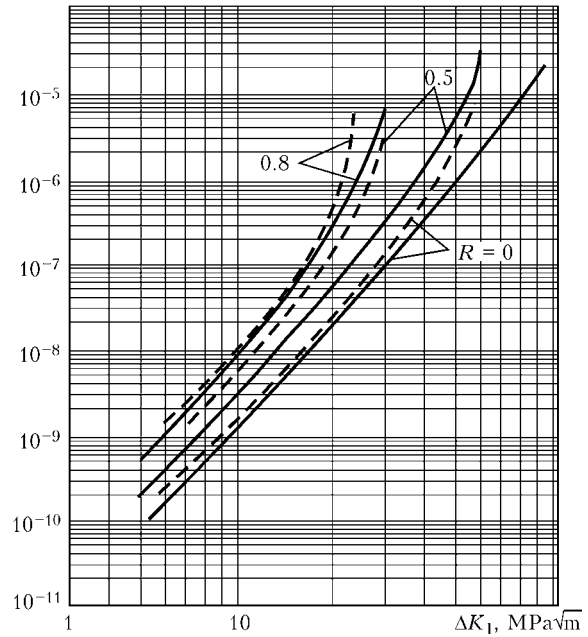
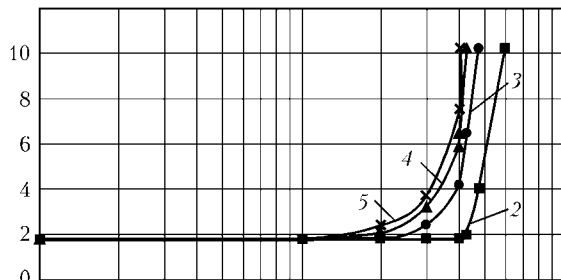


Figure 2. Fatigue fracture diagram of steel at different values of the coefficient of loading asymmetry R [4]

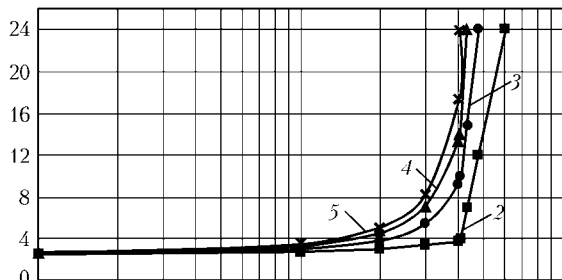
to failure. Dependence determines relative frequency of spectrum elements (2). Randomness of spectrum elements was realized using random-number generator $0 \leq D \leq 1$. A more conservative approach of tracing

a , mm



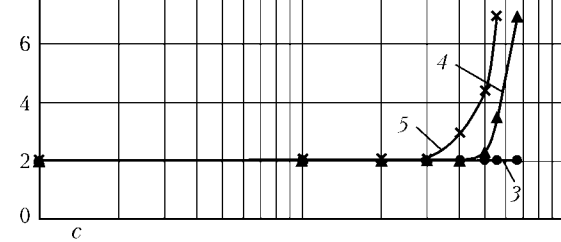
a

$2c$, mm



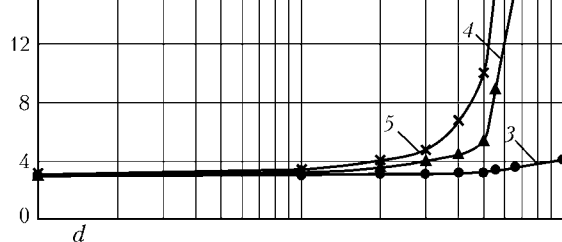
b

c



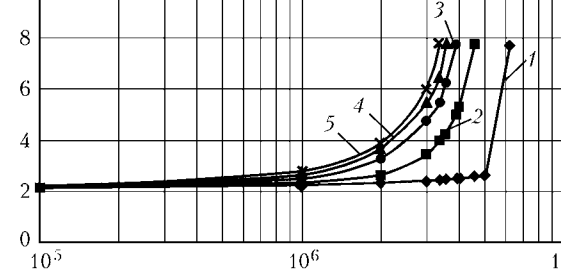
c

d



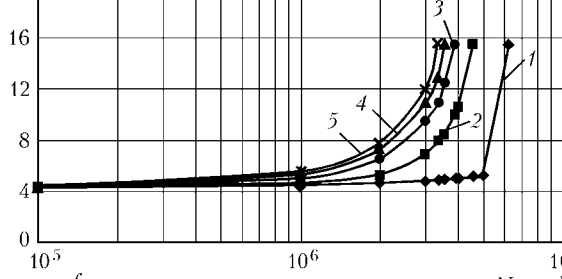
d

e



e

f



f

N , cycle

Figure 3. Kinetics of growth of defects #1 (a , b), #3 (c , d) and #4 (e , f) at car movement at a higher speed depending on safety factor γ_m : a , c , e – increase of crack depth a ; b , d , f – $2c$ growth; 1 – $\gamma_m = 1.20$; 2 – 1.25; 3 – 1.30; 4 – 1.35; 5 – 1.40



through the spectrum was used, starting from high load amplitudes and down to small amplitudes, i.e. starting from $i = 10$ and ending by $i = 1$.

Results of calculation of the kinetics of change of dimensions a and c of the initial defect #1 (cracks) in the design loading spectrum on the base of real fatigue life of the considered side beam showed that during the entire operating period of the car ($N_b = 6.47 \cdot 10^6$ cycles) the initial dimensions of the defect did not change, which is due to inequality $\Delta K_1 < \Delta K_{th} / \gamma_m$ (as shown in Table 3) for each element of the loading spectrum.

A similar situation is in place also for defects #2–5, from which secondary cracks are developing, i.e. under design operating conditions of the train the considered defects are admissible, non the less fracture did take place. Let us prove that the cause for the considered fracture can be inclusion into the loading spectrum of a higher speed of train movement. With this purpose a spectrum of speed according to [2] was considered, which corresponds to the design average technical speed of 24.7 m/s. Figure 3 gives the calculated data on the kinetics of variation of dimensions of defects #1, 3 and 4 at increased (compared to design) movement speed, from which it is seen that appearance of $v = 36.25$ m/s, $P = 0.05$ and $v = 38.75$ m/s, $P = 0.02$ in the speed spectrum noticeably changes the kinetics of the change of dimensions a and c of initial defects (cracks). Calculations showed that defects #2 and 5 do not show any growth at these input parameters. Practically, at $N = 5 \cdot 10^6$ cycles the above defects coalesce, forming a continuous crack about 10 mm deep along the base surface, at which the remaining life of the side beam is quite limited. It is characteristic that at $N = 3 \cdot 10^6$ loading cycles (approximately cor-

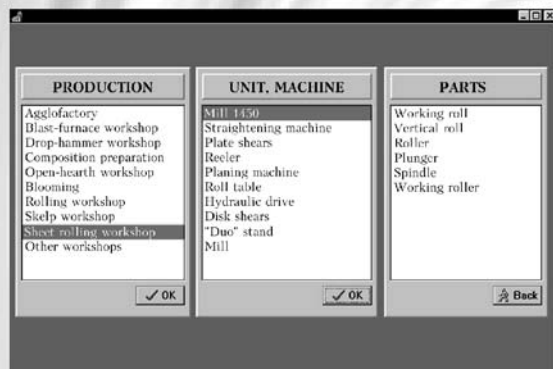
responds to the moment of setout repair 9.5 months before failure) the defects have grown noticeably and they can be detected by the non-destructive methods. Naturally, the considered variant of operation at increased speed is quite hypothetical. It shows that a quite probable cause for fracture could be the accumulated damage related to car operation in modes not envisaged by design.

Thus, calculations show that fatigue fracture of the side frame of a train car occurred because of casting defects-blowholes found in the fracture. These defects as to their geometrical dimensions are admissible at design conditions of car service. However, exceeding the design conditions of the car operation, in particular, its movement speed can be the cause for the considered defect transition into the category of inadmissible defects.

Given calculation algorithms allow prediction of the influence of variable cyclic loads applied randomly, on the growth of fatigue cracks in structural elements of railway cars and predicting their fatigue life.

1. Makhnenko, V.I., Saprykina, G.Yu. (2009) Safety service life of welded joints of bays. In: *Proc. of 4th Int. Conf. on Mathematical Modeling and Information Technologies in Welding and Related Processes* (27–30 May 2008, Katsiveli, Crimea, Ukraine). Kiev: PWI, 103–108.
2. *Codes of structural design of railway cars (non-self-propelled) of Ministry of Communications for track of 1520 mm.* Introd. 07.02.96.
3. (2009) *Technical conclusion on expert verification results in determination of causes of side frame fracture N 36213-143-06 at 2903 km PK7 in Barabinsk–Tatarskaya section behind point #6 of Kabakly station of Novosibirsk Division of West-Siberian Railway of VNIIZhT Company.* Approved 27.02.2009. Moscow.
4. Severinova, T.P. (2002) Design-theoretical substantiation of viability of side frames and bolsters with admissible defects. *Vestnik VNIIZhT*, 5, 40–45.
5. (1996) Recommendation for fatigue design of welded joints and components. *IIV Doc. XIII-1539-96/XV-845-96.*

COMPUTER SYSTEM TO DESIGN TECHNOLOGIES FOR REPAIR AND HARDENING OF METALLURGICAL EQUIPMENT PARTS



Selection of a part to be surfaced

Purpose. The system is intended to design technologies for repair and hardening of metallurgical equipment parts by the electric arc surfacing methods. The computer system is based on the experience accumulated by 16 metallurgical plants in the field of surfacing. It allows design of a surfacing technology for 350 different parts (selection of surfacing consumables, methods, conditions, equipment, etc.) at a level of a highly skilled specialist. The system operation result has the form of a process sheet.

Application. The system can be used at metallurgical enterprises. It is intended for welding technologists working at a plant engineering department.

Contacts: Prof. Makhnenko V.I.
E-mail: d34@paton.kiev.ua



PRESSURE WELDING OF MICRO-DISPERSED COMPOSITE MATERIAL AMg5 + 27 % Al₂O₃ WITH APPLICATION OF RAPIDLY SOLIDIFIED INTERLAYER OF EUTECTIC ALLOY Al + 33 % Cu

Yu.V. FALCHENKO, A.N. MURAVEJNIK, G.K. KHARCHENKO, V.E. FEDORCHUK and G.N. GORDAN
E.O. Paton Electric Welding Institute, NASU, Kiev, Ukraine

Solid-phase weldability of micro-dispersed composite material AMg5 + 27 % Al₂O₃ by using rapidly solidified interlayer of eutectic alloy Al + 33 % Cu was studied. It was established that application of the rapidly solidified strip as an interlayer activates the mating surfaces and allows decreasing the temperature and time of diffusion welding of AMg5 + 27 % Al₂O₃ material. Employment of the techniques that accelerate diffusion processes in a butt joint (forced deformation, thermal cycling) made it possible to reduce the interlayer thickness to its almost complete dissolution and improve shear strength of the welded joint to the base metal strength level.

Keywords: *vacuum pressure welding, micro-dispersed composite material, interlayer, rapidly solidified strip, plastic deformation, welding temperature, strength of joints*

Topical task of development and practical operation of different types of equipment in modern machine building is reduction of friction and wear losses in movable joints of units and mechanisms. In this connection, of high interest are composite materials (CM) based on aluminum alloys, reinforced with dispersed ceramic particles of aluminum oxide Al₂O₃ or silicon carbide SiC. These CM are characterized by high specific elasticity modulus, increased heat resistance and rigidity at room and elevated temperatures, low values of coefficients of thermal linear expansion and friction, and high wear resistance. However, successful implementation of potential capabilities of these materials and their wide application are limited by the difficulties connected with their weldability.

Fusion welding of CM involves a number of problems, e.g. significant viscosity of the weld pool, decomposition or agglomeration of the reinforcing particles, complexity of quality formation of the welds as a result of poor wetting of reinforcing particle surfaces with aluminum, and porosity of the welds. Moreover, stirring of the base metal and filler is difficult in welding using filler wire and, as a result, strength of the weld metal [1, 2] is lower than that of a composite material.

In solid-state welding of alumocomposites, for example in a diffusion welding, all the processes take place at lower temperatures (in comparison with fusion welding), and the effect of increased toughness, welds porosity, reinforcer segregation are absent in the weld pool. Therefore, in welding of alumocomposites reinforced with Al₂O₃ (SiC) dispersed particles the preference is given to solid-state joining methods [3].

The main difficulties in pressure welding of dispersion-reinforced alumocomposites are related to the presence of a dense oxide film on the surface and high

rigidity of the material, complicating deformation of its sub-surface layer.

It is hardly possible to remove the oxide film and join aluminum alloys over the «clean» surfaces. Therefore, in this case the trend is to destroy and disperse the thin oxide film remaining on the surface after etching and cleaning.

The aim of the present study was to develop a technological process for vacuum pressure welding of fine-dispersed alumocomposite, providing the welded joints with strength at a level of the base metal.

Weldability of CM based on aluminum alloy AMg5, reinforced with the dispersed particles of Al₂O₃ (AMg5 + 27 % Al₂O₃) was investigated. Thickness of the composite layer was 6 mm, and hardness was HRB 96–99 at a load of $F = 600$ N. This material is classified as difficult-to-weld and hard-to-machine.

The composite was manufactured by a casting method, i.e. mixing up the Al₂O₃ dispersed-reinforcing particles into a melt of the matrix material and subsequent pressing. Structure of the composite in the initial state consists of α -solid solution of aluminum, intermetallic inclusions characteristic of matrix aluminum alloy AMg5, and reinforcing particles of oxide aluminum Al₂O₃ of a dark-grey, almost black color, having an angular shape and size of 3–15 μ m. They are sufficiently uniformly distributed in bulk of the matrix at a distance of 3–20 μ m (Figure 1). The main defect in CM is an accumulation of particles, where the aluminum melt cannot penetrate during solidification, and where pores and discontinuities having a detrimental effect on the material properties are formed. Such defects of the base metal have a lower influence on the weld quality in solid-state welding, compared to fusion welding.

Welding of CM samples was carried out with no interlayer and with the aluminum alloy interlayer. The interlayer of aluminum alloy AD1 and interlayer in the form of a rapidly solidified strip of eutectic alloy Al + 33 % Cu were used.

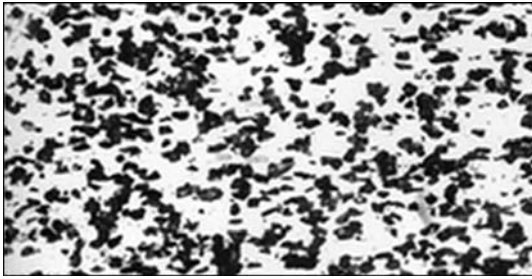


Figure 1. Microstructure ($\times 400$) of the AMg5 + 27 % Al_2O_3 CM in the initial state

Samples measuring $15 \times 15 \times 4$ mm were manufactured to optimize the technology and choose the optimum welding parameters. Preparation of the samples for welding consisted in removal of the work-hardened layer around 0.2–0.3 mm thickness and cleaning of the surface with a scraper. Shear tests of the samples were carried out for evaluation of strength of the welded joints. Cutting of the samples after welding was carried out using the EKh-1331P electroerosion machine tool. Examinations of microstructure were performed by the optical microscopy method using microscopes MIM-8 and «Neophot-32». Element composition was determined by using X-ray microanalyzer CAMEBAX. Hardness of the samples was measured with the «Rockwell» device at $F = 600$ N (ball), and microhardness – with the PMT-3 device at $F = 0.2$ N.

Production of joints with a high strength and crack resistance is a difficult problem in pressure welding of high-strength, difficult-to-weld metallic and, in particular, metal-ceramic materials. In welding of such materials, development of joint plastic deformation of the mating surfaces is complicated due to significant non-uniformity of the activation process and physical-chemical interaction on the contact area [4]. As follows from studies [5, 6] and results of our investigations, when welding CM to CM, welded joints in dispersion-reinforced CM have low strength because of its significant rigidity. Shear strength of such joints is $\sigma_{sh} = 8\text{--}9$ MPa. Metallographic examinations

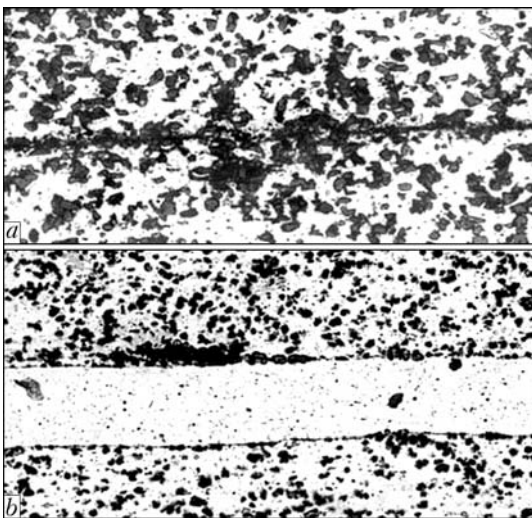


Figure 2. Microstructure of the welded joint on AMg5 + 27 % Al_2O_3 CM produced by vacuum pressure welding without interlayer (*a* – $\times 400$) and with aluminum interlayer 0.15 mm thick under free deformation conditions (*b* – $\times 250$)

showed that the reinforcing particles, matrix intermetallics and oxides are concentrated in a joining line. The interface is well recognized, in particular, in the places of accumulation of the reinforcing particles, where pores and discontinuities occur (Figure 2, *a*).

It is well known that interlayers in the form of solid materials [7, 8] of plastic alloys, such as aluminum, copper, nickel and silver, are widely used for activation of plastic deformation. In welding of dispersed-reinforced CM using a plastic interlayer eliminates such type of the contact as particle-to-particle, which weakens the joint, and replaces it by a stronger one, i.e. metal-to-particle. Besides, due to a plastic flow during the welding process, the soft solid interlayer placed in the joint provides destruction of the oxide film at the contact surfaces of the composite and improves the process of plastic deformation for near-contact volumes of the metal welded.

To optimize the technology and select the optimum welding parameters, the samples of dispersed-reinforced CM AMg5 + 27 % Al_2O_3 were welded using the 0.15 mm thick interlayer of pure aluminum (AD1 alloy) under the free deformation conditions. At that, the used optimum temperature was $T = 560$ °C, time was $t = 20$ min, welding pressure was $P = 40$ MPa, and vacuum in the working chamber was $B = 1.3 \cdot 10^{-3}$ MPa. The overall plastic deformation of the samples under the free deformation conditions was set at a level of $\epsilon = 25$ % by using steel inserts limiting the deformation.

The results of metallographic examinations showed that the sufficient adhesion of metal of the interlayer with matrix aluminum of the composite was provided in a welded joint under the free deformation conditions in vacuum pressure welding using the 0.15 mm thick interlayer of pure aluminum. There was no accumulation of the reinforcing particles at the interface. However, individual regions contained micropores and extended oxides (see Figure 2, *b*). Thickness of the aluminum interlayer in the welded joints reduced from 150 to 100–120 μm . Shear strength of the joints was $\sigma_{sh} = 40$ MPa.

As shown by investigations [4], deformation of solid interlayers take place only in a short edge area in a case of using the free-state welding scheme, this being in agreement with our investigation results. To produce stronger joints, the authors of studies [4, 9] recommend using such techniques and parameters of pressure welding, at which the joining zone material experiences plastic deformation by the pressure + shear scheme. This process was called welding with forced deformation [9], which is the case of cold welding, friction welding, resistance butt welding, etc.

In our investigations we used the scheme of welding with forced deformation for activation of plastic deformation in the joining zone. A forming device, providing a directed shear plastic deformation of metal in the joint and preset deformation of welded samples as a whole, was employed for this purpose. The forming device consisted of two dies and a guide bushing. The degree of plastic deformation of the joints at a level of $\epsilon = 15\text{--}25$ % was set by depth of the channels.

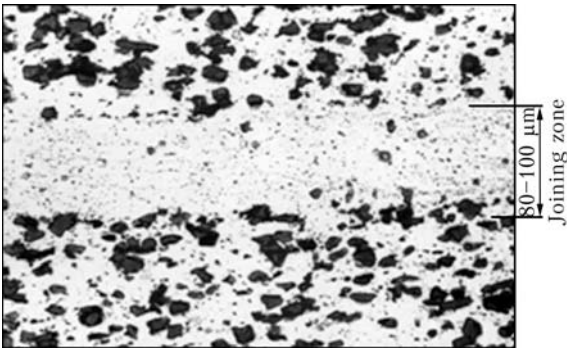


Figure 3. Microstructure ($\times 400$) of CM welded joint produced by vacuum pressure welding using aluminum interlayer 0.15 mm thick under forced deformation conditions

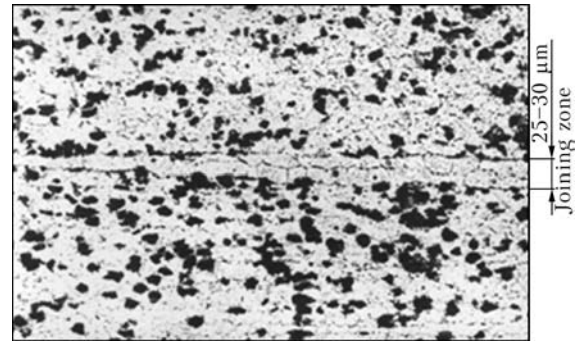


Figure 5. Microstructure ($\times 300$) of the CM joining zone in vacuum pressure welding using rapidly solidified strip (Al + 33 % Cu) 0.07 mm thick under free deformation conditions

Metallographic analysis of the welded joints produced in the forming dies using the aluminum interlayer showed the absence of defects that usually take place during welding in the free state (oxide inclusions, pores) (Figure 3).

The aluminum interlayer had non-uniform thickness along the length of a sample. In welding with the solid interlayer, thickness of aluminum was 80–100 μm in the central part of a joint and 30–60 μm at its ends, i.e. it was smaller at ends of the welded joint than in its central part. This is explained by the fact that the deformation processes on the periphery of the joint take more time than in the central part, and that the shear (tangent) deformations are longer and more intensive [10]. Microhardness of the aluminum interlayer in the welded joints is 650–750 MPa. One of the differences of the welded joints produced in the forming dies from those produced in the free state is the presence of flash no more than 1 mm thick, whereto not only the soft aluminum interlayer but also the adjacent CM layers go during welding.

In welded joints of the composite material, the character of distribution of the reinforcing particles within the welding zone, their morphology and dispersion do not change both under the free deformation conditions and when using the forming dies. Shear strength of the joints produced by welding in the forming dies using the 150 μm thick aluminum interlayer is $\sigma_{sh} = 91$ MPa. This is approximately 50 % of that of the composite in the initial condition.

Joints with sufficiently high strength characteristics can be produced by vacuum pressure welding providing that interface between the mating surfaces stops acting as a separate structural element [11]. This can be achieved by using thin interlayers, capable of intensifying diffusion processes in the joint, dispersing and redistributing remainders of the oxide film. For this, the diffusion processes have to be activated and maximum possible dissolution of the interlayer has to be achieved during the welding process, which, in our opinion, should promote significant improvement of strength of the joints. For this purpose, low-melting point interlayers of eutectic aluminum alloy, including the rapidly solidified ones, which activate the mating surfaces and easily diffuse into the base metal during welding [12], can be used.

It is also well known that the diffusion processes significantly accelerate with the grain size refinement, i.e. with increase in length of the grain boundaries, as the diffusion coefficient along the grain boundaries is several orders of magnitude higher than in the bulk of grains [13].

In this connection, the rapidly solidified strip of the Al–Cu (Al + 33 % Cu) system and eutectic composition, 0.07 mm thick and 10 mm wide, developed and manufactured by the I.M. Frantsevich Institute of Problems of Materials Science of the NAS of Ukraine, was used for welding of CM AMg5 + 27 % Al_2O_3 . Structure of the strip consists of α -solid solution of aluminum and dispersed particles of intermetallic phase Al_2Cu , uniformly distributed in the matrix volume. An X-ray diffraction pattern of the rapidly solidified trip of Al/Cu system eutectic alloy

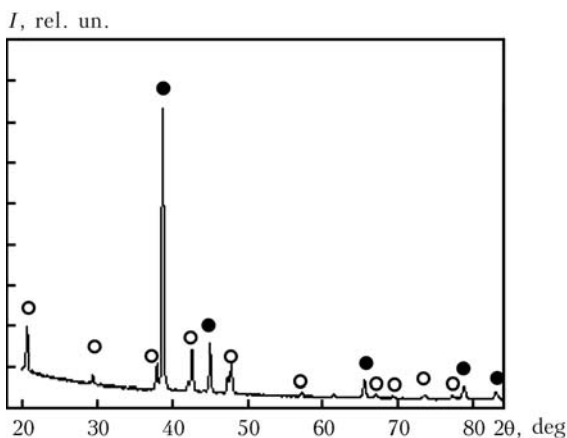


Figure 4. Spectrum of X-ray diffraction of rapidly solidified strip of Al + 33 % Cu: ● – Al; ○ – Al_2Cu

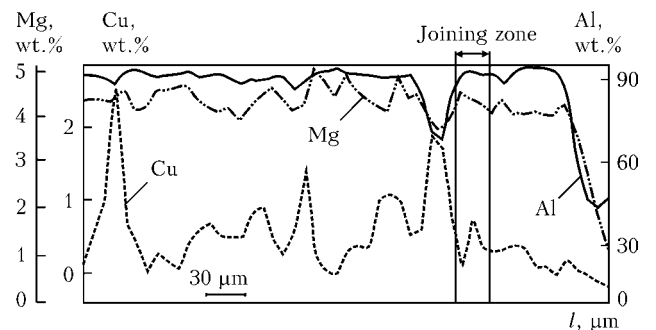


Figure 6. Character of distribution of copper, magnesium and aluminum in the CM joining zone in welding under free deformation conditions

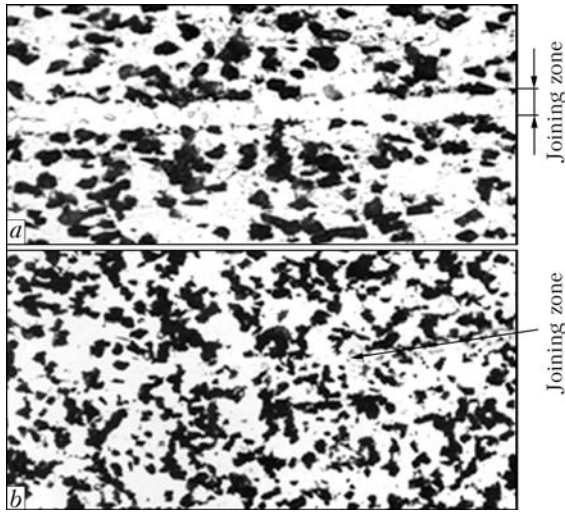


Figure 7. Microstructure of the CM joining zone ($\delta = 8\text{--}10\ \mu\text{m}$) in vacuum pressure welding using rapidly solidified strip (Al + 33 % Cu) under forced deformation conditions (*a* – $\times 600$) and with subsequent thermal cycling (*b* – $\times 400$)

Al + 33 % Cu is shown in Figure 4, in which only the Al and Al_2Cu peaks are present.

The optimal temperature in vacuum pressure welding of AMg5 + 27 % Al_2O_3 CM using the rapidly solidified strip of Al/Cu system eutectic alloy Al + 33 % Cu as an interlayer was $T_w = 500\ \text{°C}$ ($t = 10\ \text{min}$, $P = 40\ \text{MPa}$) both under the free and forced deformation conditions. It is likely that a 60 °C decrease in the welding temperature, compared with welding using the solid aluminum interlayer, is related to an increased activity of the rapidly solidified strip.

The metallographic examination results showed that thickness of the interlayer in the joint reduces from 70 up to 20–30 μm (Figure 5) in vacuum pressure welding ($T_w = 500\ \text{°C}$) under the free deformation conditions. According to the data of X-ray spectrum microanalysis, the interlayer contains 4.35 wt.% Mg, 2.3 wt.% Cu and 93.4 wt.% Al (Figure 6). During the welding process more than 4 wt.% Mg transfers to the interlayer from alumocomposite AMg5 + 27 % Al_2O_3 . Hardness of the interlayer is virtually at a level of that of the composite matrix.

Welding in forming devices allows reducing the interlayer thickness to 8–10 μm (Figure 7, *a*). Subsequent heat treatment (thermal cycling), consisting of five cycles of heating to 500 °C under pressure and cooling to 200 °C, provided practically complete dissolution of the interlayer (Figure 7, *b*). Shear strength of the welded joint after welding and heat treatment was $\sigma_{sh} = 180\ \text{MPa}$.

Therefore, application of the rapidly solidified strip of Al/Cu system eutectic alloy Al + 33 % Cu, as well as techniques aimed at acceleration of the diffusion processes in the joint, in vacuum pressure welding of composite AMg5 + 27 % Al_2O_3 allowed decreasing the welding temperature and reducing thickness of the interlayer in the welded joint to its practically complete dissolution. Shear strength of the welded joint reaches 180 MPa (Figure 8, pos. 5), which corresponds to the strength level of composite in the initial state.

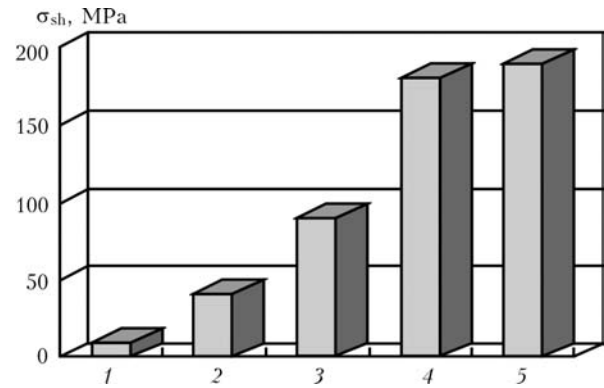


Figure 8. Diagram of changes of shear strength σ_{sh} for welded joint on AMg5 + 27 % Al_2O_3 CM depending on the technological peculiarities of vacuum pressure welding (1–4) and in the initial state (5): 1 – free state using no interlayer ($\sigma_{sh} = 8\text{--}9\ \text{MPa}$); 2 – same by using aluminum interlayer of $\delta = 150\ \mu\text{m}$ ($\sigma_{sh} = 40\ \text{MPa}$); 3 – forming die by using aluminum interlayer of $\delta = 150\ \mu\text{m}$ ($\sigma_{sh} = 91\ \text{MPa}$); 4 – same by using rapidly solidified strip Al + 33 % Cu of $\delta = 70\ \mu\text{m}$ ($\sigma_{sh} = 180\ \text{MPa}$); 5 – $\sigma_{sh} = 190\ \text{MPa}$

CONCLUSIONS

1. In vacuum pressure welding, a change of the pure aluminum interlayer to the interlayer of the rapidly solidified strip of the Al/Cu system eutectic alloy Al + 33 % Cu allowed producing the quality welded joints on composite AMg5 + 27 % Al_2O_3 at a lower temperature and shorter time of welding.

2. Application of the rapidly solidified strip of the Al/Cu system eutectic alloy provides strength of the joints at a level of that of the base metal.

- Ryabov, V.R., Budnik, V.P., Muravejnik, A.N. et al. (2001) Effect of electromagnetic stirring on properties of composite welded joints. In: *Proc. of Int. Conf. on Theory and Practice of Production Technologies of Items from Composite Materials and New Metallic Alloys – 21st Century* (30 Jan. – 2 Febr. 2001, Moscow). Moscow: MGU, 352–359.
- Ryabov, V.R., Muravejnik, A.N., Bondarev, A.A. et al. (1999) Investigation of structure of welded joints on dispersion-strengthened aluminium alloy. *Tekhnologiya Lyog. Splavov*, **1/2**, 139–144.
- Ryabov, V.R., Muravejnik, A.N., Cherepivskaya, E.N. et al. (1999) Diffusion bonding of dispersion-strengthened composite materials. *Joining of Materials*, **14(1/2)**, 6–11.
- Lyamin, Ya.V., Musin, R.A. (2002) Plastic deformation in diffusion bonding of dissimilar materials. *Svarochn. Proizvodstvo*, **5**, 24–29.
- Bushby, R.S., Scott, V.D. (1995) Joining of particulate silicon carbide reinforced 2124 aluminium alloys by diffusion bonding. *Materials Sci. and Technol.*, **11(8)**, 753–758.
- Escalera, M.D., Urena, A., Gomes de Salazar, J.M. (1997) Solid state diffusion bonding of A6061 matrix composites reinforced with aluminium particles. In: *Proc. of ASM Int. European Conf. on Welding and Joining Science and Technology* (March 10–12, 1997, Madrid, Spain). Madrid, 380–389.
- Ishchenko, A.Ya., Kharchenko, G.K., Falchenko, Yu.V. et al. (2006) Vacuum solid-state joining of dispersion-strengthened composite materials. *Nanosistemy, Nanomaterialy, Nanotekhnologii*, **4(3)**, 747–756.
- Ryabov, V.R., Muravejnik, A.N., Kharchenko, G.K. et al. (2003) Specifics of formation of structure of joints, made from dispersion-strengthened composite Al + 4 % C, in diffusion bonding. *The Paton Welding J.*, **12**, 6–9.
- Ternovsky, A.P. (1988) Diffusion bonding with forced deformation (Analytic review). *Svarochn. Proizvodstvo*, **9**, 76–83.
- Suvorov, I.K. (1973) *Pressure treatment of metals*. Moscow: Vysshaya Shkola.
- Sergeev, A.V., Chudin, V.M., Syropaeva, E.S. (1991) Diffusion welding of aluminium alloys in superplasticity state. *Automatich. Svarka*, **7**, 40–43.
- Ishchenko, Yu.Ya., Stretovich, A.D., Lozovskaya, A.V. et al. (1991) Specifics of diffusion welding of aluminium alloys. *Ibid.*, **6**, 34–35.
- Bokshtej, S.Z. (1971) *Structure and properties of metallic alloys*. Moscow: Metallurgiya.



EVALUATION OF QUALITY OF THE ARC SELF-ADJUSTMENT PROCESS

G.A. TSYBULKIN

E.O. Paton Electric Welding Institute, NASU, Kiev, Ukraine

Steady-state modes in the welding circuit during gas metal arc welding are considered. An approach is offered to evaluate quality of the arc self-adjustment process based on the use of the error index method.

Keywords: arc welding, consumable electrode, transient and steady-state process, accuracy of self-adjustment

Efficiency of control algorithms for robotic metal arc welding significantly depends on how the character of dynamic processes taking place in the welding circuit is allowed for during their development. The peculiarity of these processes is determined by the effect of self-adjustment of the arc, which, as is well known, was discovered and thoroughly investigated as far back as in the early 1940s [1]. Though there are lots of studies dedicated to investigation of the above effect, the issues of quality of the arc self-adjustment process are yet insufficiently covered in literature. We can mention only the recently published paper [2], which uses an integral performance criterion, allowing comparison of the systems close in structure (the best of them has the lowest integral estimate). The paper [2] does not consider the issues of accuracy in the steady-state modes, which, along with the transient process time, is known [3–7] to be one of the main indicators of the process quality.

Meanwhile, a smart method, described probably for the first time in study [7] and later known as an error index method, was suggested for analysis of accuracy in steady-state modes under conditions of constant, slowly varying external actions. This method makes it possible to quite easily obtain an idea of the steady-state processes in linear feedback systems of a random structure directly from coefficients of the transfer functions depending on the external actions and their derivatives. It is shown in study [8] that the above method, in principle, also applies to certain classes of non-linear systems, in which the non-linear elements are not connected by feedback circuit.

The task of this study is to investigate the steady-state process in the welding circuit during gas metal arc welding, and estimate accuracy of the arc self-adjustment process based on the error index method.

Consider the following differential equation:

$$(T_e T_s D^2 + T_s D + 1)v_m = v_e - DH + \frac{1}{E} Du_s, \quad (1)$$

which describes, according to [9], the dynamic processes taking place in the welding circuit.

The following designations are introduced in equation (1): $v_e = v_e(t)$ – consumable electrode feed speed relatively to the torch nozzle; $v_m = v_m(t)$ – electrode melting rate; $H = H(t)$ – distance between the tip of the current-conducting nozzle and free surface of the weld pool; $u_s = u_s(t)$ – voltage at output terminals of the welding current source; $E \equiv \partial u_a / \partial l$ – intensity of the electric field in the arc column; $u_a = u_a(t)$ – arc voltage; l – arc length; t – current time; $D = d/dt$ – differentiation operator; and T_e, T_s – time constants:

$$T_e = \frac{L}{R_*}; \quad T_s = \frac{R_*}{EM}. \quad (2)$$

Here L is the inductance of the welding circuit; $M \equiv \partial v_m / \partial i$ is the slope of the electrode melting characteristic at nominal values of the welding current i ; and electrode extension

$$R_* = R + S_a - S_s, \quad (3)$$

where R is the total resistance of the lead wires, electrode extension and sliding contact in the torch nozzle; $S_a \equiv \partial u_a / \partial i$; $S_s \equiv \partial u_s / \partial i$ is the slope of volt-ampere characteristics of the arc and welding current source at a nominal value of the welding current i .

Assume the following value to be a criterion of accuracy of self-adjustment:

$$\varepsilon(t) = v_e(t) - v_m(t), \quad (4)$$

which is a deviation of electrode melting rate $v_m(t)$ from electrode feed speed $v_e(t)$.

Based on (4) and (1), it can be written down that

$$\begin{aligned} (T_e T_s D^2 + T_s D + 1)\varepsilon(t) &= \\ &= (T_e T_s D^2 + T_s D)v_e(t) + DH(t) - \frac{1}{E} Du_s(t). \end{aligned} \quad (5)$$

Applying the Laplace transformation to (5), we obtain

$$\varepsilon(p) = W_1(p)v_e(p) + W_2(p)H(p) - W_3(p)u_s(p), \quad (6)$$

where p is the complex variable; and $W_1(p)$, $W_2(p)$ and $W_3(p)$ are the transfer functions:



$$W_1(p) = \frac{T_e T_s p^2 + T_s p}{T_e T_s p^2 + T_s p + 1}; \quad W_2(p) = \frac{p}{T_e T_s p^2 + T_s p + 1};$$

$$W_3(p) = \frac{E^{-1} p}{T_e T_s p^2 + T_s p + 1}. \quad (7)$$

Since transfer functions $W_1(p)$, $W_2(p)$ and $W_3(p)$ have no poles at the origin of coordinates, then, according to [7], they can be expanded into power series with regard to p . Therefore, steady-state deviation $\varepsilon_{\infty}(t)$ for each input action $v_e(t)$, $H(t)$ and $u_s(t)$ can be represented as a sum of corresponding expansions

$$\varepsilon_{\infty}(t) = \varepsilon_{1\infty}(t) + \varepsilon_{2\infty}(t) + \varepsilon_{3\infty}(t), \quad (8)$$

where

$$\begin{aligned} \varepsilon_{1\infty}(t) &= A_0 v_e(t) + A_1 D v_e(t) + A_2 D^2 v_e(t) + \dots; \\ \varepsilon_{2\infty}(t) &= B_0 H(t) + B_1 D H(t) + B_2 D^2 H(t) + \dots; \\ \varepsilon_{3\infty}(t) &= C_0 u_s(t) + C_1 D u_s(t) + C_2 D^2 u_s(t) + \dots \end{aligned} \quad (9)$$

In these expressions

$$A_n = \frac{1}{n!} \left[\frac{d^n W_1}{dp^n} \right]_{p=0}; \quad B_n = \frac{1}{n!} \left[\frac{d^n W_2}{dp^n} \right]_{p=0};$$

$$C_n = \frac{1}{n!} \left[\frac{d^n W_3}{dp^n} \right]_{p=0}, \quad n = 0, 1, 2, \dots \quad (10)$$

are the constant coefficients.

Thus, substituting coefficients A_n , B_n and C_n found from formulae (10) to expansions (9), and then summing up the results, according to (8), we will obtain the estimate of accuracy of arc self-adjustment, $\varepsilon_{\infty}(t)$.

If, for example, in expressions (9) we don't go beyond the first two terms of a series, which is quite acceptable in our case, then the approximate estimate

of accuracy $\varepsilon_{\infty}^*(t)$ will take a relatively simple form, such as

$$\varepsilon_{\infty}^*(t) = T_s D v_e + D H - \frac{1}{E} D u_s. \quad (11)$$

Numerical values of parameters T_s and E , as well as the rate of changes in input actions $v_e(t)$, $H(t)$ and $u_s(t)$ being known, we can easily calculate deviation $\varepsilon_{\infty}^*(t)$ from formula (11), i.e. obtain the estimate of accuracy of arc self-adjustment in each particular case without any additional theoretical or experimental investigations.

It can be directly seen from expression (11) that if $v_e = \text{const}$, $H = \text{const}$ and $u_s = \text{const}$, then deviation $\varepsilon_{\infty}(t)$ in the steady-state mode equals zero. Obviously, at $v_e(t) \neq \text{const}$, the lower the value of time constant T_s , which depends, according to (2), (3), on the slope of volt-ampere characteristics of the arc, $S_a \equiv \partial u_a / \partial i$, and welding current source, $S_s \equiv \partial u_s / \partial i$, the slope of electrode melting characteristic $M \equiv \partial v_m / \partial i$ and intensity of the electric field in the arc column, $E \equiv \partial u_a / \partial l$, the smaller is value of deviation $\varepsilon_{\infty}(t)$. It can be easily seen from (11), (2) and (3) that the lower the value of $R^* = R + S_a - S_s$ and higher the value of EM , the lower is the value of deviation $\varepsilon_{\infty}(t)$ in the steady-state mode, i.e. the higher is the accuracy of arc self-adjustment.

As for time τ of the transient process, which is another main characteristic of quality of self-adjustment of the arc, since $T_s \gg T_e$ in the welding circuit, this time can be estimated from the following formula:

$$\tau^* = T_s \ln(k), \quad (12)$$

where k is the number determining the degree of decrease of initial deviation ε_0 during desired time τ , i.e. $k = \varepsilon_0 / \varepsilon(t)$.

It follows from formulae (12), (2), (3), in particular, that time τ of the transient process reduces with decrease of R^* and increase of EM .

Thus, formulae (11) and (12) are very convenient for numerical estimation of the quality of the arc self-adjustment process, which to a certain extent determines the quality of the arc welding process.

Results of computer modeling of the processes described by differential equation (1) are shown in Figures 1 and 2. The following values of parameters of the welding circuit and mode of arc welding are taken: $L = 4 \cdot 10^{-4}$ H; $R = 0.015$ Ohm; $E = 2$ V/mm; $M = 0.31$ mm/(A·s), and $S_a = 0.005$ V/A.

Transient and steady-state processes $\varepsilon(t)$ obtained in changing of electrode feed speed $v_e(t)$ and at constant $H = 17$ mm and $u_s = 30$ V, are shown in Figure 1. For simplicity of verification of formula (11), the law of change in $v_e(t)$ was set by the dependence

$$v_e(t) = \begin{cases} 45, & t < 0.5 \\ 45 + 20(t - 0.5), & t \geq 0.5 \end{cases} \text{ [mm/s].}$$

Comparison of curves 1 and 2 in Figure 1 shows that the arc self-adjustment accuracy characterized by

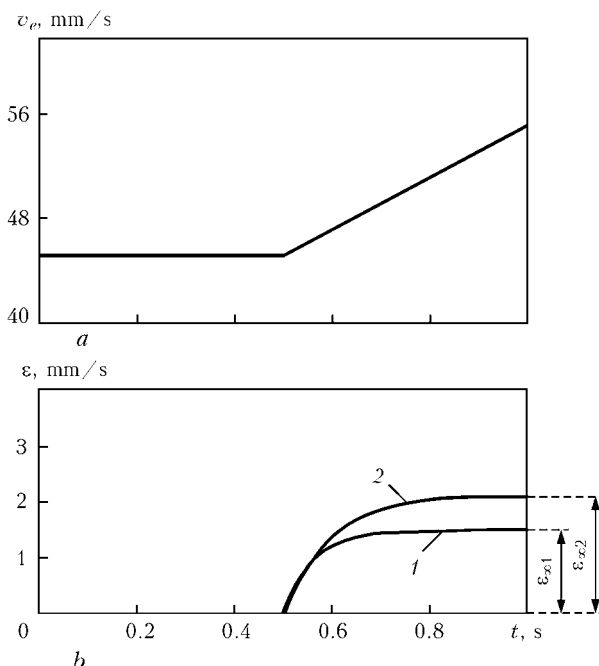


Figure 1. Linear change in electrode feed speed v_e (a), and response of deviation $\varepsilon(t)$ to this change (b): 1 - $S_s = -0.025$; 2 - -0.045 V/A



deviation $\varepsilon(t)$ increases with decrease in slope S_s of volt-ampere characteristic of the welding current source.

Transient process $\varepsilon(t)$ induced by a stepwise change in distance $H(t)$ between the tip of the current-conducting nozzle and free surface of the weld pool is shown in Figure 2:

$$H(t) = \begin{cases} 17, & t < 0.5 \\ 20, & t \geq 0.5 \end{cases} \text{ [mm].}$$

Voltage u_s was set to be equal to 30 V, and speed v_e – to 45 mm/s.

It can be seen from Figure 2 that the time of the transient process reduces with decrease in slope S_s of volt-ampere characteristic of the welding current source.

To illustrate the efficiency of application of formulae (11) and (12) for numerical estimation of the arc self-adjustment quality, calculate steady-state deviation $\varepsilon_{\infty}^*(t)$ and time τ of the transient process from these formulae for the above cases.

In case of a linear change in electrode feed speed $v_e(t)$ (see Figure 1)

$$\varepsilon_{\infty 1}^*(t) = T_s D v_e = \frac{0.015 + 0.005 + 0.025}{2 \cdot 0.31} \times 20 = 1.45 \text{ mm/s (curve 1);}$$

$$\varepsilon_{\infty 2}^*(t) = \frac{0.015 + 0.005 + 0.045}{2 \cdot 0.31} \times 20 = 2.1 \text{ mm/s (curve 2).}$$

In case of a stepwise change in distance $H(t)$ between the tip of the current-conducting nozzle and free surface of the weld pool (see Figure 2)

$$\tau_1^* = T_s \ln(k) = \frac{0.015 + 0.005 + 0.015}{2 \cdot 0.31} \times 3 = 0.17 \text{ s (curve 1);}$$

$$\tau_2^* = \frac{0.015 + 0.005 + 0.045}{2 \cdot 0.31} \times 3 = 0.31 \text{ s (curve 2).}$$

Comparing $\varepsilon_{\infty}^*(t)$ and τ^* calculated from formulae (11) and (12) with corresponding values of ε_{∞} and τ obtained by modeling (Figures 1, 2): $\varepsilon_{\infty 1}(t) = 1.45 \text{ mm/s}$, $\varepsilon_{\infty 2}(t) = 2.09 \text{ mm/s}$, $\tau_1 = 0.16 \text{ s}$, $\tau_2 = 32 \text{ s}$, it can be seen that they almost coincide.

Therefore, the computer modeling and the above calculations show that estimations (11) and (12) proposed in this study give a clear idea of the accuracy and time of the transient arc self-adjustment processes. Parameters of the welding circuit being known, it is easy to calculate the values of ε_{∞}^* and τ^* from formulae

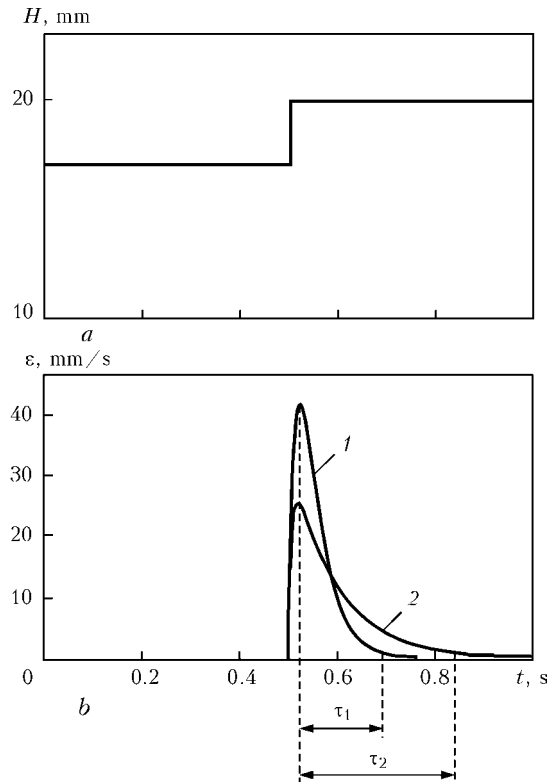


Figure 2. Stepwise change in distance H between the nozzle and weld pool (a), and response of deviation $\varepsilon(t)$ to this change (b): 1 – $S_s = -0.015$; 2 – -0.045 V/A

(11) and (12). Moreover, having the above formulae, the desirable indicators of the arc self-adjustment quality can be provided by selecting certain relationships between parameters of the welding circuit. Such a necessity, in particular, arises when using the pulsed arc welding methods [10].

We used estimations (11) and (12) in [11] for the development of the adaptive arc sensor to provide corrective control of robotized arc welding.

1. Paton, B.E. (2008) *Selected transactions*. Kiev: PWI.
2. Dyurgerov, N.G. (2001) Integral criterion of the welding arc self-adjustment quality. *Svarochm. Proizvodstvo*, **8**, 8–10.
3. Popov, E.P. (1987) *Theory of linear systems of automatic regulation and control*. Moscow: Nauka.
4. King, L.G. (1954) Decrease of steady dynamic error in closed tracking systems. *Prikl. Mekhanika i Mashino-stroenie*, **2**, 3–14.
5. Lukas, V.A. (1990) *Theory of automatic control*. Moscow: Nedra.
6. Tumanov, M.P. (2005) *Theory of control. Theory of automatic control linear systems*. Moscow: MGIEM.
7. (1951) *Theory of tracking systems*. Ed. by H. James et al. Moscow: Inostr. Literatura.
8. Tsybulkin, G.A. (1994) Analysis of steady-state modes of some classes of nonlinear dynamic systems based on recurrent estimation procedures. *Kibernetika i Vychisl. Tekhnika*, Issue 101, 74–80.
9. Tsybulkin, G.A. (2008) Stabilization of electrode melting rate in robotic arc welding. *The Paton Welding J.*, **12**, 9–11.
10. Kiji, N., Kobayashi, K., Ishii, J. et al. (2003) Development of high-efficiency arc welding methods. *Ibid.*, **10/11**, 56–60.
11. Tsybulkin, G.A. (2001) Robust digital sensor for arc welding. *Ibid.*, **11**, 44–46.



LASER WELDING OF ROOT WELDS OF THICK JOINTS OF HEAT-RESISTANT STEEL

T.I. CHERNAYA, A.K. TSARYUK, A.V. SIORA, V.D. SHELYAGIN and V.Yu. KHASKIN
E.O. Paton Electric Welding Institute, NASU, Kiev, Ukraine

Technology of laser welding of root welds from heat-resistant steel is described. Optimum conditions for sound formation of root welds with complete penetration and smooth transition from the back bead to the base metal were determined.

Keywords: laser welding, heat-resistant steel, power, beam, filler wire, welded joint, root pass, weld

Ensuring the reliability and operability of critical components of turbounits, for instance rotors of powerful steam turbines, is a challenge. One of the most urgent problems here is sound performance of root welds of the rotor joints. Considering the structural features, welding is performed under complicated conditions and performance of NDT is difficult. On the other hand, item geometry, its service life and reliability as a whole depend on welding the root welds. At present, root welds of rotors of low pressure cylinders are made by nonconsumable-electrode argon-arc welding in the gravity position or on a permanent steel backing (for low pressure cylinders of slow-speed turbines). With such a welding process, however, it is difficult to ensure a stable 100 % penetration of weld root around the entire joint perimeter, particularly in manufacturing large-sized rotors of powerful turbines. A significant drawback of making the root welds on a backing ring is formation of structural-technological lack-of-penetration, which, being a potential stress raiser, promotes lowering of the level of fatigue strength and increase of brittle fracture susceptibility. Therefore, finding a method to make the root weld with 100 % penetration and ensuring back bead formation, is a technological priority.

The objective of this work was investigation and determination of optimum conditions to produce sound root welds with back bead formation in laser welding of thick metal of heat-resistant steel. This required solving a number of procedural and technological problems, related to laser type selection, determination of its optimum power, selection of shield-

ing gas and groove geometry, establishing laser welding parameters and optimization of welding technique.

Investigation procedure envisaged application of 25Kh2NMFA rotor steel 30 mm thick as the base material, as well as steel 20, 5 mm thick, for preliminary experiments on optimization of individual parameters of the mode of welding the root face of 25Kh2NMFA steel butt joint (Figure 1). Root face thickness equal to 5 mm was selected on the grounds of convenience of assembly and minimum section of the root weld, meeting the strength requirements.

Used as the radiation source was solid-state laser of DY 044 type (Rofin Sinar, Germany). Radiation power is known to have an essential influence on the penetrability and nature of weld formation [1]. Increase of radiation power improves both the effectiveness of beam action, and penetration depth and weld width. Experiments on determination of welding mode parameters were conducted on butt samples of $300 \times 150 \times 5$ mm size from steel 20 (wt. %: 0.196 C; 0.2 Si; 0.49 Mn; 0.019 S; 0.017 P) without edge preparation at different radiation power from 2.5 up to 4.0 kW. Radiation was focused by a lens with focal distance of 200 mm. Welding was conducted with three-axis manipulator [2]. As a rule, shielding by a gas jet aimed into the zone of laser radiation action on the metal is used in laser welding. Shielding weld metal from oxidation, the gas jet deflects the vapour flow and spatter from the axis of laser radiation propagation and lowers the screening action of plasma, present in the crater and above the irradiated surface. CO_2 gas and $\text{CO}_2 + 18\%$ Ar mixture were used as shielding gases.

Welded joint quality was the main criterion for establishing the optimum conditions and parameters of laser welding. Quality control was performed by studying the macrostructure in the cross-section of templates cut out of welded joints. Joint quality was considered to be satisfactory in the absence of pores, cracks, lacks-of-fusion, slag inclusions, as well as in case of correspondence to standards of concavity and convexity of weld root from the reverse side.

It is seen from Table 1 that carbon dioxide gas provides the best shielding of weld metal. In welding in the mixture at the selected welding speed pores were formed.

Table 2 gives the data on the influence of radiation defocusing on penetration geometry in shielding with

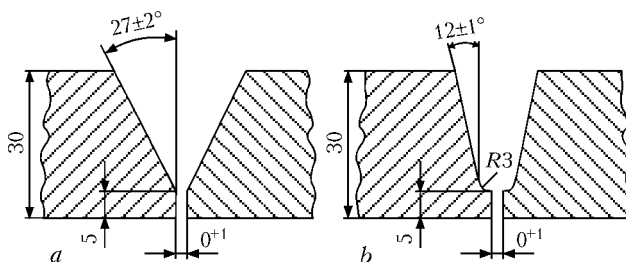


Figure 1. Schematic of edges for laser welding of V- (a) and U-shaped (b) groove



Table 1. Influence of radiation power and shielding gas on macrostructure and geometry of welded joint of steel 20, 5 mm thick

Power, kW	CO ₂	CO ₂ + 18 % Ar mixture
4.0		
3.5		
3.0		
2.8		
2.5		

carbon dioxide gas and CO₂ + Ar mixture. The surface of welded parts was located above or below the lens focal plane, where the focused beam has the smallest diameter. Focused beam diameter has direct influence on power density and on penetration geometry, respectively. The best results are achieved at lowering of the focal point under the sample surface for 2 mm. In all the variants it is rational to shield the radiation zone with carbon dioxide gas. When gas mixture and selected welding speed were used pores formed practically in all the cases. Therefore, in further experiments the main shielding was performed with carbon dioxide gas (feeding to pool head). For additional shielding of the solidifying metal, argon was fed to the pool tail part.

The main features of welding heat-resistant steels of the pearlitic class are their high sensitivity to the rate of cooling below austenitization temperatures and need to preserve structural stability, as well as me-

chanical properties, the level of which is achieved largely by thermal strengthening of steel before welding [3]. Considering the high susceptibility of these steels to formation of brittle hardening structures in the HAZ metal, welding should be performed with preheating and concurrent heating, and welded joints should be treated by high tempering. In addition, in order to reduce the risk of cold cracking in multipass welding of more than 20 mm thick metal, it is recommended to weld the weld root by a more ductile material than when filling the groove (in nonconsumable-electrode argon-arc welding Sv-08G2S or Sv-08GS

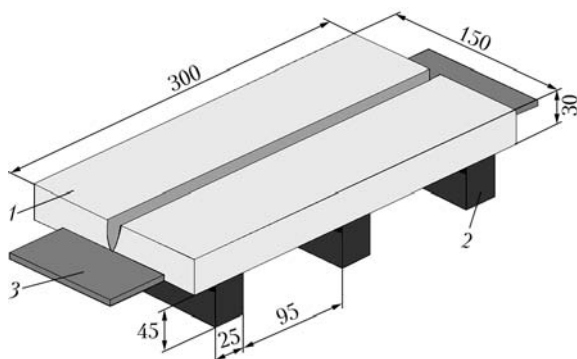


Figure 2. Schematic of rigid sample from 25Kh2NMFA steel: 1 – plate; 2 – stiffener; 3 – run-off tab

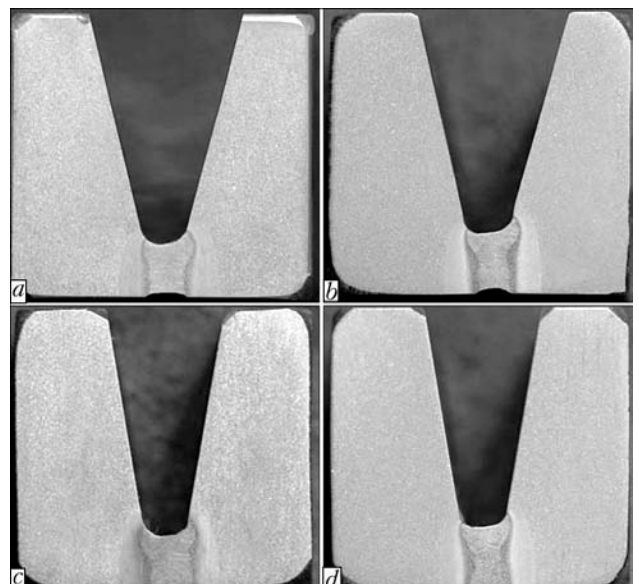
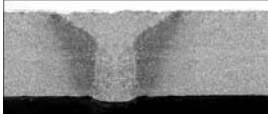
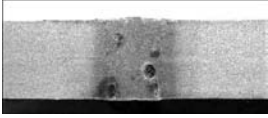
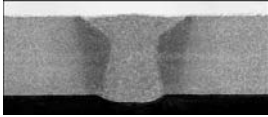
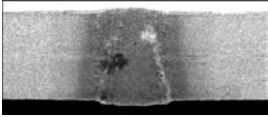
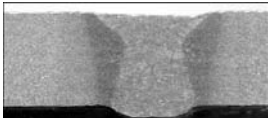
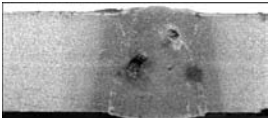
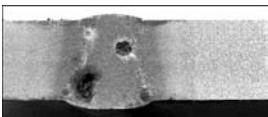
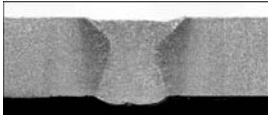
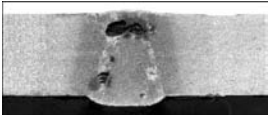
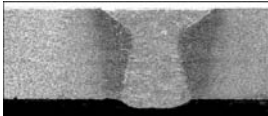
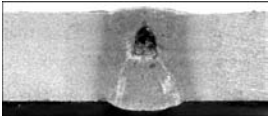
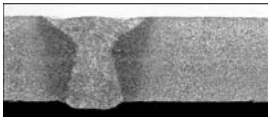
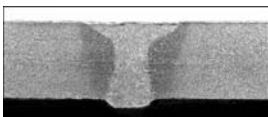
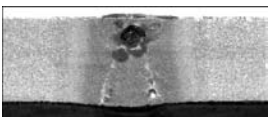
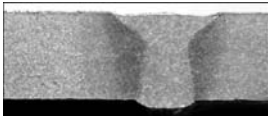
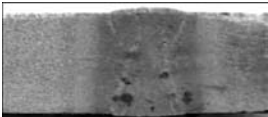


Figure 3. Macrosections of the root weld made by laser welding with V- (a, b) and U-shaped (c, d) groove and 5 mm root face

**Table 3.** Influence of radiation defocusing and shielding gas on macrostructure and geometry of welded joint of steel 20, 5 mm thick

Lowering	CO ₂	CO ₂ + 18 % Ar mixture
+5		
+3		
+2		
+1		
0		
-1		
-2		
-3		
-5		

wire is used). In this connection subsequent experiments on making the root welds of 25Kh2NMFA rotor steel joints (wt. %: 0.22 Cr; 0.3 Si; 0.44 Mn; 1.87 Cr; 1.38 Ni; 0.36 Mo; 0.04 V; 0.009 S; 0.008 P) were conducted with preheating to 250–300 °C and using ductile filler wire.

Optimisation of the technology of laser welding of root welds of butt joints on 25Kh2NMFA steel 30 mm thick was conducted on rigid samples (Figure 2) with and without filler wire feed. Sv-08G2S wire of 1.2 mm diameter was used as filler material. Several geometries of rigid butt edge preparation were studied for making the root welds (see Figure 1). U-shaped groove turned out to be the best (Figure 1, *b*). Root face was 5 mm in all the cases. Selection of groove type was aimed at obtaining a welded joint with a good weld root penetration at minimum con-

sumption of deposition metal, while keeping the groove shape simple to produce. U-shaped edge preparation compared to V-shaped groove required a smaller amount of deposited metal, and owing to a wide gap in the weld root, it facilitates the process when making the first root weld. In welding with a V-shaped groove without filler wire, the weld has a weaker section, is drawn inside from the groove reverse side (Figure 3, *a*), and the probability of fracture of such a weld is quite high. In welding with a V-shaped groove with application of filler wire (Figure 3, *b*) the section is somewhat larger, but back bead formation is unacceptable, in view of the presence of a kind of concentrator (groove instead of the root bead).

Processing and generalization of the results of investigation of welded joint quality showed that selection of laser welding parameters and filler wire feed rate



allows achieving the optimum geometry, satisfactory formation and required reinforcement of the weld root.

Conducted studies showed that radiation of Nd:YAG laser of 4.4 kW power at welding speed of 16 m/h allows making in the butt joint a root weld with complete penetration and good formation of the back bead.

Optimum mode of welding the root welds in the joints of 25Kh2NMFA steel with U-shaped groove (Figure 3, *c, d*) is as follows: radiation power of 4 kW; welding speed of 16 m/h; focal distance of 200 mm; focal point deepening to 2 mm; gas flow rate: CO₂ – 20 l/min (to pool head), Ar – 10 l/min (pool tail part); feed rate of 1.2 mm wire – 38.4 m/h.

Thus, results of experiments on laser welding of root welds in the downhand position showed that with the appropriate fit-up and following the welding modes complete penetration of the weld root without defects (pores or cracks) with good formation of the back bead is ensured.

1. Grigoriant, A.G., Shiganov, I.N. (1988) *Laser welding of metals*. Moscow: Vysshaya Shkola.
2. Shelyagin, V.D., Khaskin, V.Yu., Siora, A.V. et al. (2003) Laser welding of thin-sheet steels using special approaches. *The Paton Welding J.*, 1, 39–42.
3. (2006) *Machine-building: Technology of welding, soldering and cutting*. Ed. by B.E. Paton. Vol. 3. Moscow: Mashinostroenie.

OPTIMAL CONTROL OF FORMATION OF WELD REINFORCEMENT

V.V. DOLINENKO, T.G. SKUBA, V.A. KOLYADA and E.V. SHAPOVALOV

E.O. Paton Electric Welding Institute, NASU, Kiev, Ukraine

Method is proposed for development of the optimal system for automatic control of formation of the weld reinforcement with transportation lag in the feedback loop under MAG welding conditions. A dynamic model of formation of the weld reinforcement was developed to build the optimal controller. Mathematical modelling was performed by using the MATLAB software package. The developed control system provides a minimal duration of the process at preset limitations of dynamics of the adjustment actions.

Keywords: *MAG welding, dynamic model, weld reinforcement formation, mathematical modelling, optimal control system, transportation lag*

Achieving the optimal weld shape is one of the key tasks in fabrication of welded structures. This is explained by the fact that at the optimal shape of the weld reinforcement it is possible to decrease values of the stress concentration factor and improve performance of welded structures. Moreover, the required weld sizes allow minimising overuse of welding consumables under mass production conditions. Up to now, formation of the weld has been controlled by using an open circuit, through setting the welding process parameters. Peculiarities of design of the open systems to control formation of the welds, based on regression models, are considered in study [1]. Also, the weld shape can be controlled by using mechanical oscillations of the welding tool and magnetic control of the weld pool [2]. All open methods for control of the weld formation share one drawback, which is related to the absence of the mechanism to compensate for external disturbances, which affect a workpiece during the arc welding process and may lead to deviations of geometric parameters of the weld from the preset values. For example, such disturbances include ambient parameters, state of the surface and deviations of geometric parameters of a welding object. One of the methods to compensate for the external disturbances is to use the closed feedback systems for auto-

matic control of the weld formation. A promising area of further advancement of the arc welding control systems is development and investigation of optimal and adaptive systems, the main advantages of which are considered in studies [3–5]. The necessity of applying the optimal control theory methods to welding is associated with high requirements for reliability and durability of welded structures [6].

The purpose of this study was to develop a system to control formation of the weld in MAG welding by using a laser TV sensor (LTS) in the feedback circuit to measure geometric parameters of the weld reinforcement bead.

Formalise the control problem, i.e. replace the control object by a mathematical model that describes essential peculiarities of the control problems and goals. The process of formation of the weld bead is a multidimensional connected control object, the behaviour of which can be described in first approximation by a system of first-order differential equations. In the state space, the object equations have the following forms:

$$\mathbf{x} = \mathbf{Ax} + \mathbf{Bu} + \mathbf{V}_0, \quad (1)$$

$$\mathbf{y} = \mathbf{Cx} + \mathbf{V}_0, \quad (2)$$

where \mathbf{x} is the vector of state variables of the bead formation process ($\mathbf{x}_1, \mathbf{x}_2, \dots, \mathbf{x}_n$)^T; \mathbf{u} is the vector of control actions of the welding process ($\mathbf{u}_1, \mathbf{u}_2, \dots$,



$\mathbf{u}_m)^T$; \mathbf{y} is the vector of observations of geometric parameters of the bead ($\mathbf{y}_1, \mathbf{y}_2, \dots, \mathbf{y}_l)^T$; \mathbf{A} is the matrix of states of the system measuring $n \times n$; \mathbf{B} is the matrix of controls ($n \times m$); \mathbf{C} is the matrix of observations ($l \times n$); $\mathbf{V}_0(t)$ is the matrix of coefficients of input disturbances; $\mathbf{V}_o(t)$ is the matrix of coefficients of observation noises; and t is the time.

Matrices $\mathbf{V}_0(t)$ and $\mathbf{V}_o(t)$ are white noises with the following probability characteristics:

$$M[\mathbf{x}_0] = \bar{\mathbf{x}}_0 \text{ (average value);}$$

$$M[(\mathbf{x}_0 - \bar{\mathbf{x}}_0)(\mathbf{x}_0 - \bar{\mathbf{x}}_0)^T] = \mathbf{P}_0;$$

$$M[(\mathbf{V}_0(t) - \mathbf{V}_0^T(t'))] = \mathbf{Q}_0\delta(t - t');$$

$$M[(\mathbf{V}_o(t) - \mathbf{V}_o^T(t'))] = \mathbf{R}_0\delta(t - t');$$

$$M[\mathbf{V}_0(t)] = 0; \quad M[\mathbf{V}_o(t)] = 0; \quad M[(\mathbf{V}_0(t) \mathbf{V}_o^T(t'))] = 0,$$

where $\mathbf{x}_0 = \mathbf{x}(t_0)$; \mathbf{Q}_0 and \mathbf{P}_0 are the positively semi-definite matrices; \mathbf{R}_0 is the positively definite matrix; $\delta(t - t')$ is the Kronecker function; and t' is the time moment.

The optimality criterion, which has to be minimised, is set in the form of functional

$$J = M[\mathbf{x}^T(t_f) \mathbf{F}\mathbf{x}(t_f) + \int_0^{t_f} [\mathbf{x}^T(t) \mathbf{Q}\mathbf{x}(t) + \mathbf{u}^T(t) \mathbf{R}\mathbf{u}(t)] dt], \quad (3)$$

where M is the mathematical expectation; \mathbf{F} is the matrix of boundary conditions; and \mathbf{Q} and \mathbf{R} are the matrices of weighting coefficients.

The optimal control problem is formulated as follows [7]: at preset object equations (1) and (2), control limitations $\mathbf{u}(t) \in \mathbf{U}_t$ and $\mathbf{U}_t \subseteq \mathfrak{R}^m$ (where \mathfrak{R}^m is the m -dimensional linear space) and edge conditions $\mathbf{x}(0) = \mathbf{x}_0$ and $\mathbf{x}(t_f) = \mathbf{0}$, it is necessary to define such a control with feedback $\mathbf{u} = \mathbf{u}\{y(\tau), t_0 \leq t \leq t_f\}$, where $t_0 \leq \tau \leq t_f$, at which optimality criterion (3) would have a minimal value.

To solve the stated problem, represent the model of a control object (CO), which is the weld formation process, in the form of a connected system of dynamic links. Transition functions of the links should describe the transient processes at the CO output as precisely as possible. Welding experiments were designed and carried out to study the character of these processes and, as a result, generate the a priori information on dynamic characteristics of CO.

In the course of the experiments, the adjustment actions were formed as deviations in voltage U_a and welding current I_w , and welding speed v_w was maintained at a constant level. Welding was performed at the reverse polarity current in flat position in the atmosphere of a mixture of shielding gases (Ar + 15 % CO₂). «Fronius TransPuls Synergic-5000» was used as an arc power source, and «Fronius VR 2000» – as a wire feed mechanism. The welding object was an 8 mm thick carbon steel plate. Electrode wire Sv-08G2S with a diameter of 1.2 mm was used for welding. The nominal welding parameters were as follows: $I_{w0} = 160$ A; $U_{a0} = 19$ V and $v_{w0} = 7$ mm/s.

The amplitude of deviations of the adjustment actions for current was $\Delta I_{w \max} = 15$ A, and for voltage – $\Delta U_{a \max} = 2$ V.

It was found as a result of the experiments that stepwise variations of the adjustment signals lead to spurious oscillations of the bead surface and formation of undercuts. To prevent formation of defects in the welds, the rate of growth/fall of the adjustment signals for voltage was limited to 1 V/s, and for welding current – to 10 A/s. As shown by the experimental results, the process of the weld bead formation is characterised both by the dynamic behaviour and by the presence of two different transportation lags in formation of width and height of the bead.

Introduce the following designations: e and g – width and height of the weld bead; Δe and Δg – finite increments of width and height of the weld bead relative to nominal values e_0 and g_0 ; ΔU_a and ΔI_w – finite increments of the adjustment actions; and U_a and I_w – actual values of the adjustment actions. Therefore, the following equations are valid:

$$U_a(t) = U_{a0} + \Delta U_a(t); \quad I_w(t) = I_{w0} + \Delta I_w(t); \quad (4)$$

$$e(t) = e_0 + \Delta e(t); \quad g(t) = g_0 + \Delta g(t), \quad (5)$$

where $\Delta U_a(t) < \Delta U_{a \max}$, and $\Delta I_w(t) < \Delta I_{w \max}$.

Represent the weld bead formation model for steady-state welding conditions in the form of a static connected system linearised about the working point (U_{a0}, I_{w0}).

Write it down in the matrix form

$$\begin{bmatrix} \Delta e(t) \\ \Delta g(t) \end{bmatrix} = \begin{bmatrix} k_{11} & k_{21} \\ k_{12} & k_{22} \end{bmatrix} \begin{bmatrix} \Delta U_a(t) \\ \Delta I_w(t) \end{bmatrix}, \quad (6)$$

where k_{11}, k_{12}, k_{21} and k_{22} are the output-input gain factors, the values of which have to be determined.

Static and dynamic characteristics of the linearised weld formation process model were estimated from the welding experiments, which were conducted by using pulse adjustment actions U_a and I_w with a limited growth/fall rate. Note that in this case we actually determined the time constants of the power supply-weld pool-bead dynamic system. That is why the time constants have to be checked when changing the type of the welding equipment or technological process. Geometric parameters of the bead were measured after welding by using LTS [8] with a sampling increment of 1 mm. Mean values of $e_0 = 7.85$ mm and $g_0 = 2.2$ mm were subtracted from the obtained data arrays on geometric parameters of the beads, and then smoothed with a line filter of moving mean

$$N_O[i] = \frac{\sum_{k=i-3}^{i+3} N_I[k]}{7},$$

where N_O and N_I are the smoothed and initial data arrays, and i and k are the integers (indices of the arrays). To correctly estimate time constants of the four transit-time links that make up the model, the



data arrays were shifted towards the electrode (to the right along axis x) over corresponding calculated distances of the transportation lags. The values of the transportation lags are determined as follows. It is a known fact that width and height of the bead form at the solidification front of metal of the weld pool in its middle and tailing portions [9]. Therefore, the transportation lags of measurements of height τ_g and width τ_e of the bead can be determined from the following formulae:

$$\tau_g = \frac{L_{TV} - L_g}{v_w}; \quad \tau_e = \frac{L_{TV} - L_e}{v_w}, \quad (7)$$

where L_{TV} is the distance between the light trace of LTS and torch electrode, mm; L_g is the distance from the electrode to the end point of the weld pool tailing portion, mm; and L_e is the distance from the electrode to the middle point of the weld pool, mm.

A regression model was synthesised to calculate distances L_e and L_g . The model was developed by using a calculation experiment with the presented model of the process of propagation of heat in a semi-infinite body heated with a moving normal-rotary heat source [10]:

$$L_g = -0.69 + 0.041U_a + 0.0048I_w + 0.3v_w \text{ [cm];}$$

$$L_e = 0.08 + 0.004U_a + 0.0016I_w + 0.4v_w \text{ [cm].}$$

Figure 1 shows the plots of variations in geometric parameters of the beads depending upon the lineally varying adjustment actions with reactions of transit-time elements superimposed on them for comparison. Noteworthy is non-linear dynamics of variations in width and height of the bead under the effect of a welding current pulse, which shows up as decrease in duration of the output pulse due to the phase shift of its leading edge (Figure 1, I).

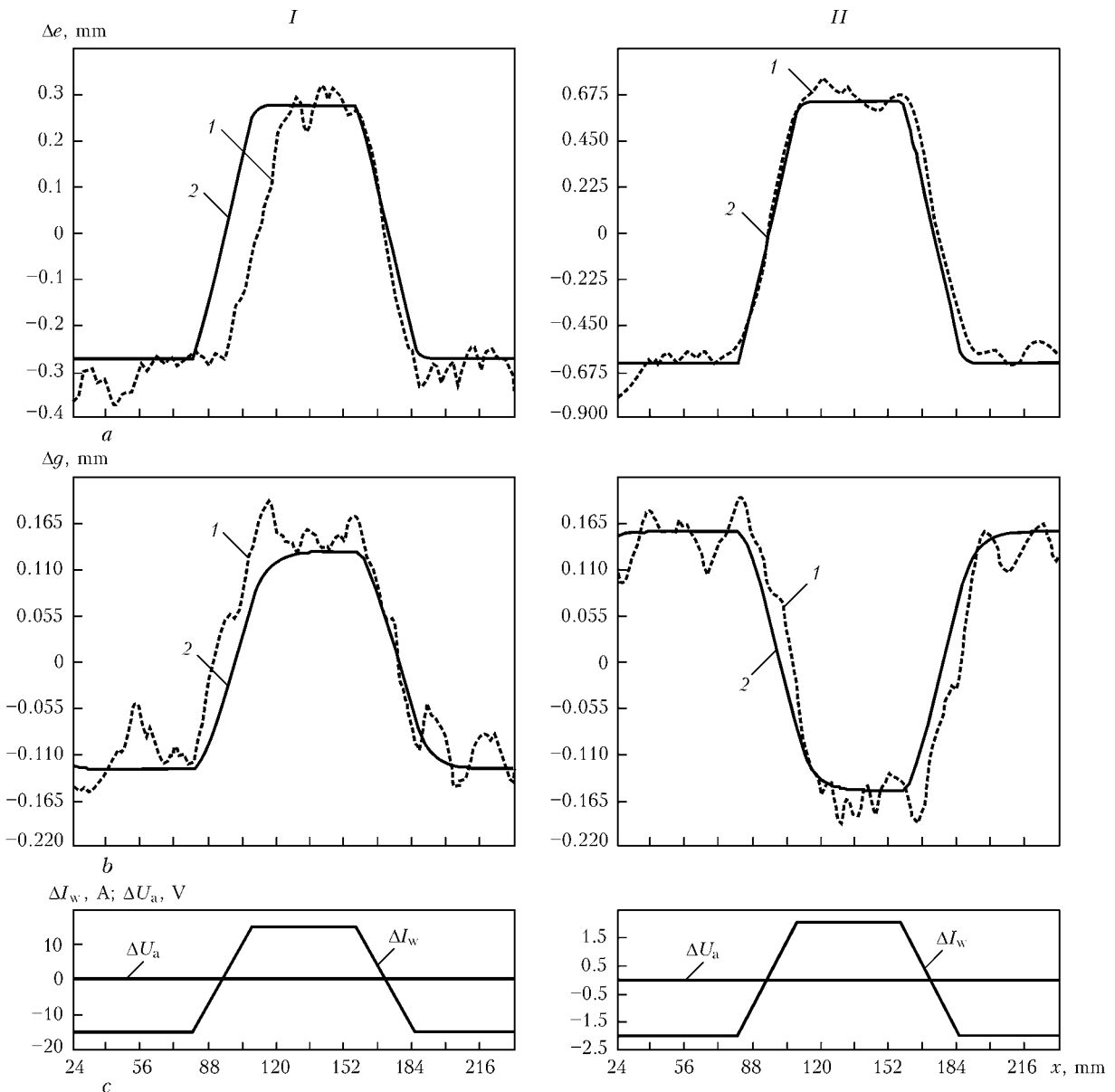


Figure 1. Results of identification of parameters of dynamic links of the weld reinforcement formation model for a pulse of welding current (I) and voltage (II); a, b – variations in width and height of the reinforcement bead, respectively; c – increments of welding current and voltage adjustment actions, respectively: 1 – reaction of dynamic links of the model; 2 – geometric parameters of the reinforcement bead measured with LTS



The dynamic control object is synthesised as follows. As it is necessary to limit dynamics of variations in adjustment actions U_a and I_w , the control vector is set in the form of time derivatives $\mathbf{u} = \left[\frac{dU_a}{dt} \frac{dI_w}{dt} \right]^T$. Then, to match the control and adjustment actions it is necessary to add an ideal integrating link to the CO composition. The output vector (observation vector) is set as $\mathbf{y} = [\Delta e(t) \Delta g(t)]^T$. The resulting output equation in the operator form is written down as follows:

$$\mathbf{y} = W(p)\mathbf{u}, \tag{8}$$

where $W(p) = W_3(p)W_2(p)W_1(p)$; p is the Laplace operator; $W_3(p)$ is the transfer function of an ideal link of the transportation lag; $W_2(p)$ is the transfer function of the first-order aperiodic link; and $W_1(p)$ is the transfer function of the ideal integrating link.

These transfer functions in the matrix form look like as follows:

$$W_1(p) = \begin{bmatrix} \frac{1}{p} & 0 \\ 0 & \frac{1}{p} \end{bmatrix}; \quad W_2(p) = \begin{bmatrix} \frac{k_{11}}{1+T_{11}p} & \frac{k_{21}}{1+T_{21}p} \\ \frac{k_{12}}{1+T_{12}p} & \frac{k_{22}}{1+T_{22}p} \end{bmatrix};$$

$$W_3(p) = \begin{bmatrix} e^{-\tau_e p} & 0 \\ 0 & e^{-\tau_g p} \end{bmatrix}.$$

After substitution of transfer functions $W_3(p)$, $W_2(p)$ and $W_1(p)$ in (8), the output equation will be written down as follows:

$$\mathbf{y} = \begin{bmatrix} \frac{k_{11}}{(1+T_{11}p)p} e^{-\tau_e p} & \frac{k_{21}}{(1+T_{21}p)p} e^{-\tau_e p} \\ \frac{k_{12}}{(1+T_{12}p)p} e^{-\tau_g p} & \frac{k_{22}}{(1+T_{22}p)p} e^{-\tau_g p} \end{bmatrix} \mathbf{u}. \tag{9}$$

The limitations have the following form:

$$\left| \frac{dU_a(e)}{dt} \leq u_{\max 1} \right|, \quad \left| \frac{dI_w(e)}{dt} \leq u_{\max 2} \right|, \tag{10}$$

where $u_{\max 1} \in \mathbf{U}$; $u_{\max 2} \in \mathbf{U}$; $\mathbf{U} \subseteq \mathfrak{R}_+^2$; \mathfrak{R}_+^2 is the two-dimensional space of non-negative numbers.

Figure 2 shows a structure chart of transfer function $W(p)$.

To make use of the known procedure of synthesis of the optimal automatic control system (ACS), ex-

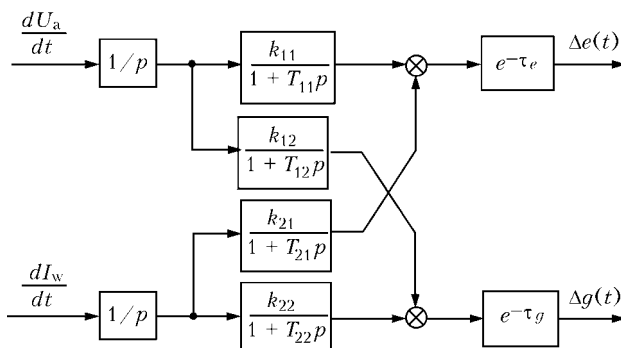


Figure 2. Structure chart of the dynamic weld reinforcement formation model

ponential functions are replaced by rational polynomials. $e^{-\tau p}$ is approximated to a sufficient accuracy by Pade polynomial [11] of the 5th degree:

$$e^{-\tau p} = \frac{\tau^5 p^5 - 30\tau^4 p^4 + 420\tau^3 p^3 - 3360\tau^2 p^2 + 15120\tau p - 30240}{\tau^5 p^5 + 30\tau^4 p^4 + 420\tau^3 p^3 + 3360\tau^2 p^2 + 15120\tau p + 30240}. \tag{11}$$

The resulting transfer function should be represented by a system in the state space. Mean values of the transportation lags, i.e. $\tau_e = 9.52$ s and $\tau_g = 8.38$ s, were determined based on the welding conditions ($v_w = \text{const}$) and preset distance $L_{TV} = 70$ mm. The calculations were made proceeding from an assumption that transportation lags τ_g and τ_e vary but insignificantly at the chosen range of the welding parameters. Hence, it follows that CO is stationary.

Control object matrices in the state spaces \mathbf{A} (14×14), \mathbf{B} (14×2) and \mathbf{C} (2×14), were calculated with the MATLAB package by using function *ss* [12].

Analysis of the obtained matrices shows that the quantity of lines of output matrix \mathbf{C} is smaller than the dimension of matrix \mathbf{A} that determines the state vector, for the restoration of which it is reasonable to use the Kalman–Bucy filter, i.e. optimal state observer.

Synthesis of the optimal control system for the weld bead formation is performed according to the procedure [7] based on the known principle of distribution or stochastic equivalence [13, 14]. It is used to solve the following interconnected problems: development of the deterministic optimal state controller and synthesis of the Kalman–Bucy filter. Development of the deterministic optimal controller is formulated as a problem of determination of optimal feedback control for object (1), (2) at optimality criterion (3)

$$\mathbf{u} = \mathbf{R}^{-1} \mathbf{B}^T \mathbf{K} \hat{\mathbf{x}}, \tag{12}$$

where $\hat{\mathbf{x}}$ is the optimal estimate of the CO state, which is determined by using the optimal state observer, i.e. Kalman–Bucy filter; and \mathbf{K} is the symmetric matrix determined from the Riccati matrix equation

$$\dot{\mathbf{K}} = -\mathbf{K}\mathbf{A} - \mathbf{A}^T \mathbf{K} + \mathbf{K}\mathbf{B}\mathbf{R}^{-1} \mathbf{B}^T \mathbf{K} - \mathbf{Q} \tag{13}$$

at boundary condition $\mathbf{K}(t_f) = \mathbf{F}$.

The required limitations on control are provided by a corresponding choice of matrix \mathbf{R} and inclusion of the optimal controller of an auxiliary element into the system, which is described by function $u_{\text{out } k} = \text{sat}(u_{\text{in } k}, u_{\max k})$:

$$u_{\text{out } k} = \begin{cases} u_{\text{out } k}, & \text{if } u_{\text{in } k} < u_{\max k}, \\ u_{\max k}, & \text{if } u_{\text{in } k} \geq u_{\max k}, \end{cases} \text{ at } k = (1, 2, \dots, m). \tag{14}$$

Synthesis of the Kalman–Bucy filter is made as follows. As noises of the welding process and observations are uncorrelated ($\mathbf{S}_0(t) \equiv 0$), the $\hat{\mathbf{x}}(t)$ estimate is unbiased and optimal if it satisfies equation

$$\dot{\hat{\mathbf{x}}} = \hat{\mathbf{A}}\hat{\mathbf{x}} + \mathbf{B}\mathbf{u} + \mathbf{K}^0(\mathbf{y} - \hat{\mathbf{C}}\hat{\mathbf{x}}); \quad \hat{\mathbf{x}}(t_0) = \bar{\mathbf{x}}_0 \tag{15}$$

with a matrix of gain factors $\mathbf{K}^0 = \mathbf{P}\mathbf{C}^T \mathbf{R}_0^{-1}$, where matrix \mathbf{P} is the solution of the Riccati equation:

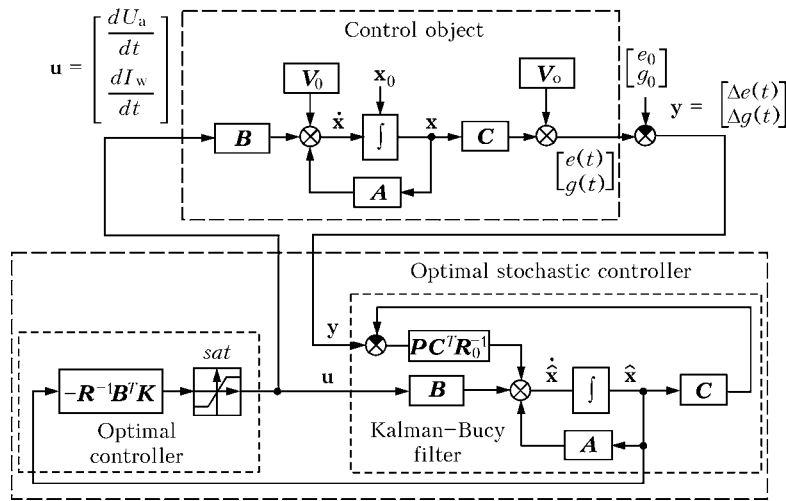


Figure 3. Structure chart of the optimal ACS model

$$P = AP + PA^T - PC^T R_0^{-1} CP + Q_0; P(t_0) = P_0. \quad (16)$$

Calculation of the stochastic optimal controller was made with the MATLAB package tools (by using function *lqry*). The resulting solution of the Riccati equation had the form of matrix **K** (14 × 14). The calculation was made by using matrices of weighting coefficients of the observation vector, **Q** (2 × 2), and control vector, **R** (2 × 2), in the following form:

$$Q = \begin{bmatrix} 5 & 0 \\ 0 & 20 \end{bmatrix}; R = \begin{bmatrix} 2 & 0 \\ 0 & 0.015 \end{bmatrix}.$$

Function *kalman* was used to calculate the Kalman-Bucy filter. Matrices of CO in the state space, matrices of coefficients of input disturbances, **V**₀ (14 × 2), matrices of variation noises, **V**_o (2 × 2), and covariance matrices of noises

$$Q_0 = \begin{bmatrix} 0.01 & 0 \\ 0 & 0.2 \end{bmatrix}; R_0 = \begin{bmatrix} 0.01 & 0 \\ 0 & 0.004 \end{bmatrix},$$

were set as input conditions.

Structure chart of the optimal ACS model (Figure 3) includes the CO model and model of the stochastic optimal controller, which consists of the optimal state controller, element of limitations of the control actions and optimal state controller, i.e. Kalman-Bucy filter. The optimal controller forms controls by way of derivative adjustment actions *U*_a and *I*_w. Vector of the optimal observer state, **x̂**, is used as feedback signals. This vector is calculated on the basis of the a priori information on control object matrices **A**, **B** and **C**, as well as allowing for current values of the vector of controls and output vector $[\Delta e(t) \Delta g(t)]^T$.

Transient characteristics of the CO model were investigated. Figure 4 shows curves of the input and output signals in formation of pulse controls with a duration of 5 s and amplitude of 1 V/s and 10 A/s, respectively. These curves simulate the signals in hypothetical ACS with LTS, which forms a light trace on the workpiece surface at distance *L*_{TV} = 70 mm from the electrode axis. A change in values of geometric parameters of the bead with some transportation lags

relative to the time point of feeding the control actions occurs in this case.

The transient and stationary processes in ACS were modelled by formation of the weld bead (Figures 5 and 6), considerable levels of noises of observation of the reinforcement width and height, equal to 0.2 and 0.05 mm, respectively, being simulated in this case. It was determined that fluctuations of output parameters insignificantly changed under the steady-state conditions, i.e. a change in fluctuations of the reinforcement width and height was no more than 0.05 and 0.02 mm, respectively. The modelling results al-

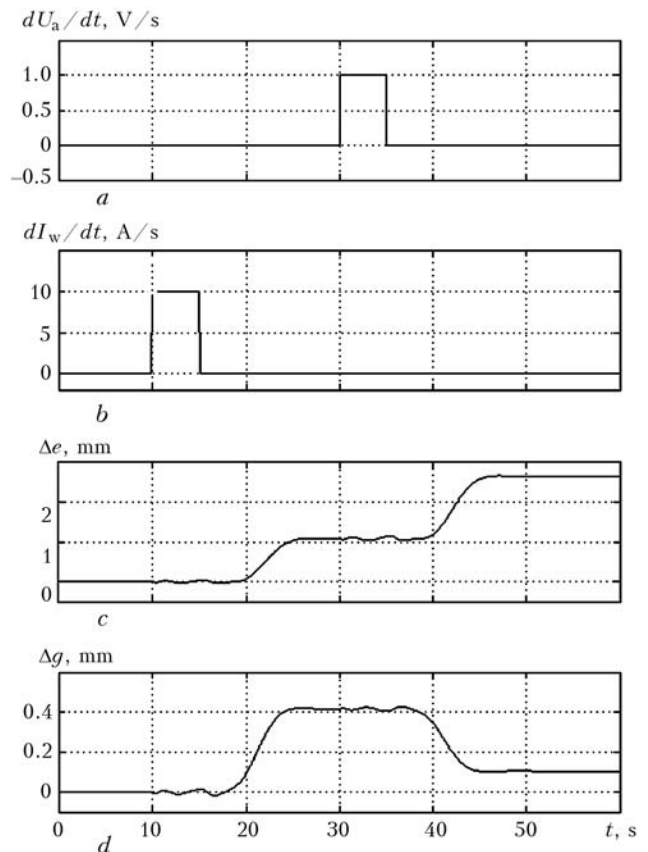


Figure 4. Transient characteristics of the dynamic control object model: a, b – voltage and welding current control actions, respectively; c, d – variations in weld width and height, respectively

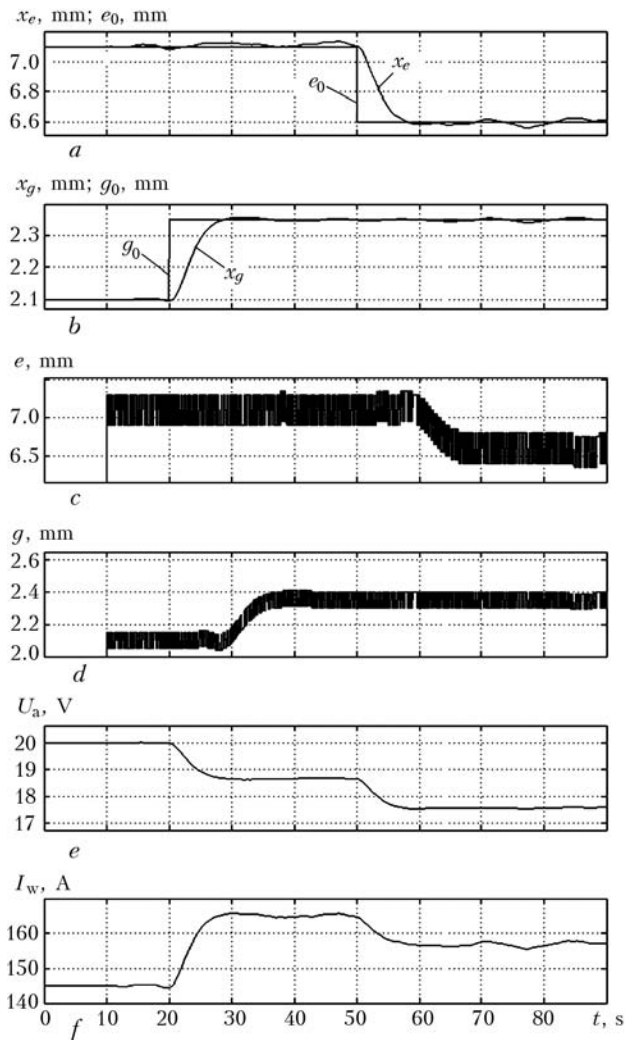


Figure 5. Curves of the transient process in optimal ACS with a change in master controls e_0 and g_0 at the 20th and 50th second: a, b – width x_e and height x_g of the bead at a current time point; c, d – signals of observation of width and height of the bead; e, f – adjustment actions

low a conclusion that developed optimal stochastic ACS with a transportation lag in the feedback loop forms an acceptable path of control of the MAG welding process. Control of the weld reinforcement formation process described by the multidimensional dynamic system provides a minimal time of the transient process (no more than 8 s) at the absence of overcontrol. According to Figure 5, the control actions start simultaneously changing with a stepwise change in the master controls at time points of 20 and 50 s, this causing movement of CO state variables x_e and x_g . The paths of changes in the controlled parameters are of an aperiodic character.

The developed optimal controller provides limitations of dynamics of the adjustment actions. As follows from Figure 6, despite the transportation lag present in CO and a substantial level of noises, the control signals do not exceed the limitation levels of 1 V/s (for dU_a/dt) and 10 A/s (for dI_w/dt).

Therefore, it is likely that the approach proposed for synthesis of optimal ACS to control the MAG welding process can be further developed towards both

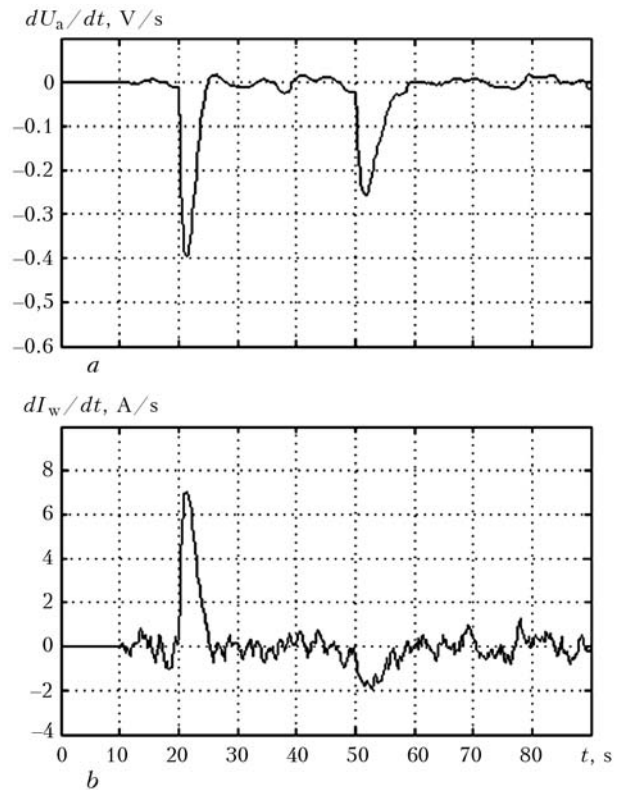


Figure 6. Curves of voltage (a) and welding current (b) signals in optimal ACS

refinement of the structure of the weld formation dynamic model and widening of the vector of control actions (e.g. adjustment of the welding speed) or observation vector (e.g. measurement of the joint gap).

1. Sergatsky, G.N., Dubovetsky, S.V. (1986) Systems for open-loop control of weld formation in arc welding. *Avtomatich. Svarka*, **6**, 37–48.
2. Razmyshlyayev, A.D. (1996) *Physical principles of bead and weld shape formation in arc surfacing and welding with control actions*: Syn. of Thesis for Dr. of Techn. Sci. Degree. Mariupol.
3. Gurevich, V.I. (1983) Dynamics of heat systems for automatic control of welding conditions. In: *Transact. on Control of Welding Processes*. Tula: TPI.
4. Trigubov, G.P., Gorbach, V.D. (2003) Optimisation of weld sizes due to adaptive control of the arc welding process. *Svarochn. Proizvodstvo*, **7**, 19–21.
5. Gladkov, E.A. (1996) Problems of quality prediction and weld formation control in welding using the neural network models. *Ibid.*, **10**, 36–41.
6. Paton, B.E., Podola, N.V., Kvachev, V.G. et al. (1971) Mathematical modelling of welding processes for development of systems for prediction of quality of the joints and optimal control. *Avtomatich. Svarka*, **7**, 1–5.
7. Kim, D.P. (2004) *Theory of automatic control: Manual*. Vol. 2: Multidimensional, nonlinear, optimal and adaptive systems. Moscow: Fizmatlit.
8. Kisilevsky, F.N., Shapovalov, E.V., Kolyada, V.A. (2006) System of laser following of weld reinforcement. *The Paton Welding J.*, **1**, 42–44.
9. Erokhin, A.A. (1973) *Fundamentals of fusion welding. Physical-chemical principles*. Moscow: Mashinostroenie.
10. Rykalin, N.N., Uglov, A.A. (1951) *Calculations of thermal processes in welding*. Moscow: Mashgiz.
11. Baker, J., Graves-Morris, P. (1986) *Pade approximations*. Moscow: Mir.
12. Perelmuter, V.M. (2008) *MATLAB extension packages. Control System Toolbox and Robust Control Toolbox*. Moscow: SOLOMON-PRESS.
13. Quakernak, H., Sivan, R. (1977) *Linear optimal control systems*. Moscow: Mir.
14. Brighson, A., Ho Yu-Shi (1972) *Applied theory of optimal control*. Moscow: Mir.

PROSPECTS OF INCREASING ENERGY CHARACTERISTICS OF FLASH BUTT WELDING (Review)

S.I. KUCHUK-YATSENKO, Yu.S. NEJLO, V.S. GAVRISH and R.V. GUSHCHIN

E.O. Paton Electric Welding Institute, NASU, Kiev, Ukraine

Developments aimed at increasing energy characteristics of flash butt welding are reviewed, and possible investigation trends in this area are analysed.

Keywords: flash butt welding, technology, equipment, power supply, direct current, alternating current, low-frequency current, secondary circuit, circuit resistance, energy characteristics

Power of the equipment used for flash butt welding (FBW) amounts to tens and hundreds of kilowatts. One of the problems of current importance is to find ways of uniformly loading the three-phase mains at a single-phase load in the welding circuit, which is characteristic of resistance heating. Non-uniform loading causes a higher drop in the distribution mains, this leading to unfavourable conditions for operation of other equipment connected to this mains. While selecting power supplies for single-phase FBW machines, producers have to orient themselves to increased phase loads and, accordingly, total capacity of a power supply.

Most standard FBW machines use the technology that provides for repeated short-time resistance heating of parts, when a load changes from zero to its limiting value, this also having a negative effect on consumers of power in the general mains.

Power factor of standard FBW machines is 0.5–0.6, and thermal efficiency is no more than 30 %. This is attributable to the fact that resistance of the welding circuit of the machines is commensurable with and, in many cases, higher than resistance in contact between the parts during heating [1, 2].

Various control systems for power circuits of FBW machines, intended for splitting the single-phase load into three phases, have been developed in the last decades [2, 3]. As to their operation principle, the power components used can be subdivided into two categories. In the first category, switching of the electric currents takes place in primary windings of a welding transformer, the decreased-frequency (5–30 Hz) current, compared with 50 Hz in the power mains, being maintained in the secondary loop of the welding circuit. In the second category, secondary windings of the welding transformer comprise rectifiers installed there to provide flow of the direct current in the welding circuit. Detailed analysis of converters of the first category is given in studies [2, 3]. Such converters find application in spot and capaci-

tor-discharge welding machines with a capacity of up to 100–150 kW.

The first frequency and phase converter for FBW was developed by the E.O. Paton Electric Welding Institute in the early 1960s [4]. Later on, similar converters were developed by other companies, e.g. «Sciaky». The converter (Figure 1) consists of six thyristors (the first machines used ignitrons).

High-power machines for spot and projection welding still use this type of the «Sciaky» low-frequency converters. Their utilisation for butt welding was limited to production of single specimens and did not receive further development. This was caused, first of all, by substantial complication of design of a low-frequency welding transformer, considerable increase in its weight, dimensions and, hence, cost.

New generations of high-power FBW machines supplied by leading manufacturers of this equipment in the last decade have used converters of the second

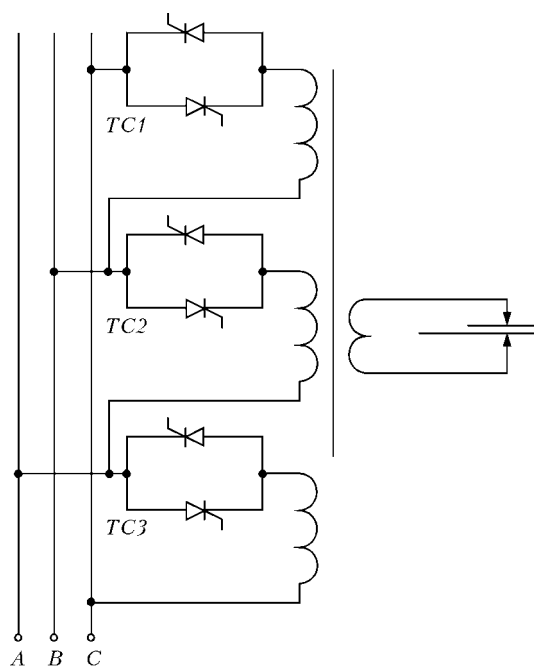


Figure 1. Circuit of frequency converter with four-winding transformer (TC1–TC3 – thyristor contactors)

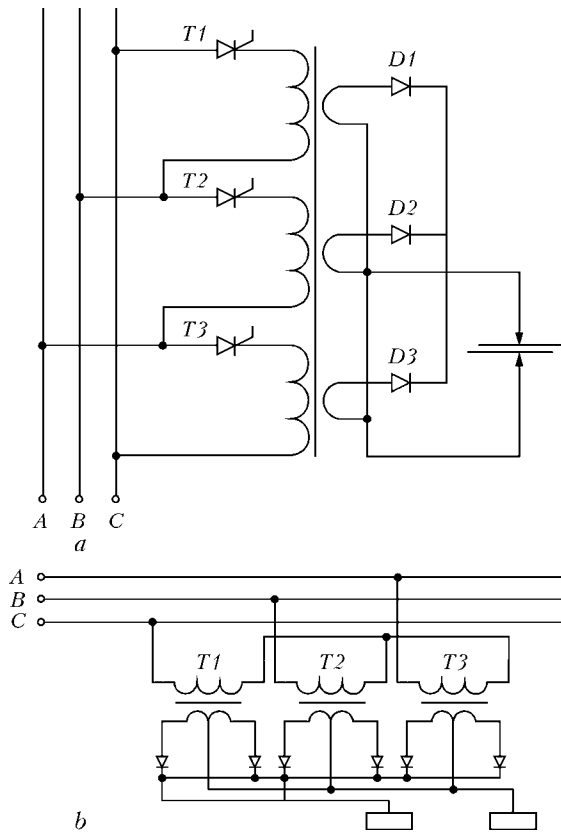


Figure 2. Circuits of three- (a) and six-phase (b) rectifiers ($T1-T3$ – thyristors, $D1-D3$ – diodes)

category, which provide for rectification of the current in the secondary circuit.

Figure 2 shows circuits of the three- and six-phase rectifiers used in modern FBW machines.

Separate transformers with delta or star connection of their primary windings are used most frequently. The primary winding circuit comprises thyristor contactors, which allow adjustment of voltage supplied to the transformer. One- and two-arm rectifiers are included into each circuit of secondary windings of the transformers, the secondary windings being star connected. Physically, a rectifier is a single module. Transformers and rectifying cells have a cooling system. The rectified welding current is practically of the direct type, pulsation factor for the three-phase star rectifier is 25 %, and for the six-phase star rectifier

is 5.7 %. Six-phase rectifiers with a delta connection of the primary windings are mainly used for the high-power FBW machines. In the last years, companies «Roman Transformer», «Safco System s.r.l.» and «Dalex Schweisstechnik» have been supplying the above types of the modules for currents of 17 to 100 kA. Emergence of such systems on the world market has substantially widened potentialities for development of new generations of specialised and versatile FBW equipment for different industrial sectors. Application of DC converters allows solving the problem of uniform loading of the mains when using high-power FBW machines, and increasing the efficiency of their utilisation. Moreover, this leads to increase in power factor of such equipment because of decrease in reactive losses in the secondary loop of the welding circuit. Along with the noted advantages, in general the use of the direct current did not allow the total consumed power in the welding circuit to be considerably decreased, compared to the similar indicators with a power supplied from the 50 Hz mains. This is attributable to the fact that in resistance heating of heavy-section parts (5,000–10,000 mm²) a voltage drop in contact between the parts is 1.5–2.0 V. The voltage drop at modern silicon rectifying cells is approximately the same, and losses of power in the cells are commensurable with the power consumed for welding. In welding of aluminium parts the power losses are even higher. Therefore, the thermal efficiency of the resistance heating process at the direct current is lower than in the case of using the first group of the converters, e.g. low-frequency converters [4]. The Table gives technical characteristics of some modern machines for FBW of rails. They use high-power rectifiers, allowing the currents of 50–100 kA to be provided in the secondary circuit. To compare, the Table also gives similar characteristics of the machines designed for a single-phase load.

At an identical productivity and power of the welding machines, machines with a three-phase load have a power distributed into three phases. As a result, their installed power decreases three times.

Judging from the experience of operation of such equipment, utilisation of the direct current provides a number of advantages, in addition to improvement

Technical characteristics of «Schlatter» machines for DC and AC FBW of rails

Type of machine	Maximal cross section to be welded S , mm ²	Rated power of welding machine P_r , kV·A	Short-circuit power of welding machine P_{max} , kV·A	Maximal secondary current I_{2max} , kA
Direct current				
GAAS-80	12000	580	630	80
GAAS-100	20000	580	630	100
Alternating current				
Aa 50/500u	10000	500	1500	90
Aa 50/450s	10000	450	1300	80
Aa 35/400s	8000	400	1000	70
BHVR 43/120	6000	450	–	–



of power indicators. In particular, as noted in promotion materials [5], the use of the direct current provides a more uniform heating of parts over their entire cross section.

The data given apply to the welding technologies at which the main heating of parts is provided by resistance at short-circuits from the ends.

The possibilities of further increasing the thermal efficiency and decreasing the consumed power through using these technologies have been exhausted to a considerable degree, at least for the systems that use modern semiconductor rectifying cells. A more radical improvement of these characteristics is likely if methods are found for increasing the efficiency of resistance heating providing for increase in contact resistance $R_{sh.c}$ or decrease in $Z_{sh.c}$ of the welding circuit.

In the last decades the E.O. Paton Electric Welding Institute has developed several generations of the machines for FBW of parts from different steels and aluminium-, titanium- and chromium-base alloys with a cross section area of up to 100,000 mm² or more. They are characterised by a relatively low specific power consumption (15 W/mm²), high power factor (0.80–0.95) and high thermal efficiency (60–70 %). Design of the machines and control systems is based on the technology of continuous FBW with program control of main process parameters. Modifications of this technology, called pulsed FBW, have found commercial application in the last years [6]. Along with high productivity, the technology provides a considerable decrease (2–3 times) in power consumption, compared to the machines that use the welding technology with resistance heating. First of all, this is explained by the possibility of achieving a highly concentrated heating through automatic control of resistance in contact between the parts welded, $R_{sh.c}$, at a level of $R_{sh.c} \geq Z_{sh.c}$. Implementation of the continuous flashing process requires that the $Z_{sh.c}$ value be decreased 2–3 times, and in specialised machines – more than 10 times, which can be achieved owing to a special design of the welding circuit. Although such machines do not provide three-phase loading of the mains, their power in phase is lower than that of conventional machines with three-phase loading. As most of such machines are made particularly for welding certain parts (pipes, rails), they have individual power supplies (mobile electric stations), when requirements for three-phase loading are not that important. In a number of cases the continuous FBW technologies are used to advantage with versatile butt welding machines, where it is difficult to make substantial reconstruction of the secondary loop. Very effective was re-equipment of versatile standard single-phase rail welding machine MSGU-500 by using a low-frequency and phase converters. Utilisation of the 5 Hz frequency in the secondary loop allowed decreasing its resistance from 280 to 120 μ Ohm. This made it possible to decrease the voltage required to excite continuous flashing in welding of heavy types of rails from 11.5 to 6.26 V [4]. Application of the

continuous FBW technology in this case provided a 2.5 times decrease in power consumption, and 1.5–2 times reduction in welding time and power input.

Considering prospects for further improvement of this equipment, it seems reasonable to develop the first category of the converters designed for medium frequencies of up to 30 Hz, along with finding rational designs of the secondary loop to minimise its resistance.

Using the direct current for continuous FBW allows expecting improvement of energy indicators of the welding process, as an average value of $R_{sh.c}$ in flashing is higher than in resistance heating. This deteriorates operation of the rectifying cells requiring synchronisation of loads. The world practice does not know so far any examples of commercial application of the machines with the DC converters for continuous FBW of heavy-section parts. Experiments on DC welding of plates and thin-walled pipes of heating surfaces 30–50 m in diameter were conducted under laboratory conditions [7, 8]. Resistance in contact between the parts in FBW is higher than in short circuits, which are characteristic of resistance heating. So, it may be expected that relative losses of power in rectifying cells will be lower. In this case it is difficult to determine their values, as resistance in contact during flashing gradually varies from values close to the short-circuit ones to complete breaking of the circuit. It is noted that mostly fine contacts form at the direct current. In this case the process is more stable than at the alternating current, and the flashed surface is smoother. As a result, sound joints can be provided at flash and upset allowances that are lower than 20 %. In general, the authors of the study came to a conclusion that transition to the direct current in FBW of the said parts would give the same technological advantages as decrease in $Z_{sh.c}$ of the machines by reconstructing their welding circuit at 50 Hz, which is less expensive.

The sinusoidal wave form of the voltage supplied to the parts welded is not optimal, because the efficient heating of elementary electric contacts occurs only in the amplitude portion of a sinusoid, the duration of which during a half-period is insignificant.

It is reported that abroad such drawbacks of FBW are eliminated by using inverter power supplies, which consist of a rectifier and inverter. The rectifier provides uniform loading of all three phases of the power supplier and converts the three-phase voltage into the single-phase one, while the inverter converts the single-phase direct voltage into the single-phase alternating one, having a square wave form. Moreover, the presence of the inverter in a new power supply is attributed to the fact that to provide the direct current flashing process it is difficult to solve the problem of commutation of the high direct current power, whereas the square wave form of the voltage is caused primarily by a difficulty of providing the sinusoidal form of the voltage at the inverter output. Study [6] gives data on development and testing of a pilot sample



of the inverter power unit. As follows from the data, the highest energy indicators in FBW can be obtained with the machines having a sufficiently low resistance of $Z_{sh.c} \leq 100 \mu\Omega$ by using the phase converter in the primary circuit of transformers. Converters designed for frequencies of 20–30 Hz are also used for FBW and provide uniform loading of the mains. Furthermore, standard transformers of FBW machines can be used in this case. While considering the FBW progress trends, it is necessary to account also for the possibility of using this process for highly concentrated heating in solid-state resistance welding. Machines that use the stored energy, and most often these are the capacitor-discharge spot welding machines, are characterised by the most efficient utilisation of energy in welding. At low charging powers, such energy storages generate the currents during welding that are dozens and hundred of times higher than the charging currents. For example, spot welding of aluminium alloys 1.5 + 1.5 mm thick can be performed with AC machine MT-4019 and capacitor-discharge machine MTK-5502. Electrode extension is identical in both cases. The power consumed from the mains by machine MT-4019 will be 300 kV·A, and by machine MTK-5502 – 20 kV·A [3]. The time of welding with the capacitor-discharge machines is tens of milliseconds.

In FBW of parts with a relatively small cross section area (up to 1000 mm²), the duration of heating is tens of seconds. Building of capacitor-discharge storages for such loads seems economically inexpedient, if we orient ourselves to technical characteristics of standard modern capacitors. Considering continuous development efforts in this area, emergence of such converters in the nearest future is highly possible.

Ionistors, which are also called supercapacitors (SC), are electric devices characterised by an enormous output capacity achieved within a very short period of time. Owing to this capacity, they have received wide acceptance in many fields of electronics and electrical engineering. The latest changes made in their design, as well as new achievements in the production technology make them ones of the most promising electronic devices [9]. SC are superior to other types of capacitors in density of capacitance ρ_C , charge ρ_Q and energy ρ_E . SC can provide operation of different systems at increased pulse current loads. That is why in a number of cases they replace chemical current sources. SC are characterised by a unique combination of important characteristics. Compared to lithium elements, advantages of SC include an order of magnitude higher power density ρ_W , long shelf life

(about 10 years), absence of toxic and hazardous components, and a large number of re-charging cycles with no change in capacitance (up to 10 million cycles). Capacitance of modern SC and batteries on their base is 1–10,000 F [10]. Characteristics of SC allow using them as energy storages, e.g. uninterruptible power supplies (UPS), components of pulse power devices, and in other instruments requiring fast energy sources [9]. Widening of their application can be accelerated by finding more perfect processes of contact resistance heating. The E.O. Paton Electric Welding Institute completed investigations [10] that showed the possibility of resistance welding of parts with compact and developed cross sections of 2,000–3,000 mm² using a highly concentrated heating. Increase in heating concentration is achieved owing to the use of intermediate inserts having a composite structure. The heating duration in this case was 1.5–2.0 s, and current density – 1.5–2.0 A/mm². This process can be implemented by using not only capacitor-type energy storages, but also other storages of the energy, e.g. kinetic energy in mechanical converters.

In this connection, of interest are the long-time development efforts [7] in the field of a unipolar generator to power the machines for FBW of pipes, the idea of building of which was a subject of many discussions [8]. Here the point is that the unipolar generator designed for low voltage is built into the secondary circuit of the welding machine (Figure 3) instead of a transformer.

Special current conductors feed currents amounting to hundreds of thousands of amperes from a generator collector directly to electrodes of the welding machine, which makes it possible to minimise losses in the secondary loop. Electric motor *EM* of a drive of generator *G* is built into the generator stator casing, which excludes intermediate elements in kinematics of the drive experiencing considerable peak loads. Big mass and sizes of rotating elements of the drive at high rotation speeds provide storing of the substantial kinetic energy in the generator that is consumed for welding. This provides a uniform loading of three phases of the mains, and power of the drive can be decreased tens of times compared to the peak one consumed in welding. This source can be efficiently utilised in repeated short-time operation of the welding machine, where pauses between welding cycles are sufficiently long to restore the required level of the stored energy.

Many years' developments [11] aimed at building different-power unipolar generators were accompanied by looking for optimal technologies for resistance heating of parts with big cross section areas (up to 12,000 mm²), including the pipes. They were concluded with manufacture of a commercial batch of the systems comprising generators of the machines for welding of pipes with a diameter of 80–320 mm and wall thickness of 8–12 mm [11]. Different-power welding machines use 10–60 MJ energy storages, this allowing the 1.5–9.0 MA currents to be produced in

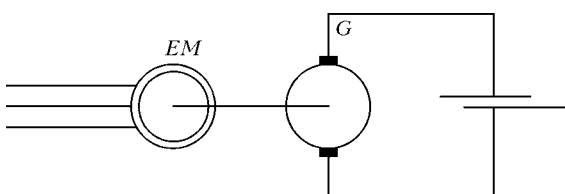


Figure 3. Unipolar generator scheme

the welding circuit. The heating duration in welding is no more than 3 s, and power consumed from mains of the electric drive is 230–420 kW. Application of high-rate high-concentration heating at current densities of 50–60 A/mm² made it possible to produce the high-quality joints on 80–320 mm diameter pipes with wall thickness of 8–12 mm, made from X65 type steels and steels of the austenitic and martensitic grades belonging to the hard-to-weld ones. Along with high strength values, the joints exhibited the high properties in impact toughness tests.

Further improvement of this type of energy storages creates conditions for widening of the application fields for the FBW technologies, especially for hard-to-weld materials.

As noted for the machines for FBW of 114–320 mm diameter pipes, utilisation of a power supply with square wave pulses and frequency of 50 Hz provides a 25 % reduction in the welding time [6].

1. Kuchuk-Yatsenko, S.I. (1992) *Flash butt welding*. Kiev: Naukova Dumka.
2. Paton, B.E., Lebedev, V.K. (1969) *Electric equipment for flash butt welding*. Moscow: Mashinostroenie.
3. Smirnov, V.V. (2000) *Equipment for flash butt welding*. St.-Petersburg: Energoatomizdat.
4. Podola, N.V., Kuchuk-Yatsenko, S.I. (1957) Low-frequency current flash butt welding. *Avtomatich. Svarka*, **1**, 63–72.
5. (1985) *Catalogue of Schlatter Company*. Prosp. 2. Schlatter AG.
6. Khomenko, V.I., Pankov, O.G., Sergeev, S.K. et al. (1991) Application of inverter power supplies for flash butt welding in construction of pipelines. *Svarochm. Proizvodstvo*, **9**, 16–17.
7. Bertinov, A.I., Alievsky, B.L., Troitsky, S.R. (1966) *Unipolar electric machines with liquid metal current pickup*. Ed. by A.I. Bertinov. Moscow; Leningrad: Energiya.
8. Haase, P.W., Carries, R.W., Hudson, R.S. (1995) The University of Texas at Austin, Center for Electromechanics. Homopolar pulsed welding for offshore deep water pipelines. *Welding J.*, **5**, 35–39.
9. Shurygina, V. (2003) Supercapacitors. *Elektronika, Nauka, Tekhnologiya, Biznes*, **3**.
10. Despotuli, A.L., Andreeva, A.V. (2006) Supercapacitors for electronics. *Sovrem. Elektronika*, **5**, 10–14.
11. James, C., Wright, P.E. (1999) *Homopolar pulsed welding for pipeline application*: Report of Int. Symp. on Exploiting Solid State Joining. Cambridge.

PORTABLE SYSTEM OF MONITORING AND CONTROL OF RESISTANCE SPOT WELDING PROCESS

P.M. RUDENKO and V.S. GAVRISH

E.O. Paton Electric Welding Institute, NASU, Kiev, Ukraine

The paper presents the schematic diagram and operative algorithm of system of quality control of welded joints made by resistance spot welding, based on a pocket PC. In addition to real-time quality control, the system also implements functions of expert system for technology selection and production analysis.

Keywords: *resistance spot welding, welded joints, quality control, process control, weld spot nugget diameter, expert system, pocket PC*

The quality of resistance spot welding depends on many factors, mainly on the selected technology, applied equipment and automatic control of process in real time.

A lot of stationary and pocket devices, systems, based on the office and industrial PCs and laptops, designed for control of process of resistance spot and seam welding is known.

These devices and systems allow investigation of process of welding the new and well-known materials and structures, automation of selection of welding condition and its optimization, presetting and verification of acceptable limits of variables of condition parameters, welding quality control in real time. With their use it is possible to perform accumulation, statistical processing and analysis of data, certification of production, calibration of sensors, to realize the technical maintenance of welding machines and electrodes.

As an example of resistance spot welding control systems it is possible to mention the wide nomenclature of devices of Miyachi Uniteck [1], monitors of WeldCom-

puter Corp., ATek Resistance Welding and Dengensha America (USA), pocket tester of TECNA (Italy) [2], measuring systems of VNIIESO (Russia) [3].

The E.O. Paton Electric Welding Institute has also developed the series of devices for monitoring and diagnostics of process (UDK-01 -02, -05) [4] and welding condition control systems with wide package of functions on control of condition parameters and quality of a welded joint (RVK-100, KSU KS-02) [5, 6].

The above-mentioned devices on controllable parameters are differed negligibly. This is in general the welding current or current in primary winding of welding transformer, voltage between electrodes, pressure or compression force of electrodes, movement of electrodes and time of optimizing operations in cyclogram. However they can considerably differ in technical realization. For instance, the series of Miyachi Uniteck includes stationary MG3, MM-370 (of 5 kg weight) with a graphical display, more compact MM-122A (1.9 kg) with possibility of connection to outer PC (e.g. laptop) and printing device, so-called palm MM-380 (0.9 kg) and, finally, pocket devices for measuring of current parameters (MM-315A) and compression forces (MM-601A). At the same time the monitors WeldComputer Corp. are similar to industrial working stations with a full-scale graphical screen with

options of working as a local, remote or net device, controlling several welding machines.

The E.O. Paton Electric Welding Institute has developed an expert system for resistance spot welding [7] which, basing on databases and experience, gives recommendations on technology of welding of products with a preset thickness of parts, condition of their surface, peculiarities of design and grade of material. To increase competitiveness it is desirable to develop control devices with functions of expert system. Besides the work of reference system there is also option of the most efficient method of evaluation of quality for considered product and automatic switching of a device to a required monitoring mode.

The UDK devices were developed on the basis of the industrial controllers. The realization of algorithms in them, similar to expert systems is impossible due to a limited memory capacity for storage of software and data. The data output displays have limited possibilities as to volume of produced textual and graphic information. Nevertheless, the full output of information is very important and its absence results in limitation of possibilities of expert systems. Meantime, the devices of monitoring and control are complex computer devices and their small-batch production leads to a high cost.

Nowadays, the mobile computer computing means with screens from 3–4 inches to represent textual and graphic information, such as the pocket PCs, smartphones, communicators, netbooks and laptops find a wide application in everyday life (entertainment, organizing of working day, text translation, GPS, health control and other). Their technical characteristics in providing output of information about welding process parameters from the welding machine can successfully replace the above-mentioned devices and, moreover, obtain additional advantages by realizing required functions of expert system.

The purpose of the work is the development of a portable computer system where functions of expert system and those of welding process monitoring, typical of specialized devices, are realised simultaneously. Moreover, the system should maximum apply the widely spread serial equipment of high reliability, low cost and can be adopted for the application under the conditions of welding shop.

One of the basic tasks at the design of such system is the development of equipment and software to interface the mobile computers with sensors of process parameters.

To interface the resistance spot machine with universal mobile computer devices, the E.O. Paton Electric Welding Institute has developed a system KSU KS-03 of monitoring the spot welding process parameters, designed for measuring process parameters and transfer of these data to the computer of upper level. The unit is developed on the basis of a single-crystal controller C8051 F020 of company «Silicon Laboratory», the main advantage of which is presence of necessary resources for design of measuring system: 12-charge 8-channel ADC of efficiency of up to 100 K measurements per 1 s and input amplifier with a programmable amplification factor at high productivity as to calculations and control. The schematic diagram of the system is given in Figure 1.

Technical characteristics of measuring unit

Range of welding current measurement, kA	2–25 4–50
Range of voltage measurement between electrodes, V	0–5
Range of measurement of compression force of electrodes, kN	0–10; 0–20
Range of measurement of acceleration of electrodes movement, <i>g</i>	±1.7
Given error in parameters measurement, %	not more than 3
Speed of data transfer on the radio channel, Kbit/s	19.2–115.2
Mains voltage, V	220–380
Dimensions, mm	260 × 220 × 160

The main distinction of the unit from control devices is the presence of one of two communication channels, which are available practically in all portable computers, USB and Bluetooth. In the first case exchange speed is 921.6 Kbit/s, in the second Bluetooth the adapter operates in the mode of series channel RS232 and maximal speed of transfer is 115.2 Kbit/s. Although radiochannel has a lower speed, its application can be more preferable as it does not need the wire communication between the devices, the distance between receiver and transmitter can be up to 100 m excluding high voltages at the input of computer system, the connection is simple.

In capacity of base package the unit consists of the following sensors: a Rogowski belt of a split type of manufacture of the Engineering Pressure Welding Centre of the E.O. Paton Electric Welding Institute; sensor of compression force MEGATRON KMB 31K 10KN 0000D; acceleration sensor ANALOG DEVICE ADXL 103.

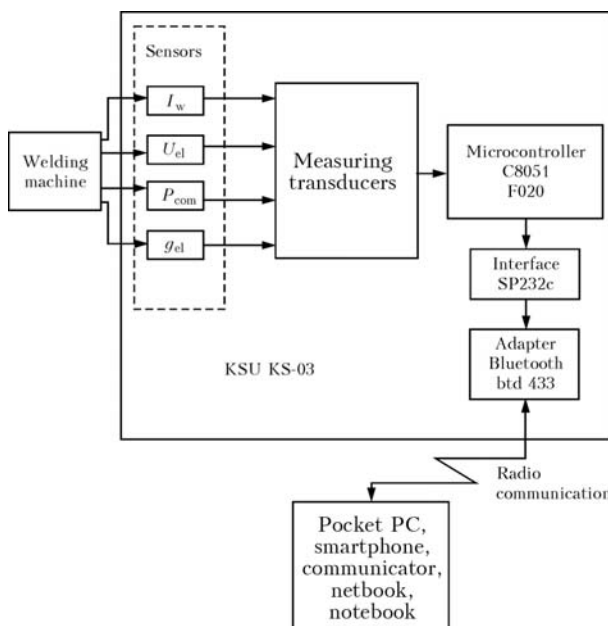


Figure 1. Schematic diagram of control system of resistance spot welding

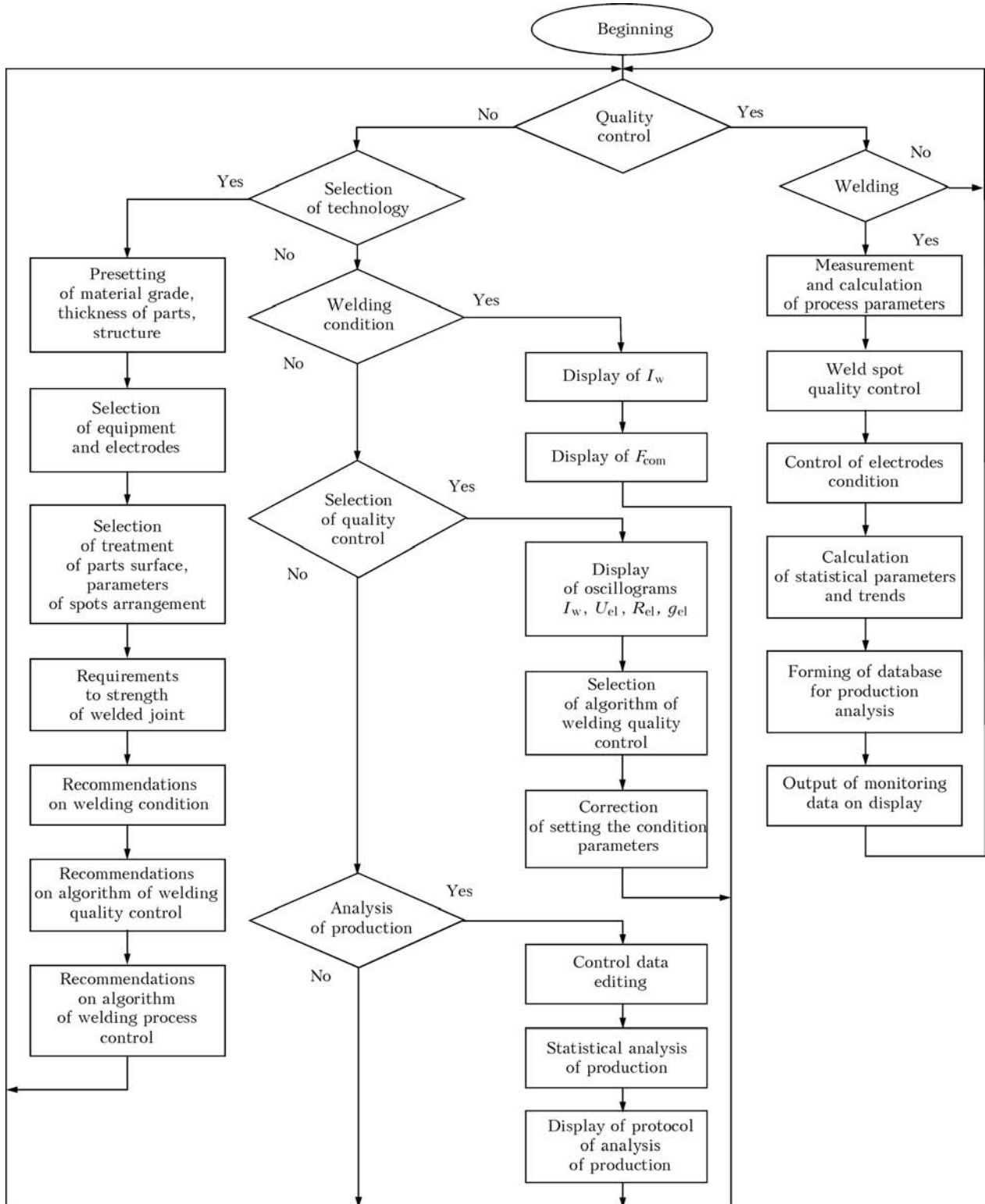


Figure 2. Algorithm of monitoring system operation

Besides there is a pair of measuring conductors with special terminals to measure voltage between electrodes.

Current sensor is flexible and split and has 150 mm diameter, sensitivity of 1 V/s/kA, current measuring error does not depend on position of the sensor. The sensor of compression force is manufactured of high-quality steel, the working temperature range is $-10 -$

$+40$ °C, variant IP66. The acceleration sensor is uniaxial, sensitivity of 1 V/g, zero shift at 0 g is 2.5 V.

Measuring sensor transducers are also included into the unit. In the package with a sensor of compression force the measuring transducer MEGATRON IMA 3-DMS-2405 is used. The measuring transducer of voltage sensor eliminates interference brought by welding current and allows measuring of signal di-

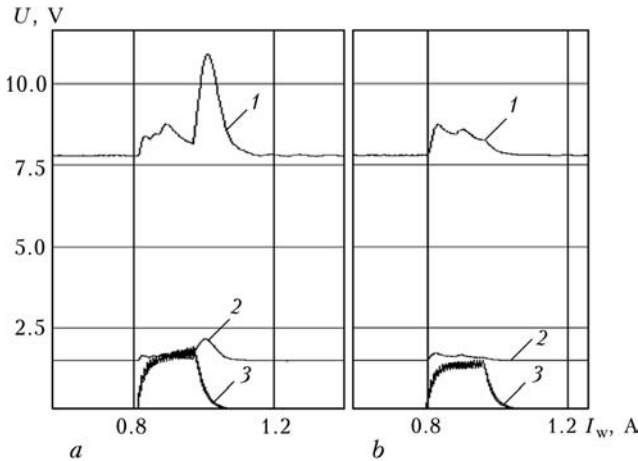


Figure 3. Oscillogram of signals from outputs of measuring transducers of accelerometer 1 and current 3 during splash (a) and without it (b) (2 – signal at the output of accelerometer)

rectly on the electrodes with laying of measuring circuits along the welding circuit.

The algorithm of monitoring system operation is given in Figure 2.

During the monitoring of technological process the control unit at a period of 10 ms issues integral values of a current, voltage, forces of compression and acceleration of electrodes for the computer of upper level to calculate input values of algorithm of quality control and stability of production:

- input parameters of tolerance control: current, voltage, displacement and resistance in the last period of welding, relative variation of resistance, integral error evaluations in correction of curves of current,

voltage, displacement (the sum of absolute values of deviation of current values relative to reference curves);

- input parameters of regression model: energy Q , generated in welding contact;
- input parameters of neuron network: average values of current and voltage at four sequential and possibly equal intervals which in sum are equal to time of welding.

During the tolerance control of quality the algorithms are used based on the fuzzy logics [8].

The monitoring of diameter of weld spot nugget according to regression equations was performed using following expression:

$$d = a_0 + a_1Q + a_2Q^2,$$

where a_0, a_1, a_2 are the coefficients of equation.

During the monitoring of welding quality according to the neuron networks the dependencies, given in the work [9], were used.

To monitor the splash, the indications of the accelerometer are used (Figure 3), which is mounted on electrode holder. Here, the time of its occurrence is taken into account: splash at the beginning of welding is not admissible and can indicate an insufficient force of compression of electrodes, non-quality preparation of surface of parts being welded or wear of the working surface of electrodes. In any of these cases it is necessary to interrupt the welding of workpiece and to detect the cause of instable process. At the same time the splash at the end of welding is not a rejection feature in many cases.

According to obtained value of weld spot nugget diameter the following values are further calculated: average value, mean square deviation, and also sliding average value and sliding mean square deviation which can help in determination of undesirable tendencies in welding quality. For clearness, except of data about welding quality the data, plots and histograms on the whole file and sliding average values are shown on display.

There is a possibility to reset data on the last point to exclude them from general evaluation, to reset the



Figure 4. Data on welding technology on pocket PC display

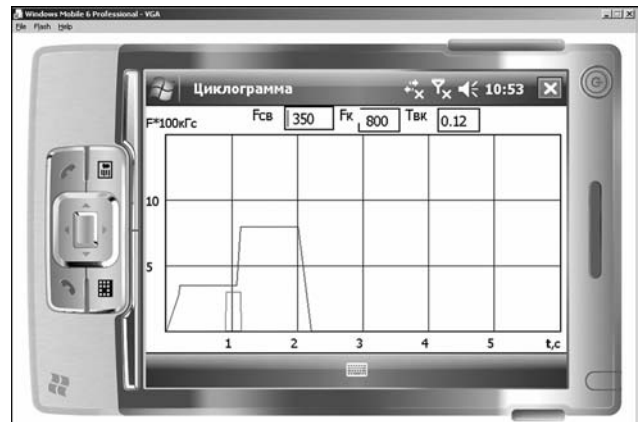


Figure 5. Cyclogram of compression force of electrodes on pocket PC display

whole database or to store it in the computer memory in the form a separate file for the further analysis.

The selection of welding technology, adjusting of parameters of algorithm of quality control and statistic analysis of production are performed in a dialogue mode.

The recommendations on selection of welding condition and equipment are issued on pocket PC display on the basis of the preset grade of material, thickness of parts, structure, method of surface treatment and also requirements specified to the quality of welding (Figure 4).

To measure the cyclogram parameters of compression force, it is necessary to optimize the preset condition with a switched welding current at the compression force sensor fixed between the electrodes. In this case the duration of current and its time in general cyclogram are determined by the sensor of voltage between electrodes (Figure 5).

In the process of welding of a workpiece or specimens during selection of the condition the values of current in the last period I_1 , average current in the time of welding I_{av} and durability of current T_w are measured. For mentioned values the average values, mean-square and maximal relative deviations for mentioned values are calculated and shown on the display. Here, the database for calculation of these values in any time of tests can be reset to zero values or completely or only on the last point.

During statistical analysis of production any file of control of welding process can be selected from the memory of device. Usually one file corresponds to the operation of welding machine within a day and its name is chosen by the date of its creation (day, month, year). A protocol as a document of a programme Mi-

crosoft WORD is formed of it, where quantity of welded spots, data on welding quality, data on errors of reproduction of controllable parameters, recommendations on cleaning and change of electrodes are indicated. The histograms of controllable parameters can be produced on the display and compared with their similar histograms at selection of the condition.

Thus, the developed system of monitoring and control of resistance spot welding process on the basis of the modern devices of computer engineering widens greatly the possibilities of control, increases its validity and provides the required quality of welded joints.

1. (2007) *Miyachi Uniteck 991-041 03/07*: Resistance welding. Weld checkers. Spirit of innovation.
2. (2007) *TECNA*. Test and measurement instruments. 1000-10/2007.
3. Ioffe, Yu.E. (2006) System for control and monitoring of resistance welding. In: *Proc. of 3rd Int. Sci.-Pract. Seminar on Resistance Welding and Other Types of Pressure Welding, Technologies and Equipment* (13-15 June 2006, St.-Petersburg). St.-Petersburg.
4. Podola, N.V., Gavrish, V.S., Rudenko, P.M. (1994) Computer diagnostics of resistance welding. *Avtomatich. Svarka*, **7/8**, 32-35.
5. Podola, N.V., Rudenko, P.M., Gejts, V.I. et al. (1991) Computer system of RVK-100 type for control of resistance spot welding machine. *Ibid.*, **7**, 61-68.
6. Rudenko, P.M., Gavrish, V.S. (2007) KSU KS 02 system for automatic control and monitoring of resistance spot welding process. *The Paton Welding J.*, **11**, 34-36.
7. Gavrish, V.S., Rudenko, P.M., Podola, N.V. (2007) System of automatic control and monitoring of resistance spot welding. *Ibid.*, **9**, 45-48.
8. Podola, N.V., Rudenko, P.M., Gorun, N.P. et al. (1999) Quality control of resistance welding of accumulator element-to-element joints on the base of fuzzy logic. *Avtomatich. Svarka*, **5**, 42-45.
9. Podola, N.V., Rudenko, P.M., Gavrish, V.S. (1991) Application of adaptive algorithm for welding quality control in control systems of resistance spot machines. *Ibid.*, **7**, 61-68.

MEASURING SYSTEM FOR DETERMINATION OF RESIDUAL STRESSES IN ELEMENTS OF STRUCTURES USING THE ESPI METHOD



At the E.O. Paton Electric Welding Institute a compact measuring system and technology for determination of residual stresses, occurring in welded, brazed, cast and other metallic structures, have been developed. The developed system and technology can be also used for determination of stresses, caused in structures by applying the loads.

Residual stresses are determined on the basis of data about the value of in-plane displacements, measured by the method of electron speckle-interferometry in the vicinity of a blind hole. The in-plane displacements are the result of an elastic unloading of residual stresses after drilling of a blind hole.

The accuracy of determination of residual stresses is 10 % of value of yield strength of the material examined.

The measuring system consists of speckle-interferometer 1, CCD-camera 2, light guide 3, laser 4, computer with a board of pattern interference fringes figuring 5.

Proposals for co-operation. Measurement of residual stresses in elements of metallic structures, parts and sub-assemblies of machines. Manufacture of the measuring system and its delivery to the Customer, training of personnel.

Contacts: Prof. Lobanov L.M.
Tel.: (38044) 289 95 78



TECHNOLOGY FOR WIDE-LAYER HARD-FACING OF CRANKSHAFTS

A.P. ZHUDRA, S.Yu. KRIVCHIKOV and V.V. PETROV
E.O. Paton Electric Welding Institute, NASU, Kiev, Ukraine

Results of experimental investigations of the effect of wide-layer hard-facing parameters on characteristics of the deposited layer are presented. Optimal ranges of variations of the process parameters in hard-facing of cylindrical parts 180–300 mm in diameter were determined. Application of the investigation results to development of the technology for repair of large-size diesel generator crankshafts is shown.

Keywords: wide-layer arc hard-facing, large-size crankshafts, self-shielding flux-cored wire, optimisation of hard-facing parameters, hard-facing technology

Large-size crankshafts (crankshafts of main gas pipeline compressors, diesel generators, marine and diesel locomotive engines, etc.) are metal-consuming parts with weight of up to 6 t and length of about 6 m. Average price of such a crankshaft is US \$ 70,000. Physically, a crankshaft is a crank made from medium-carbon steel and consisting of two groups of cylindrical journals, i.e. rod and main ones. The rod group consists of up to eight journals, and the main group — up to ten journals, their diameter being 180–280 mm.

Key parameters of the loads that determine service life of a crankshaft are high contact pressure at interfaces between the journal and bushing in friction, and quantity of alternating loading cycles. They lead to wear out of working surfaces and decrease in nominal diameters of the rod and main journals. In turn, a change in geometric parameters of the interfaces in friction leads to occurrence of an emergency situation: violation of lubrication of the friction interfaces, creation of «dry» friction conditions, «seizure» and burning out of bushings that interface the journals. Therefore, a crankshaft that spent about 30 % of its design safety factor for strength may fail because of an insignificant wear ranging from 1.5 to 2.5 mm, depending upon its operational conditions and real service life.

Hard-facing on a helical line by the submerged- or open-arc welding method is used to repair large-diameter cylindrical parts with a substantial wear (over 5 mm). If wear is less than 3 mm, it is recommended to apply wide-layer hard-facing by using a self-shielding flux-cored wire, the productivity of which is 1.8–2 times higher than that of the helical hard-facing process. Moreover, wide-layer hard-facing is characterised by a favourable thermal cycle (self-heating of a workpiece treated)*, which is very important for improving crack resistance of hardening steels in hard-facing.

Figure 1 shows the flow diagram of wide-layer hard-facing of a cylindrical surface by using a self-

shielding flux-cored wire. In hard-facing, rotation of a workpiece with diameter D occurs at welding speed v_w . The flux-cored wire (electrode) is fed to the melting zone at speed $v_{w,f}$, and, at the same time, it makes reciprocal movements (oscillations) to width B of the surface treated (oscillation amplitude or range) at preset radius r and oscillation speed v_o . A deposited layer forms on the workpiece surface during welding and gradual solidification of the weld pool. Welding cycle time t_w corresponds to the time of one revolution of the workpiece. Apparently, parameters of wide-layer hard-facing affect thickness of the deposited layer, δ , and quality of its formation. In this case, optimisation of the wide-layer hard-facing process is often hampered by a big quantity of the process parameters and the probability of their variations over wide ranges.

The purpose of this study was to experimentally investigate the effect of individual parameters of the wide-layer hard-facing process on characteristics of the deposited layer, as well as determine the optimal ranges of their variations in hard-facing of cylindrical parts 180–300 mm in diameter.

Experimental welding runs were performed at a direct current of reversed polarity on samples of steel St3, the geometric dimensions of which corresponded to those of the rod and main journals of large-size crankshafts. 2 mm diameter self-shielding flux-cored wire PP-Np-30Kh4G2SM, which gave good results in hard-facing of steel crankshafts, was used as an electrode material.

Average thickness δ of the deposited layer and quality of its formation are the key characteristics used as a basis to choose such wide-layer welding process parameters as I_w , U_a , v_w , $v_{w,f}$, v_o , electrode extension l_e , and electrode displacement from zenith, e . The following formula can be used to set the δ value (with machining allowance taken into account):

$$\delta = (1.0 - 1.2)(W + 0.5A),$$

where W is the wear or thickness of the deposited layer, mm; A is the machining allowance for diameter, mm; and 1.0–1.2 is the coefficient that accounts for

* Krivchikov, S.Yu., Zhudra, A.P., Petrov, V.V. (1998) Thermal cycle in wide-layer hard-facing of cylindrical cast iron parts. *Avtomaticheskaya Svarka*, 4, 49–50.

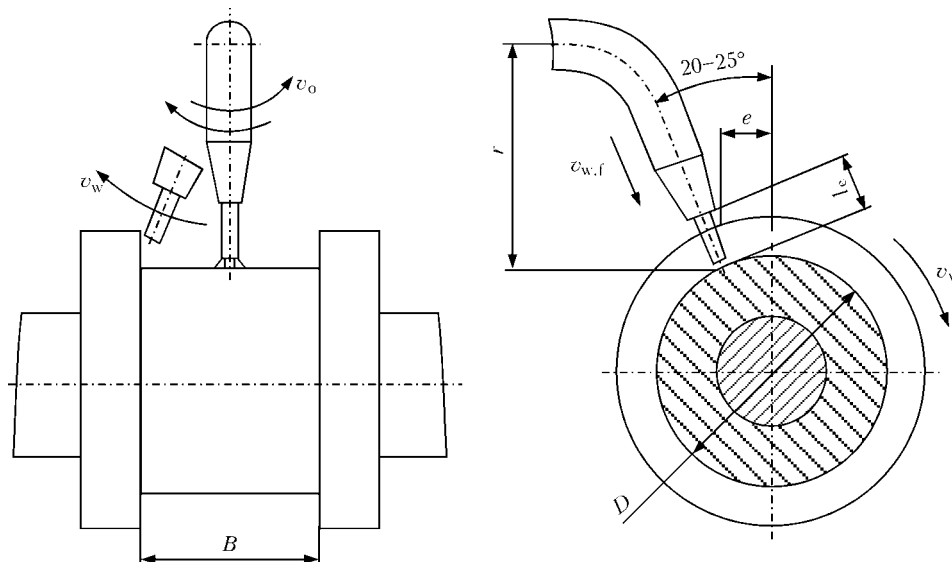


Figure 1. Flow diagram of the method of wide-layer hard-facing of cylindrical parts using oscillating electrode (self-shielding flux-cored wire) (see designations in the text)

surface roughness of the deposited layer. As noted above, $W = 1.5\text{--}3.0$ mm for large-size crankshafts. Wide-layer deposition of this thickness of the metal layer on a large-diameter cylindrical surface can be performed over a wide range of welding currents. However, for the flux-cored wire employed, the technologically efficient ranges of the welding current and arc voltage are $I_w = 200\text{--}400$ A and $U_a = 26\text{--}28$ V, respectively, at $l_e = 20\text{--}25$ mm. It should be noted that for such values of the welding current the maximal width of the deposited layer should not exceed 70 mm in order to provide the acceptable quality of its formation and productivity of the process. Also, the absolute values of I_w (A) and $v_{w,f}$ (m/h) were found to be almost identical (Figure 2) in the case of wide-layer welding using the 2 mm diameter medium-alloyed flux-cored wire. This makes it possible to use the $v_{w,f}$ parameter as a more general characteristic of the process and exclude the welding current from the range of the process optimisation parameters.

Surface roughness of the deposited layer taking place in wide-layer hard-facing, was evaluated on the basis of the coefficient of variations of real thickness of the layer, CV_δ . The maximal value of $CV_\delta = 30\%$ was assumed for the investigations, by accounting for the value of allowance for subsequent machining of the deposited surface. It was established that a welding speed of 3–8 m/h corresponds to the range of variations in the real layer thickness equal to 15–30%. In this case, the displacement of electrode from zenith providing good formation of the deposited layer also varies within a rather narrow range. For example, at a welding speed of 5.5 m/h and current of 200–400 A, the optimal quality of formation of the deposited layer was provided at a displacement of electrode from zenith equal to 8–12 mm (dashed region in Figure 3). Outside this range, formation of the deposited layer is disturbed, this leading to the risk of flow of part of the weld pool down from the surface being treated. It should be taken into account that the higher the values of v_w and I_w , the higher should be the value

of e . The effect of the v_w and I_w values on average thickness of the deposited layer is shown in Figure 4.

Electrode oscillation speed v_o affects the process of formation of the weld pool, the length of which in wide-layer hard-facing is approximately equal to the electrode oscillation amplitude (or range). If the v_o value is low, the deposited metal has the form of isolated transverse beads. And if this value is too high, then regions of the lack of fusion form between the base and deposited metal, and stability of the arc and uniformity of melting of the flux-cored wire deteriorate. In both cases the quality of formation of the deposited layer is unsatisfactory. In this connection, the optimal value of v_o in terms of ensuring the good quality of formation is such at which the common liquid weld pool with a length equal to the electrode oscillation amplitude forms at the beginning of the welding process. It was experimentally proved that in deposition of layers with width of 40–70 mm and

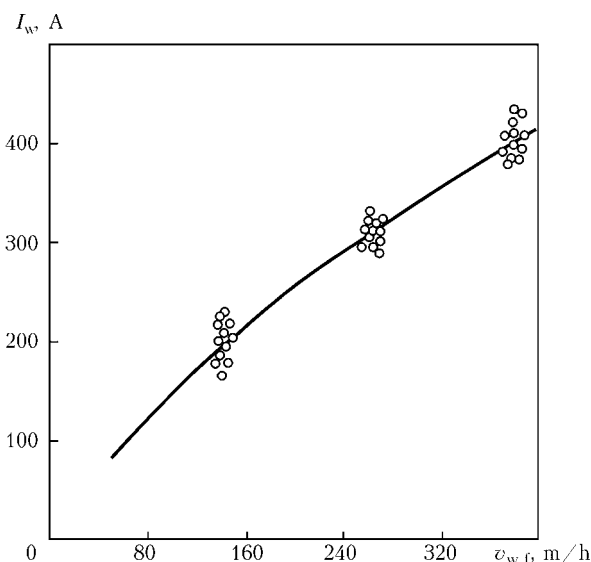


Figure 2. Current I_w versus wire (2 mm diameter flux-cored wire PP-Np-30Kh4G2SM) feed speed $v_{w,f}$ in wide-layer hard-facing ($U_a = 26\text{--}28$ V, $l_e = 20\text{--}25$ mm, $v_o = 155\text{--}215$ m/h)

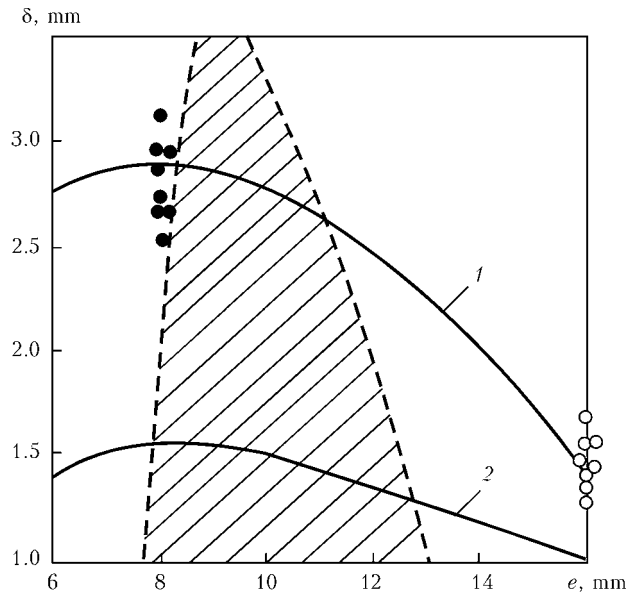


Figure 3. Average thickness δ of deposited layer versus displacement e of electrode from zenith at $v_w = 5.5$ m/h, $CV_\delta = 30\%$ and $I_w = 400$ (1) and 200 (2) A; ●, ○ – forward and backward flow of liquid metal

at $I_w = 200\text{--}400$ A, the optimal values of v_o may vary from 120 to 250 m/h, and that it depends upon the welding current and width of the deposited layer. It should be noted that the oscillation speed exerts the substantial effect only on the time of formation of the common weld pool at the beginning of the welding process. After its formation the v_o value can be varied over a wide range without any loss in the quality of formation of the deposited layer.

However, adjustment of the v_o parameter is time-consuming. To exclude this operation, it is enough to determine the time required for formation of the common weld pool and use it as a constant parameter of the welding process. It was established that within the investigated ranges of the welding currents (200–400 A) and width of the deposited layer (30–70 mm), this time

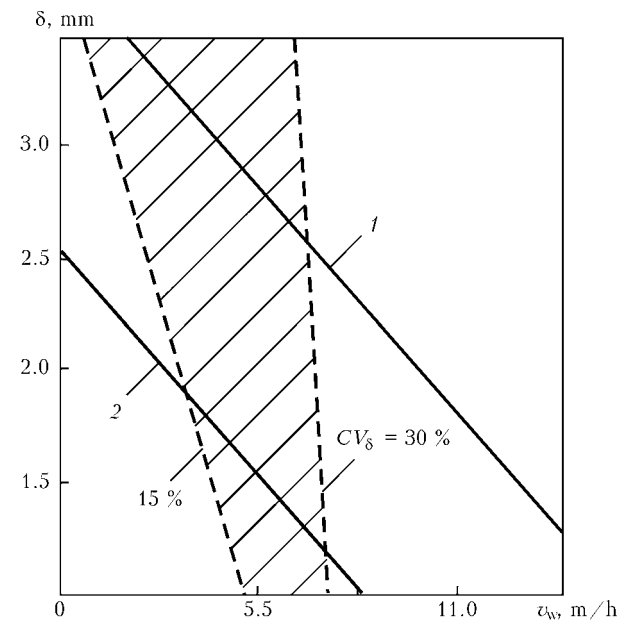


Figure 4. Average thickness δ of deposited layer versus welding speed v_w at $l_c = 8$ mm: 1, 2 – see Figure 3

is 2–3 s, which corresponds to electrode oscillation frequency $n_o = 60 \text{ min}^{-1}$. This oscillation frequency provides a good quality of formation of the deposited layer. Therefore, it can be used as a universal value. It should be taken in consideration in this case that for a welding process beginning lag time of 2–3 s the welding speed should be equal to zero. When this time expires, v_w grows to the preset value. The use of the n_o parameter instead of v_o permitted the electrode oscillation mechanism to be substantially simplified.

One of the requirements imposed on the technology for wide-layer hard-facing of crankshaft journals is compulsory welding of fillets, i.e. regions of transition from a cylindrical surface of a journal to normal surfaces of webs. As experimentally found, if an electrode during the welding process makes oscillatory movements at a constant speed, at the moments of its approaching the fillets (at extreme positions) the arc and electrode metal heat is not enough for their reliable fusion. This results in formation of a defect in the form of a region of lack of fusion between the deposited layer and near-fillet region of the crankshaft journal web. To eliminate this drawback, one more characteristic, i.e. the time of dwelling of the electrode at the extreme positions, should be added to the set of the wide-layer welding parameters. The quality of the deposited near-fillet regions varies depending upon τ : the longer the lag time and the lower the welding speed, the higher is the quality of formation of the deposited metal. Other conditions being equal, τ also depends upon the heat removal conditions: the heavier the weight of the webs adjoining the journal, the higher is the τ value. The character of the oscillatory movement of the electrode is set by a shaped cam, which is kinematically connected to the flux-cored wire feed nozzle. The shape of the cam is set such that the total cycle of one oscillatory movement of the electrode consists of three regions: regions 1 and 2 – dwelling of the electrode near the fillets for time t , and region 3 – movement of the electrode at a preset constant speed. For the studied ranges of the wide-layer hard-facing parameters, the maximal value of τ is not in excess of 0.26 s.

Including radius r of oscillations of the electrode into the range of the optimisation parameters is attributed to the fact that surfaces of the fillet regions are more convenient to deposit at a curvilinear path of movement of the electrode tip. This eliminates the probability of short circuits between the nozzle and webs. According to the calculations, a change in extension of the electrode at its oscillations to a width of 30–70 mm is 0.6–4.8 mm. However, as shown by the experiments, such a change in the extension at a flux-cored wire feed speed of over 180 m/h does not have a marked effect on length of the arc, its electrical parameters and quality of formation of the deposited layer. A change in the oscillation radius exerts a considerable effect on the process of welding of the fillet regions and losses of the electrode metal. As follows from the data obtained, the quality of formation of metal deposited on the fillet regions deteriorates, and losses of the electrode metal grow from 8.1 to 15.8 %

Optimal parameters of wide-layer hard-facing of rod and main journals of diesel generator crankshafts

Process parameter	Type of crankshaft journal	
	Main journal	Rod journal
I_w, A	320–340	340–360
U_w, V	27–28	27–28
$v_w, m/h$	4.5	5.0
Electrode oscillation amplitude, mm	50	65
e, mm	8–10	8–10
n_w, min^{-1}	60	60
Quantity of adjacent layers, pcs	2	2
t_w, min	6.0	4.0
l_e, mm	25–28	25–28

with increase in the r values from 81 to 145 mm. This is associated with decrease in the electrode inclination angle to the plane of a web of the journal being welded, which, in turn, leads to incidental contacts of the web with the side surface of the flux-cored wire sheath, formation of short circuits that shunt the arc, and spattering of the electrode metal. Therefore, to deposit layers no more than 70 mm wide, the optimal value of r should be 80–90 mm.

The investigations conducted served as a basis for the technology developed by the E.O. Paton Electric Welding Institute for hard-facing of large-size diesel generator crankshafts. The technology consists of three successively performed stages: preparation of a crankshaft, wide-layer welding of rod and main journals, and machining of the hard-faced crankshaft. If defects (e.g. regions with large pores or voids, etc.) are detected in the deposited layer after hard-facing or during machining, method for removing them is added to the technology.

Preparation of the crankshaft for hard-facing includes inspection of the shaft surfaces subject to hard-facing in order to detect cracks. In the case of cracks escaping to the journal surfaces and having a length of more than 20 mm, they are subjected to machining and repair welding.

Equipment for hard-facing of crankshafts includes a rotation mechanism and welding device (e.g. welding head A-580) fitted with the electrode oscillation mechanism. The rotation mechanism is a specialised screw-cutting lathe intended for machining of billets of diesel generator crankshafts. Wide-layer hard-facing is performed by using the 2 mm diameter self-shielding flux-cored wire, the journal to be welded being preheated to a temperature of 220–240 °C. The optimal hard-facing parameters are given in the Table.

With wide-layer hard-facing by the open-arc welding method using flux-cored wire PP-Np-30Kh4G2SM, the deposited metal has the following chemical composition, wt.%: 0.3 C, 4.0 Cr, 2.0 Mn, 0.8 Si, 0.8 Mo, and 0.45 Ti.

Figure 5, *a* shows appearance of the 65 mm wide crankshaft journal after hard-facing. Width of the diesel generator shaft journal is 135 mm, which is

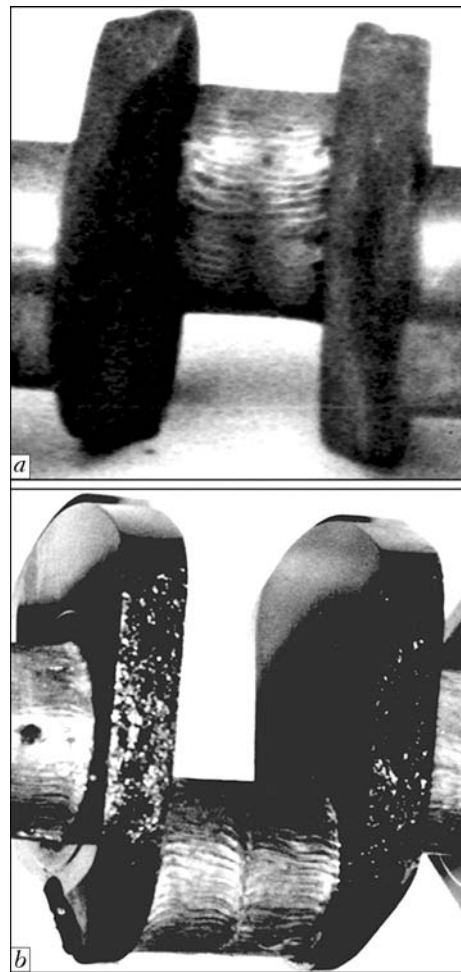


Figure 5. Appearance of crankshaft journals after wide-layer hard-facing using self-shielding flux-cored wire PP-Np-30Kh4G2SM under optimal conditions with one layer (*a*) and two adjacent layers (*b*)

much in excess of the maximum permissible width of the layer deposited with the above grade of the flux-cored wire. Therefore, the process of hard-facing of the journal consists of two stages: first the wide-layer hard-facing process is performed on one part of the journal at the electrode oscillation amplitude equal to its half-width, and then the other half of the journal is subjected to hard-facing. As a result of performing hard-facing in two stages, two adjacent layers are formed on the journal, thus fully covering its worn-out working surface (Figure 5, *b*).

The developed technology for wide-layer hard-facing passed the experimental-industrial verification at Company «Pervomajskdizelmash» (Pervomajsk, Ukraine). A batch of crankshafts was hard-faced and machined, after which the crankshafts successfully passed the bench tests. At present, these crankshafts are commercially applied. No data are available on the effect of wide-layer hard-facing on fatigue strength of the repaired large-size crankshafts. However, a long-time experience of application of wide-layer hard-facing to different types of crankshafts proves that it exerts no significant effect on this characteristic.

Application of the technology for wide-layer hard-facing of diesel generator crankshafts showed that the hard-facing costs constituted 22 % of the price of a new crankshaft.

DETERMINATION OF ADDITIONAL RESISTANCES TO SHEET PANEL DISPLACEMENT OVER DEAD ROLLER TABLE OF ASSEMBLY AND WELDING LINES

V.A. ROYANOV¹ and P.V. KOROSTASHEVSKY²
¹Priazovsky State Technical University, Mariupol, Ukraine
²OJSC «GSKTI», Mariupol, Ukraine

The nature of force interaction of the front edge of sheet panels in displacement along the dead roller table of assembly and welding lines was investigated. The value of additional resistance to displacement of panels for a case of arrangement of rollers with a critical pitch, as well as relationship between its components, was determined. Load cyclograms, allowing for additional resistance to displacement, to be used in calculation of power of the transportation device drives, and recommendations for decrease of the additional resistance were developed.

Keywords: arc welding, steel sheets, assembly and welding lines, roller table, displacement resistance, load cyclograms

Assembly and welding of sheets into panels is one of the main technological operations in fabrication of railway tank-cars and other vessels. At displacement of sheet panels over the rollers of dead roller table in their assembly and welding lines, the transporting device drives overcome the resistance directly proportional to panel weight and dependent on roller parameters. This resistance is calculated from the known formulas, similar to calculation of the displacement resistance, for instance, for travel mechanisms of the traverser and hoisting cranes [1]. However, when the panel front edge moves over the rollers, unlike smooth movement of wheel over rail, a resistance jump occurs — an additional resistance appears, due to front edge sagging below the panel displacement plane and its running against the rollers. Additional resistances reach maximum values, when the rollers are mounted with a pitch equal to or close to the critical one, when the panel front edge runs against the roller barrel at such a distance below the transportation plane, increase of which, i.e. further sagging of the front edge, leads to a complete stop of the panel or its slipping under the roller (sagging of the panel front edge and

its overhang are also critical at critical roller pitch) [2]. Power of the drives of devices transporting the panels is proportional to the resistance to panel displacement over the roller table (in the currently used structures of assembly and welding lines of large-sized panels from up to 16 mm sheets it is equal to about 10–15 kW). Increase of the total resistance to panel displacement at appearance of additional resistance requires a proportional increase of the forces to achieve this displacement, this automatically leading to overloading of the motors and other drive elements. In order to prevent the above situation, it is necessary to increase the power of transportation device drives adequately to the increased resistance, thus leading to an increase of their overall dimensions, power consumption and increased product cost. Such an additional load should be taken into account in selection of the optimum roller pitch and calculation of transporting device drive power, so that determination of additional resistances to sheet panel displacement over dead roller table is a highly important scientific and practical task.

In publications devoted to the problems of item transportation over roller tables and conveyers [2–6], attention was given to conditions of normal transportation of sheet panels and long cargoes and determination of their displacement resistance. Conditions for normal movement of sheet panel front edge onto the rollers are considered in detail in [2, 3]. Works [4, 6] analyze the methods of determination of additional resistance to displacement of extended cargoes over roller conveyors with drive rollers and beds installed between them. However, the above materials do not permit calculation of additional resistance to displacement of sheet panels along their assembly and welding lines, arising at panel front edge moving onto dead rollers of the roller table mounted without any intermediate beds (Figure 1).

The purpose of this work is determination of additional resistances to displacement of sheet panels along their assembly and welding lines, arising at

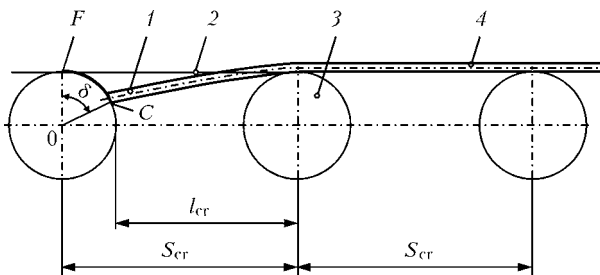


Figure 1. Schematic of panel front edge movement over the roller: 1 — panel front edge; 2 — panel transportation level; 3 — roller; 4 — panel; C, F — initial and final contact point of front edge with roller; l_{cr} — panel critical overhang; S_{cr} — critical roller pitch

panel front edge moving onto the rollers at displacement over the roller table with dead rollers mounted without intermediate beds.

To determine additional resistances, let us consider the schematic of force action at contact of panel front edge with the roller at its critical sagging on the roller table with critical roller pitch (Figure 2).

In the point of front edge contact, force Q of panel displacement, equal to its displacement resistance, is decomposed into two components, namely radial force Q_R , directed away from the point of contact to roller rotation axis, and circumferential force Q_c . In its turn, reaction from radial force $Q_R = Q_{R'}$ is decomposed into horizontal Q_h and vertical Q_v components. Additional resistance W_r to panel displacement is made up of two components: resistance W_{rol} from roller rotation at front edge moving onto them and resistance W_h to panel horizontal displacement at front edge contact with rollers:

$$W_r = W_{rol} + W_h. \quad (1)$$

Influence of the weight of overhanging front edge is not considered in this case, as the panel weight is fully allowed for in determination of the main resistance to panel displacement over the roller table.

Resistance W_{rol} due to roller rotation at front edge moving onto them is induced during roller rotation at the pressure of radial component on them similar to that induced in rollers at normal displacement of panels over them. It can be calculated by known formulas [1], for instance, by formula, converted from the formula of calculation of resistance to bridge crane trolley displacement in a steady-state operation mode:

$$W_{rol} = Q_R(f_{fr}d + 2\mu) / D_{rol}, \quad (2)$$

where f_{fr} is the coefficient of friction in roller journals; d is the roller journal diameter; μ is the coefficient of rolling friction; D_{rol} is the roller diameter in the rolling circle; $Q_R = Q \cos \alpha$; and from right triangle AOC at critical panel overhang and roller pitch (Figure 1) we obtain

$$\alpha = \arcsin (r / R_{rol}). \quad (3)$$

After transformations we obtain:

$$W_{rol} = Q \cos [\arcsin (r_{rol} / R_{rol})] \times (f_{fr}d + 2\mu) / D_{rol} = QK_{rol}; \quad (4)$$

$$K_{rol} = \cos [\arcsin (r_{rol} / R_{rol})] \times (f_{fr}d + 2\mu) / D_{rol}, \quad (5)$$

where K_{rol} is the coefficient of additional resistance to displacement due to roller rotation at panel front edge moving onto the roller table rollers; r_{rol} is the roller axis radius (bearing inner radius) equal to $d_{rol}/2$; R_{rol} is the roller radius in the rolling circle equal to $D_{rol}/2$.

From formulas (4) and (5) it is seen that additional resistance to roller rotation at contact with the front edge, does not depend on transported panel parame-

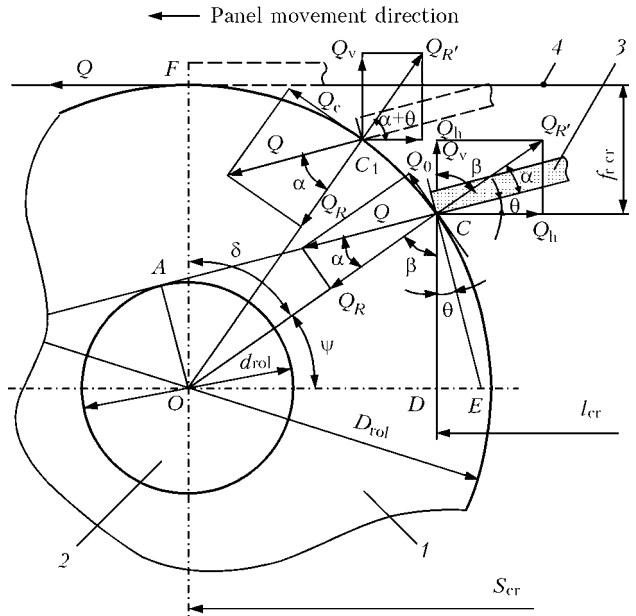


Figure 2. Schematic of force action at contact of panel front edge with the roller at panel critical sagging on a roller table with critical roller pitch: 1 – roller; 2 – journal; 3 – panel front edge; 4 – panel transportation level

ters, and only depends on roller parameters and their bearings.

Additional resistance to panel horizontal displacement at its front edge contact with rollers is the horizontal component of the reaction of radial force $Q_R = Q_{R'}$:

$$W_h = Q_R \sin \beta = Q \cos \alpha \cos (\alpha + \theta) = QK_h; \quad (6)$$

$$K_h = \cos \alpha \cos (\alpha + \theta), \quad (7)$$

where K_h is the coefficient of additional horizontal displacement resistance at contact of panel front edge with rollers; θ is the angle of rotation of front edge end plane at its critical sagging, equal to $K_{\theta}l_{cr}^3$ [2].

Expanding additional resistance formula (1) using formulas (4) and (6), we obtain:

$$W_r = Q(K_{rol} + K_h) = QK_r; \quad (8)$$

$$K_r = K_{rol} + K_h, \quad (9)$$

where K_r is the coefficient of additional resistance to displacement at panel front edge moving over the rollers.

At determination of K_r for different rollers, let us precise the value of calculated diameters for roller journals d . Journal calculated diameter is equal to average diameter of a roller bearing:

$$d = (d_{rol} + D_n) / 2, \quad (10)$$

where d_{rol} ($d_{rol} = 2r_{rol}$) and D_n is the roller bearing inner and outer diameter, respectively.

As in terms of design the rollers can have rolling bearings with the same inner, but different outer diameters, the journal diameter for the same rollers and, accordingly, resistance to panel displacement over

Table 1. Values of coefficients K_{rol} of additional resistance to displacement due to rotation of rollers with different parameters

Rollers d_{rol}/D_{rol}	Parameter·10 ³ , m		Roller journal diameter $d·10^3$, m	$K_{rol}·100$ %	
	d_{rol}	Bearings D_{rol}		Limit	Average
25/100	25	37, 42, 47, 52, 62, 80	31.0–52.5	1.225–1.538	1.38
30/120	30	47, 55, 62, 72, 90	38.5–60.0	1.113–1.372	1.24
35/160	35	47, 55, 62, 72, 80, 100	41.0–67.5	0.863–1.106	0.99
40/200	40	62, 68, 80, 90, 110	51.0–75.0	0.767–0.944	0.86
45/250	45	68, 75, 85, 100, 120	56.5–82.5	0.648–0.802	0.73
50/280	50	80, 90, 110, 130	56.0–90.0	0.624–0.756	0.69
50/300				0.584–0.707	0.65
55/320	55	80, 90, 100, 120, 140	67.5–97.5	0.558–0.696	0.63
60/360	60	78, 85, 95, 110, 130, 150	69.0–105.0	0.503–0.651	0.58

Table 2. Values of coefficients K_r of additional resistance for sheet panels from 12Kh18N10T steel of different thickness at transportation over rollers of different diameters

$h·10^3$, m	$d_{rol}/D_{rol}·10^3$, m	Coefficients of resistance, %		
		$K_{rol,cr}$	K_h	K_r
4	25/100, 30/120,	1.38, 1.24, 0.99, 0.86, 0.73, 0.69, 0.63, 0.58	92.49–94.40	93.87–94.98
6	35/160, 40/200,		92.72–94.79	94.10–95.37
8	45/250, 50/280,		92.86–95.31	94.24–95.89
10	55/320, 60/360		92.96–95.53	94.34–96.11
12			93.03–95.70	94.41–96.28
16			93.13–95.92	94.51–96.50

such rollers, will be different at their same outer diameters.

Results of calculation of the coefficients of additional resistance to panel displacement for rollers of the most optimum outer diameters of 100, 120, 160, 200, 250, 280, 300, 320 and 360 mm, mounted on different bearings and having different journal diame-

ters, are presented in Table 1 and in Figure 3. Parameters of the most common ball radial single-row rolling bearings [7], as well as $f_{fr} = 0.015$ and $\mu = 0.04$ cm were used [1].

Results of calculation of the coefficients of additional horizontal displacement resistance at panel front edge running against the rollers K_h and coefficients of full additional resistance in transportation of sheet panels K_r for sheet panels from 12Kh18N10T steel 4, 6, 8, 10, 12 and 16 mm thick over rollers of diameter $D_{rol} = 100, 120, 160, 200, 250, 280, 300$ and 360 mm, are given in Table 2. Values of panel critical overhang l_{cr} and angles of rotation of front edge end plane at its critical sagging θ (angles of section rotation at critical overhang values) were obtained from the respective graphs and formulas [2].

Analysis of the obtained results shows that the coefficient of additional resistance to displacement at panel front edge moving onto the rollers at critical panel overhang for sheets of different thickness, is equal to 93.87–96.50 % (almost 100 %), i.e. a unity. Coefficient of resistance to displacement due to roller rotation is up to 2 %, it decreases with increase of journal diameter and roller diameter and rises with increase of journal diameter at unchanged roller diameter. The main part of additional resistance is cre-

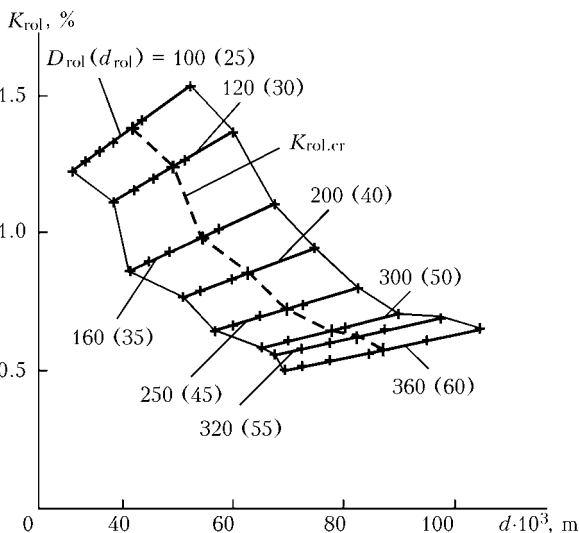


Figure 3. Coefficients K_{rol} of additional resistance to panel displacement due to roller rotation for rollers of different diameters with different journal diameters

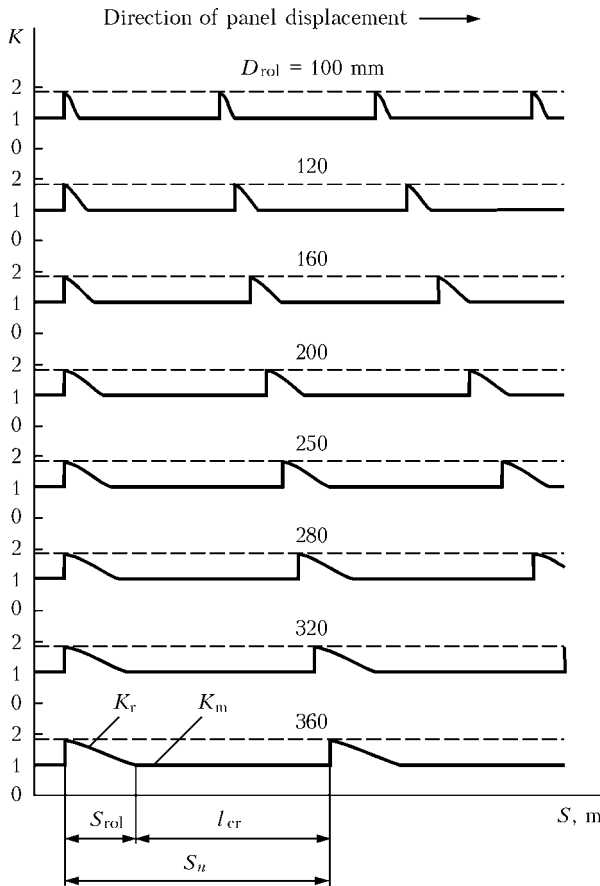


Figure 4. Cyclograms of the coefficients of resistance to displacement of 8 mm sheet panel from 12Kh18N10T steel over rollers of various diameters mounted with a critical pitch: K_m – coefficient of the main resistance equal to 1; K – total coefficient of resistance

acted by resistance to panel horizontal displacement at contact of its front edge with rollers, increasing slightly with increase of sheet thickness and roller diameter. Value of additional resistance decreases with decrease of roller pitch (and panel front edge overhang, respectively).

Duration of action of additional resistance at constant speed of panel displacement is directly proportional to path S_{rol} of front edge over the roller – length of arc CF (see Figures 1 and 2). Value of displacement of front edge from one roller to another

Table 3. Length of path of front edge of sheet panels from 8 mm 12Kh18N10T steel at transportation along the generatrix of rollers of different diameters

$d_{rol}/D_{rol} \cdot 10^3, m$	$l_{cr} \cdot 10^3, m$	$K_r, \%$	$S_{rol} \cdot 10^3, m$	$\frac{S_{rol}}{S_{rol} + l_{cr}}$
25/100	1400	94.24	64.2	4.39
30/120	1460	94.10	76.8	5.00
35/160	1585	95.03	10.40	6.16
40/200	1680	95.53	13.10	7.23
45/250	1785	96.00	16.49	8.46
50/280	1830	95.87	18.41	9.14
55/320	1895	95.89	21.01	9.98
60/360	1945	95.89	23.60	10.82

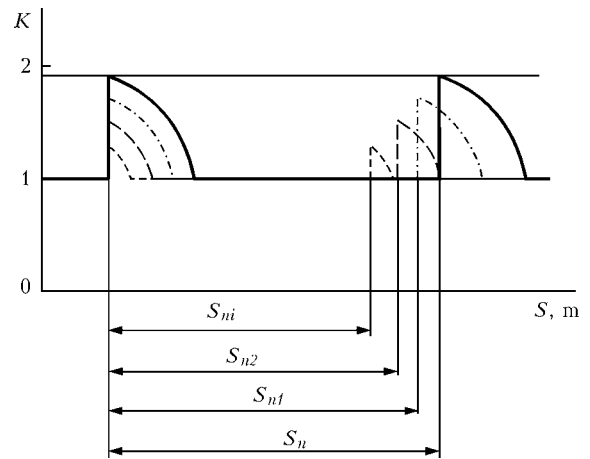


Figure 5. Nature of variation of coefficient of additional resistance at reduction of roller pitch: $S_n - S_{ni}$ – front edge path at panel displacement by different (decreasing) roller pitch

(by roller pitch in plan view) at roller mounting with critical pitch will be

$$S_n = S_{rol} + l_{cr}. \quad (10)$$

The path of front edge over the roller (along the roller barrel arc CF) is

$$S_{rol} = \pi D_{rol} \delta / 360, \quad (11)$$

where δ is the central angle of arc of roller of diameter D_{rol} (see Figures 1 and 2) equal to

$$\delta = 90^\circ - \psi = 90^\circ - (90^\circ - \beta) = 90^\circ - (\alpha + \theta). \quad (12)$$

Making the required transformations and calculations, we will get the values of the path, as well as value of the path relative to full displacement (in percent) of sheet panel front edge over the rollers. For sheet panels from 12Kh18N10T steel 8 mm thick at transportation over rollers of different diameters calculation results are given in Table 3, and cyclograms of the coefficients of the main and additional resistances to front edge displacements – in Figure 4.

The value, periodicity and duration of the action of additional resistance to panel displacement at its

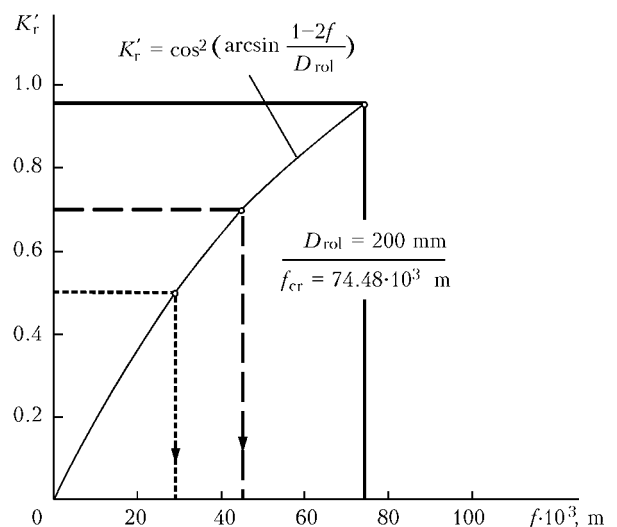


Figure 6. Dependence of the coefficient of additional resistance on sagging of front edge of sheet panel from 8 mm 12Kh18N10T steel



movement over the roller table with critical roller pitch are traceable by the cyclograms. One can see that with increase of roller diameter and critical overhang of panel front edge the length of front edge path over the roller and the duration of additional resistance action increase, respectively. At increase of roller pitch from the critical value, panel front edge overhang and sagging automatically decrease from the critical values, additional resistance to panel displacement and duration of its action decreasing, respectively (Figure 5). The given cyclograms actually are graphs of the transporting device drive loads, forming the basis for motor power calculation. At the known speed of panel displacement the time of covering certain sections of the path and influence of additional resistance on transporting device drive power are readily found.

Having analyzed the formulas of the coefficients of resistance (5), (7) and (9) and their calculated values in Table 2, we can see that additional resistance from the roller rotation (coefficient $K_{r,av}$) is equal to about 2 % of the total additional resistance. Value of angle θ in the formula of the coefficient of horizontal resistance K_h is also small. In addition, at decrease of front edge sagging from the critical value, angles α and ψ become larger, and angle θ decreases, value of angle α becoming close to value of angle ψ . Having transformed formulas (6) and (7), taking it into account, we obtain a simplified formula of the coefficient of additional resistance K'_r for calculation of its value at sagging of panel front edge below the critical values:

$$K'_r = \cos^2 \psi. \quad (13)$$

Considering that at minimum roller diameters of 100 mm and their journals of 25 mm maximum angle α (see Figure 2) is equal to 14.48° , and maximum angle ($\alpha + \theta$) is 17.21° , formula (13) can be used in the range of values $\psi = 20-90^\circ$. Having expressed value ψ through sagging of front edge (see Figure 2), we obtain a formula of the coefficient of panel additional resistance at sagging below the critical values:

$$K'_r = \cos^2 \psi = \cos^2 [\arcsin (1 - 2f/D_{rol})], \quad (14)$$

where f is the sagging of panel front edge below the critical one.

The graph of this dependence for sheets from 12Kh18N10T steel 8 mm thick and rollers of 200 mm diameter, having critical sagging of 74.48 mm, is given

in Figure 6. Taking the admissible for this case coefficient of additional resistance, we use the above graph to determine front edge sagging with this coefficient, and by sagging value we determine the required roller pitch from the known dependencies.

The direction of further research is development of criteria of selection of the optimum roller pitch for dead rollers of roller tables, allowing for the influence of additional resistance to panel displacement on transporting device drive power.

CONCLUSIONS

1. At panel front edge moving onto the rollers of dead roller table, the panel is exposed to additional resistance to displacement on each roller, which is practically equal to the main resistance at critical roller pitch.

2. It is confirmed that the main part of additional resistance to panel displacement over the roller table (at its maximum value) is made up by resistance to horizontal displacement at contact of front edge with the roller, and a small part — up to 2 % — is resistance to displacement due to roller rotation.

3. It is established that the value of additional resistance decreases with reduction of roller pitch, and at panel front edge displacement over the roller it decreases from its maximum value to zero.

4. The pitch of roller table rollers should be selected, allowing for the admissible value of additional resistance to panel displacement, and at calculation of transporting device drive power the load graphs should allow for the value and duration of the action of additional resistance.

1. Ivanchenko, F.K., Bondarev, V.S., Kolesnik, N.P. et al. (1978) *Calculations of lifting and transporting machines*. Kiev: Vishcha Shkola.
2. Royanov, V.A., Korostashevsky, P.V. (2007) Selection of parameters of roller table of the line of sheet panel assembly and welding. *The Paton Welding J.*, 7, 14–18.
3. Royanov, V.A., Korostashevsky, P.V. (2008) Determination of optimal relationship of roller pitch and distance between roller rows of transport systems of sheet panel assembly and welding lines. *Visnyk Pryazovskiy DTU*, Issue 18, Pt 1, 184–187.
4. Ivanovsky, K.E., Rakovshchik, A.N., Tsoglin, A.N. (1973) *Roller and disk conveyors and devices*. Moscow: Mashinostroenie.
5. Plavinsky, V.I. (1969) *Continuous transportation machines*. Moscow: Mashinostroenie.
6. Zenkov, R.L., Ivashkov, I.I., Kolobov, L.N. (1987) *Continuous transportation machines*. 2nd ed. Moscow: Mashinostroenie.
7. (1985) *GOST 8338-75: Radial single-row ball bearings*. Moscow: Standart.



NEWS

NKMZ CONFIRMED AGAIN THE BRAND OF ENTERPRISE OF HIGH QUALITY

At the International exhibition «All-Russian Brand «Quality Mark of XXI Century» the gold marks of quality were given to more 11 kinds of products of Novokramatorsk Machine-Building Works (NKMZ Company, Kramatorsk, Donetsk region). These are steel forged rolls for hot and cold rolling mills, universal hydraulic recoilers for strip reeling, arc steel melting furnace DSP-50, automated transport systems of storage and supply of bulk materials of efficiency of up to 250 t per hour, foundry cranes of load-carrying capacity up to 500 t, loading cranes of carrying capacity up to 40 t, forge cranes up to 500 t, mills of semi-self-grinding and self-grinding with drum of up

to 10 m diameter, stationary mixers of capacity up to 2500 t for storage of liquid cast iron, worm-gear crushers, crank hot stamp presses of up to 8000 t force.

Products of none of other enterprises, participated in the exhibition, were awarded such considerable package of decorations.

Today 45 kinds of products of NKMZ are recommended for application at the Russian market, 24 kinds are marked with platinum Quality mark «All-Russian Brand».

At this exhibition NKMZ proved also his right for possession of Passport of enterprise of high quality for the fourth time.

WELDING MANIPULATOR MS-101

OJSC «Elektromashinostroitelny Zavod «Firma SELMA» mastered the production of welding manipulator MS-101 designed for inclination and rotation of workpieces in the position convenient for welding (cutting) at a preset speed in automatic, semi-automatic or manual electric arc welding.

The control system of manipulator provides smooth control of rotation speed of a workpiece in a wide range, high accuracy, stability of work and function of self-protection. Using control panel it is possible to set required rotation speed, perform rotation of a part in both directions.

The delivery package of manipulator MS-101 includes manipulator, control unit, control panel.

Technical characteristics

Maximal loading capacity, kg	100
Rotation speed of faceplate, rpm	1-5
Range of inclination angle of faceplate, deg	0-120



Diameter of faceplate, mm	350
Welding current at 60 % duty cycle, A	500
Supply voltage of control unit, V	2 × 380 (50 Hz)
Weight (without unit and control panel), kg	47

XIII REPUBLICAN SCIENTIFIC-TECHNICAL CONFERENCE OF KAZAKHSTAN WELDERS



On December 10–11, 2009 the XIII Republican Scientific-Technical Conference «Welding and Control» was held at Karaganda State Technical University (KarSTU) (Kazakhstan Republic). Chief welding engineers, specialists on welding and non-destructive testing, lecturers of educational establishments from more than 30 enterprises and organizations of Kazakhstan participated in the Conference.

Before the Conference opening, F. Jabbur and D. Konysova, Managers of Italian-Kazakhstan Company ERSAl, presented to the KarSTU eight pieces of modern multimedia training equipment for the total sum of 1 mln tenge for training students of welding speciality and for the jointly established training center «Svarka». In June 2009 this Company already supplied free-of-charge filter-ventilation unit EMK-1600, the cost of which is 1.2 mln tenge, for the welding laboratory. Speaking at the Conference opening,



Conference session in progress

Conference Chairman I.A. Bartenev, Cand. of Sci. (Eng.), Assistant Professor of KarSTU, expressed his gratitude to ERSAl Company.

During the Conference activities 16 papers were presented and discussed, which were devoted to different aspects of theory and practice of welding fabrication and non-destructive testing, as well as training personnel for welding fabrication in Kazakhstan Republic.

I.A. Bartenev spoke about the International Exhibition of modern welding equipment and technologies «Weldex 2009», which was held from 12 to 16.10.2009 in Moscow, demonstrating photo slides and videos. A fundamentally new technology MicroTack™ developed by KEMPPi for tack welding thin metal was described in his presentation by S. Linovsky, Chief Welder of «Welding Group» Company from Almaty, with his co-author P. Yarnstrom, Dr. of Sci. (Eng.), KEMPPi Oy, Lachti, Finland. V.I. Bochenin, Cand. of Sci. (Eng.), one of the oldest lecturers of welding subjects in KarSTU, made a presentation on the prospects for development of welding fabrication. A.F. Kuritsyn, academician of KR Academy of Arts, Director of Karaganda Division of KR Union of Artists, spoke about interesting work on application of argon-arc welding in creation of original monumental sculptures from bronze, which are mounted in such major cities of Kazakhstan as Astana, Karaganda, Atyrau, Ust-Kamenogorsk, with demonstration of illustrations.

Presentation by F. Jabbur, Manager of ERSAl Ltd. from Aktau on the Caspian Sea, and I.A. Bartenev was devoted to the experience of fruitful cooperation of Italian-Kazakhstan ERSAl Company and KarSTU in the area of training and probation of young specialists on welding. Two papers on wear-resistant arc surfacing by strip electrode in manufacture of welded sliding shutters and on nanonitride strengthening of chromium-nickel-silicon deposited metal for pipeline fittings were presented by Yu.I. Lopukhov, Cand of Sci. (Eng.), Assistant Professor from East-Kazakhstan State Technical University (Ust-Kamenogorsk).

Information on the influence of plasma surfacing and welding parameters on metal properties was presented by I.A. Bartenev and B.M. Marinushkin from «Vetromashservis» Ltd., Almaty. Three papers were presented by young lecturers and undergraduates from KarSTU. These were «Nature of strains and stresses developing in welded structures», «Cladding of hammer mill beaters» (D.K. Absatov, postgraduate); «CAE systems – systems of engineering analysis in simulation of welding processes» (E.A. Telenkova, postgraduate, G.R. Gurba, lecturer).



E.M. Kvitko, Deputy Director of Karaganda Professional Lyceum #26, talked about development of KR state general education standards of technical and professional post-secondary education. A paper on technological features of welding and control of pipeline root weld was delivered by Zh.E. Abilov, engineer, first graduate of Welding Chair of KarSTU. I.M. Pokasov, Director of SPA «Tekhnik» Ltd., Karaganda, reported on development of a procedure of control and assessment of weld quality by defect area, which gave rise to lively discussion in the Conference. Another serious discussion was held in connection with the presentation of S. Linovsky, Chief Welder of «Welding Group», Almaty, on FastROOT technology of welding the weld root by a modified short arc.

In conclusion of the first day of the Conference, I.A. Bartenev talked about the experience of student training in the welding speciality at KarSTU in keeping with the Bacheloriata system, and assigning the graduates to work in major companies and firms in Western and Central Kazakhstan.

On the Conference first day a tour to KarSTU welding laboratory was conducted, where presentation of new KEMPPi equipment was held. In particular, Master TIG MLS™ 3000/3003 ACDC machine for welding and tack welding of sheet metal by Microtack technology was demonstrated in operation. Setting up of the modes and welding by this machine were demonstrated by S. Linovsky. The new technology excited great interest of Conference participants, who themselves tried welding with Maser TIG MLS™ 3000/3003 ACDC machine. On the second day of the Conference activities, a meeting of chief welders of enterprises, head of welding laboratories and welding and NDT specialists was held, where the draft of new Rules of Certification of Welders and Welding Fabrication Specialists of KR, as well as development of a system of welding fabrication certification in the country, was discussed. I.A. Bartenev delivered a paper on this subject.

Candidates for the National Certification Committee on welding fabrication of KR were nominated and



Presentation by S. Linovsky

its functions were outlined. Specialists present in the meeting approved these proposals and spoke in favour of as prompt as possible approval of the new Rules of Certification of Welders and Welding Fabrication Specialists of KR in the Ministry of Emergency Situations of KR and introduction of a system of welding fabrication certification in the country.

The subject of collective subscription to «Avtomaticheskaya Svarka» journal was also discussed in the Conference. More than 10 representatives of companies and enterprises expressed their wish to become collective subscribers to this prestigious journal.

After completion of the Conference A.G. Kozmin, Director of «Welding Technologies» Ltd., Atyrau, expressed a wish to provide assistance to the welding laboratory and supply free of charge three advanced welding machines of KEMPPi for training KarSTU students, which will promote an improvement of the quality of training young specialists of welding fabrication in Kazakhstan's only higher educational establishment with such a speciality.

Dr. I.A. Bartenev, KarSTU

PROBLEMS OF LIFE AND SAFE OPERATION OF STRUCTURES, CONSTRUCTIONS AND MACHINES (Final Scientific Conference at the E.O. Paton Electric Welding Institute of the NAS of Ukraine)

On January 22, 2010 the Final Scientific Conference devoted to consideration of scientific and applied results obtained during 2007–2009 in fulfillment of projects of purpose-oriented program of the NAS of Ukraine «Problems of Life and Safe Operation of Structures, Constructions and Machines» was held at PWI. Scientific leaders and performers of projects, as

well as representatives of interested ministries, departments, educational and branch institutes, industrial enterprises and organizations participated in the Conference activities.

The Conference was opened by academician B.E. Paton, President of the National Academy of Sciences of Ukraine, who noted that «...problems of controlling



Conference Presidium (from left to right): I.K. Pokhodnya, academician of NASU, academician B.E. Paton and L.M. Lobanov, academician of NASU

the operating reliability and fatigue life of critical constructions by determination of their technical condition, residual life and establishing scientifically-grounded operating lives are now becoming particularly urgent». The integrated program of the NAS of Ukraine is aimed at solving exactly these problems. Its purpose is establishing methodological fundamentals, technical means and technologies for assessment and extension of the residual life of critical constructions in long-term operation. 26 institutes of eight divisions of the NAS of Ukraine were involved in fulfillment of this program, consisting of nine sections, including 118 projects. In the opinion of B.E. Paton, important scientific-technical and practical results were obtained during the three years. Among them are:

- development of the procedure for evaluation of strength and fatigue life of pipelines based on two-criteria fracture diagram in the presence of stress-corrosion defects with specifying of the admissible strength margin and proposed procedure of calculation of its real value;
- development of technologies of repair welding of steam turbine casing parts and high-pressure fittings for extension of service life of TPS turbounits;
- calculation by the criteria of fracture mechanics of admissible dimensions of crack-like defects in the walls of delivery pipelines of TPS supercritical pressure power units, depending on their shape and content of impurities in the operating environment;
- optimization of the technology of manufacturing low-frequency piezoceramic two-component accelerometers for vibration testing of NPP main circulating pumps in operation under the conditions of up to 300 °C temperatures. Test samples of accelerometers were made and their characteristics were studied;
- work on optimization of welding technologies and materials for reconditioning and extension of the life of operating bridges has been performed. A semi-automatic machine has been developed for reconditioning of underwater metal structures by arc welding to extend their service life;

- technology and equipment for diagnostics of structural elements from composite materials by laser interferometry methods have been developed and introduced in DB «Yuzhnoe»;

- samples of lamellar-combined fibrous composite materials have been developed and tested, forming the basis for development of explosion-proof chambers for safe cutting and treatment of metal structures;

- a test batch of enamel for petrochemical industry, using modified polyurethane paintwork materials for anti-corrosion coatings, has been made for petrochemical industry and pilot-production verification has been performed with its application on elements of equipment and pipelines of Lisichansk Petroleum Refinery;

- technology has been developed, which enables 3–4 times extension of operating life of drill bits for drilling wells in production of scattered or mine metal;

- it is established that long-term operation induces considerable changes of electrical properties of wall metal in the main pipelines. Correlation dependencies between the changes of mechanical and electrochemical properties were plotted, which open up possibilities for forecasting the operating reliability of pipeline metal.

Other important scientific-technical results have also been obtained during Program fulfillment. On the other hand, in the opinion of B.E. Paton, the Program contained a number of small projects, not having clear perspectives for application of the obtained results.

It is important to note that the Program scientific council ensured preparation of publishing of a final collection of scientific papers of projects of the Program «Problems of Life and Safe Operation of Structures, Construction and Machines» (Kiev: PWI, 2009, 710 pp.). The collection contains the main scientific and applied work results obtained during fulfillment of the Projects (the collection can be ordered from PWI by phone: 529-26-23).

After that the scientific leaders of Program Sections delivered their papers at the Conference.

V.I. Makhnenko, academician of the NAS of Ukraine, Scientific Leader of the Section «Development of procedural fundamentals of assessment of the technical condition and substantiation of safe life of structural elements of higher risk objects in the territory of Ukraine», in his presentation reported that all the six projects of this Program Section are related to critical objects such as steam generators (nuclear power engineering), main pipelines, railway transportation, apartment and industrial buildings in mine working areas. Important results have been obtained in all these fields.

Z.T. Nazarchuk, academician of the NAS of Ukraine, Scientific Leader of the Section «Development of the methods and new technical means of NDT and diagnostics of the state of materials and items in long-term operation», noted in his presentation that an effective monitoring system, new means of NDT of elements of a number of vitally important objects



have been developed, and new diagnostic equipment has been prepared for batch production.

V.I. Pokhmursky, Corresp. Member of the NAS of Ukraine, Scientific Leader of the Section «Development of the methods of corrosion protection of structural elements of objects in long-term operation», noted that the list of the most important results of the fulfilled projects should include development of a coating for improvement of operational reliability of pipes and boilers of electric power stations, development of coatings for protection from fretting corrosion, development of methods of corrosion protection of steel R-bars for extension of the residual life of concrete structures. He noted the importance of development of a state purpose-oriented program on corrosion protection of the structures of bridges and other objects in base sectors of the industry of Ukraine till as far as 2015.

Presentation on the Section «Development of effective methods of evaluation and extension of the service life of nuclear engineering facilities» (Scientific Leader is I.M. Neklyudov, academician of the NAS of Ukraine) was made by *V.N. Voevodin*, Dr. of Sci. (Eng.). He emphasized that most of the projects in this section have been fulfilled with the participation of Ukrainian NPPs. Analysis of the stress-strain state of WWER-1000 reactor cases, steam generators and welds of turbine section piping of power units in Zaporozhskaya and Yuzhno-Ukrainskaya NPP has been performed. The main causes for failure of pressure piping have been established, an expert procedure for their control by magnetic methods has been proposed.

B.S. Stogny, academician of the NAS of Ukraine, summing up the results of investigations on the Section «Improvement of reliability and extension of service life of power equipment and systems», noted that important results have been obtained, which will be used for improvement of reliability and extension of operating life of turbines, generators, equipment of gas pumping stations, as well as upgrading of boiler equipment of municipal power generation and coal-fired power units. Conducted studies allowed outlining and substantiating the main measures for extension of operating life of boiler equipment elements of load-area thermal power generation.

Scientific results obtained in the Section «Development of systems of monitoring of technical condition of pipelines and objects of gas and petroleum-processing industry» were reported by its Scientific Leader *A.Ya. Krasovsky*, Corresp. Member of the NAS of Ukraine. Among the most important achievements, he mentioned development of a computer system of ensuring the integrity of the main pipeline, development of an all-purpose algorithm for pressure calculation in pipeline system components, evaluation of structural strength of pipelines with defects.

Presentation by *L.M. Lobanov*, academician of the NAS of Ukraine, was devoted to the results obtained on 22 projects of the Section «Improvement of reliability and extension of the life of bridges, build-



ing, industrial and transport structures». Among them are development of the technology of repair welding of turbine casing parts, development of low-hydrogen electrodes for welding and repair of bridge and transport structures, etc.

Results obtained on the projects of the Section «Development of technologies of repair and reconditioning of structural elements of higher risk facilities in order to extend their operating life» (Scientific Leader is K.A. Yushchenko, academician of the NAS of Ukraine) were reported by *O.G. Kasatkin*, Dr. of Sci. (Eng.).

V.V. Panasyuk, academician of the NAS of Ukraine, Scientific Leader of Program Section «Preparation and publishing of normative documents and scientific-technical manuals on evaluation of the life of long-term operation objects», noted in his presentation that during 2007–2009 modern scientific-technical reference books have been prepared and published for engineering-technical staff of design and industrial enterprises for evaluation of the fatigue life and reliability (life) of elements of long-term operation structures, in particular bridge and building structures, thermal and nuclear power stations, pipelines, etc.



Conference session in progress

This was followed by discussion of scientific results set forth in the presentations of scientific leaders of Program Section. *V.I. Korol*, Dr. of Sci. (Eng.), Director of Donbass Center of Technological Safety, *P.I. Krivosheev*, Director of Building Structures RI, *A.I. Lantukh-Lyashchenko*, Professor of the Chair of Bridges and Tunnels of the National Transport University, *V.I. Bolshakov*, Director of Z.I. Nekrasov Iron and Steel Institute participated in the discussion.

All the presenters have noted the urgency and importance of the obtained results for solving the problem of life of long-term operation objects, expressed their opinion on the rationality of continuation of fulfillment of Program «Problems of Life and Operation of Structures, Constructions and Machines» in 2010–2012.

In conclusion, academician B.E. Paton said «...I believe that we have to support the proposal of the scientific council on extension of fulfillment of Program «Resurs» for the next three years. It is necessary to entrust the scientific council with defining new stages of work performance, focusing the scientific efforts on the most urgent directions of investigations, envisaging, primarily, practical application of the obtained results. I would like to particularly emphasize that during the competition primary attention should be given to funding of integrated major efforts, the without dispersing funds for small projects fulfillment».

In conclusion the resolutions of the Final Conference were approved.

Profs O.G. Kasatkin and V.N. Lipodaev, PWI

«FRONIUS» WELDING DEVICES FOUND APPLICATION IN MANUFACTURE OF ELECTRON BEAM REMELTING EQUIPMENT

Production base of International Company «Antares» relies on two electron beam vacuum furnaces VT01, each with an installed power of 2.5 MW and annual output of titanium equal to 2500 t. At present the Company is completing manufacture of a new generation of furnace VT02, which is an in-house development, featuring an installed power of 3.2 MW and annual titanium output of 3000 t. Design of the furnace will allow producing round ingots and slabs of titanium and its alloys with a weight of up to 14 t and length of up to 5.5 m.

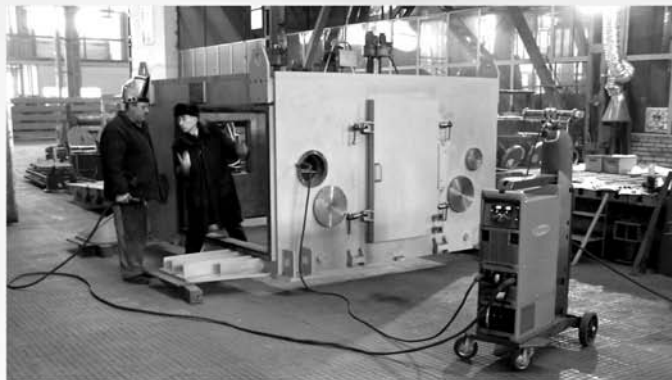


Photo in the cover page illustrates performance of welding of a melting chamber of furnace VT02 (steel 09G2S, lining of steel 10Kh18N10T) by using the welding equipment of the «Fronius» Company (Austria). IC «Antares» is currently using a range of the «Fronius» welding equipment, such as Magic Wave 2200, Magic Wave 5000 and Vario Star 457-2. Application of the above equipment allows «Antares» to improve economic indices of manufacture of assemblies of unit VT02 and provide the welded joints with high strength properties, and vacuum tightness of the welds in particular. Moreover, the Company achieved a substantial (up to 10 %) increase in productivity of welding operations, 5–5.5 % drop in consumption of welding wire, decrease in losses for its spattering, and reduction of costs for dressing of welds and removal of defects.

The Company managed to decrease residual stresses and strains and provide the preset accuracy of sizes and shapes of weldments due to decreased heat input and high reproducibility of welding parameters. This made it possible to reduce scopes of machining of vacuum flange connections.

Reduction of up to 15 % in operating costs was achieved in welding of conventional and stainless steels and copper owing to decrease in consumption of shielding gases, i.e. argon and helium.

As a result, robustness and failure-free operation of the «Fronius» welding equipment enables improving operating reliability of the electron beam units manufactured by IC «Antares».



LOYALTY PROGRAM OF FRONIUS UKRAINA Ltd. IN CRISIS PERIOD AND ITS RESULTS

In the period of June 25–September 25, 2009 the Fronius Ukraina Ltd. presented «Loyalty Program and Sales Stimulation» to its clients. The purpose of the Program is stimulation of purchases of the Fronius welding systems and machines for plasma cutting of the Powermax type, and support of Ukrainian enterprises-manufacturers.

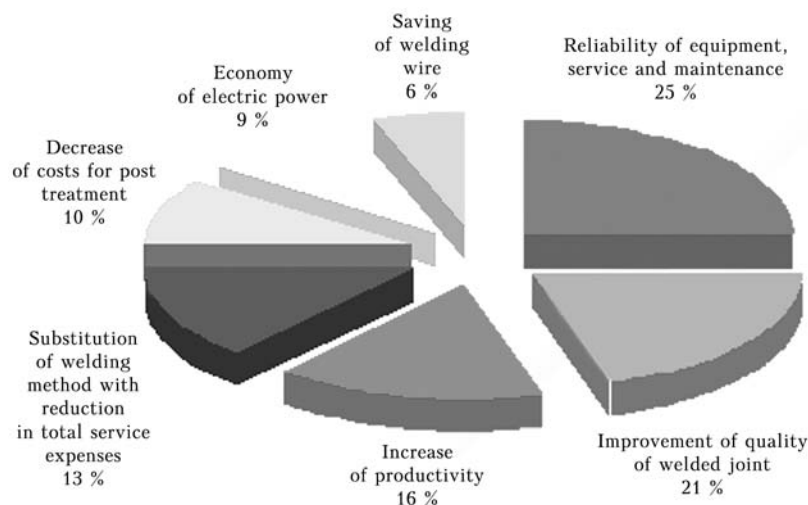
Owing to excellent welding-technological characteristics, high reliability and flexibility, the Fronius welding systems and machines for plasma cutting of the Powermax type give an opportunity to increase quality and appearance of products and to reduce as a whole the cost of operations and to decrease the total industrial expenses. This is very important in nowadays economic situation and complex market conditions, when industrial companies are looking for new possibilities to cut expenses and save the funds.

The enterprises, using welding technologies in their production cycle, could choose in purchase of equipment one of three most suitable variants of Loyalty Program from Fronius Ukraina Ltd.:

- receiving an additional discount on welding system;
- delay of payment (120 days);
- program «from rent to property».

In all cases the customers together with specialists of Fronius Ukraina had to evaluate efficiency of implementation of purchased welding system (or cutting system); determine main criteria of obtained advantages and *predict finally the saving costs at further service of these systems.*

The mentioned efficiency of implementation of systems into the production was evaluated on the basis of the following criteria for different types of equipment.



Criteria influencing efficiency:

- substitution of welding method with reduction of total service costs;
- saving of electric power (consumed current at welding currents 100/200/300/400 A — earlier and now);
- saving of welding wire due to decrease of spattering (measurement of wire mass for welding of the first workpiece — earlier and now);
- decrease of expenses for post treatment;
- increase of productivity (welding speed or coefficient of deposition);
- reliability of equipment, service and maintenance;
- improvement of quality of welded joint.

Type of equipment:

- MIG/MAG
- TIG



- MMA (electrode)
- Plasma cutting «Hypertherm»

Required welding samples with relative measurements were made at the territory of customers or in the Fronius Ukraina Technological Centre.

Over the period of validity of the program more than 50 domestic enterprises participated in it having put into their production new highly-efficient welding equipment and technologies (based on the analysis of efficiency of payback of their investments to the new equipment).

The generalized data on main criteria of selection of equipment «Fronius» are given in the Figure.

Six technological advantages why plasma «Hypertherm» overcomes oxygen cutting are as follows:

- excellent cut quality;
- high flexibility;
- high productivity;
- low cost of cut;
- simple in use;
- increased safety.

We hope that the presented information will be useful to wide range of specialists in welding at modernization or improvement of welding processes of production with the purpose of increase of compatibility of enterprises.

The Fronius Ukraina Ltd. thanks to all participants of given program and is looking forward to the further mutual cooperation.

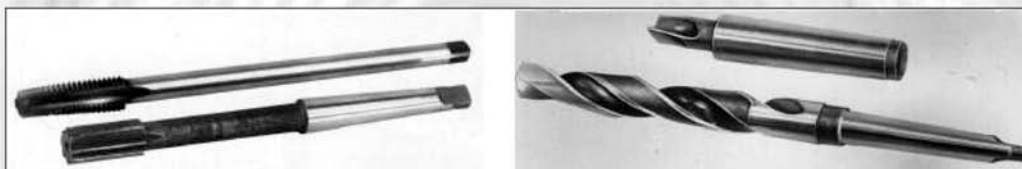
Dr. A.T. Zelnichenko, PWI

TECHNOLOGY AND EQUIPMENT FOR FLASH-BUTT WELDING OF CUTTING TOOLS

E.O. Paton Electric Welding Institute developed technology and equipment for flash-butt welding of tool steel to structural steel, in particular, high-speed steel of R6M5 grade to structural steels 45, 20Kh, 40Kh, etc., for making bimetal metal-cutting point tools (drills, taps, broaches, finger mills).

The developed technology guarantees producing sound flash-butt welded joints of cutting tools equivalent to the base metal.

The welding process is fully automated, has program control and a system for real time monitoring of welding parameters.



Samples of welded bimetal tools

The developed technology was the basis for designing specialized and upgrading all-purpose flash-butt welding machines K802, K793, K724A, K838, which allow welding tool billets of 7 to 8000 mm² cross-section. This equipment can be applied independently or as part of automated lines of tool manufacturing.

Purpose and application. Technologies and equipment for flash-butt welding of bimetal tools are designed for application in the tool and machine-tool construction industries.

Status and level of development. Developed technologies and equipment for their implementation correspond to the world standards and are protected by foreign patents and authors' certificates.

Forms of co-operation. To be determined during negotiations. Technology and equipment can be introduced, and all-purpose equipment can be upgraded on contract basis.

Contacts: Prof. Kuchuk-Yatsenko S.I.
E-mail: chvertko@paton.kiev.ua

INFORMATION FOR CONTRIBUTORS TO THE PATON WELDING JOURNAL

«The Paton Welding Journal» is an English translation of the monthly «Avtomaticheskaya Svarka» journal published in Russian since 1948.

THE PATON WELDING JOURNAL is a scientific journal publishing fundamental and applied papers and short notes in the area of:

- weldability of structural materials
- welding different types of steels and cast irons
- welding non-ferrous metals, including aluminium, titanium, etc.
- joining dissimilar and composite materials
- welding refractory metals and alloys
- welding cryogenic materials
- arc welding
- flash-butt welding
- electron beam and laser welding
- explosion welding and cutting
- friction welding
- electroslag welding
- soldering and brazing
- advanced structural materials
- surfacing and coating deposition
- cutting
- computer technologies in welding
- strength of welded joints and structures
- residual stresses and strains
- calculation and design of welded joints and structures
- automation of welding fabrication
- estimation of residual life of welded structures
- welding for fabrication of unique structures
- welding and repair in thermal and nuclear power engineering
- advances in underwater welding, cutting and repair

The journal accepts also advertisements and announcements of conferences and publications on related topics.

THE PATON WELDING JOURNAL is published monthly. Subscription requests should be sent to the Editorial Office. Manuscripts should be submitted in duplicate in English, and supplemented with a text file and figures on a diskette. An electronic copy may be submitted by e-mail.

The rules for submission of electronic copies are as follows:

- an electronic copy should be submitted on a diskette or by e-mail simultaneously with sending a hard copy of the manuscript;
- acceptable text formats: MSWord (rtf, doc);
- acceptable graphic formats for figures: EPS, TIFF, CDR. Figures created using software for mathematical and statistical calculations should be converted to one of these formats.

Manuscripts should be supplemented with:

- official letter signed by a chief manager of the institution where the work was performed. This rule does not apply to papers submitted by international groups of authors.

Title page:

- title of the paper and name(s) of the author(s);
- name of affiliated institution, full address, telephone and fax numbers, e-mail addresses (if available) for each author.

Abstract: up to 100 words, must be presented in English. Before the abstract text one should indicate in the same language: the paper title, surnames and initials of all authors.

Key words: their amount must not exceed eight word units. In the specific cases it is acceptable to use two- or three-word terms. These words must be placed under the abstract and written in the same language.

Text should be printed double-spaced on white paper (A4 format) with a 12-point font. Titles of the paper and sections should be typed with bold capitals.

Tables should be submitted on separate pages in the format of appropriate text processors, or in the text format (with columns separated by periods, commas, semicolons, or tabulation characters). Use of pseudo-graphic characters is not allowed.

List of references should be double-spaced, with references numbered in order of their appearance in the text.

Captions for figures and tables should be printed in the manuscript double-spaced after the list of references.

Pictures will be scanned for digital reproduction. Only high-quality pictures can be accepted. Inscriptions and symbols should be printed inside. Negatives, slides and transparencies are accepted.

Figures: each figure should be printed on a separate page of the manuscript and have a size not exceeding 160 × 200 mm. For text in figures, use 10-point fonts. All figures are to be numbered in order of their appearance in the text, with sections denoted as (a), (b), etc. Placing figure numbers and captions inside figures is not allowed. On the back side, write with a pencil the paper title, author(s) name(s) and figure number, and mark the top side with an arrow.

Photographs should be submitted as original prints.

Color printing is possible if its cost is covered by the authors. For information about the rules and costs, contact the Executive Director.

No author's fee is provided for.

Publication in TPWJ is free of charge.

Manuscripts should be sent to:

Dr. Alexander T. Zelnichenko
Executive Director of
«The Paton Welding Journal»,
11, Bozhenko Str.,
03680, Kiev, Ukraine
International Association «Welding»
Tel.: (38044) 287 67 57, 529 26 23
Fax: (38044) 528 04 86
E-mail: journal@paton.kiev.ua
www.nas.gov.ua/pwj

SUBSCRIPTION FOR «THE PATON WELDING JOURNAL»

If You are interested in making subscription directly via Editorial Board, fill, please, the coupon and send application by fax or e-mail.

The cost of annual subscription via Editorial Board is \$324.

Telephones and faxes of Editorial Board of «The Paton Welding Journal»:

Tel.: (38044) 287 6302, 271 2403, 529 2623

Fax: (38044) 528 3484, 528 0486, 529 2623.

«The Paton Welding Journal» can be also subscribed worldwide from catalogues of subscription agency EBSCO.

SUBSCRIPTION COUPON			
Address for journal delivery			
Term of subscription since	200	till	200
Name, initials	_____		
Affiliation	_____		
Position	_____		
Tel., Fax, E-mail	_____		



ADVERTISEMENT IN «THE PATON WELDING JOURNAL» (DISTRIBUTED ALL OVER THE WORLD)

«АВТОМАТИЧЕСКАЯ СВАРКА»

RUSSIAN VERSION OF «THE PATON WELDING JOURNAL» (DISTRIBUTED IN UKRAINE, RUSSIA AND OTHER CIS COUNTRIES)

External cover, fully-colored:

- First page of cover (190×190 mm) – \$700
- Second page of cover (200×290 mm) – \$550
- Third page of cover (200×290 mm) – \$500
- Fourth page of cover (200×290 mm) – \$600

Internal cover, fully-colored:

- First page of cover (200×290 mm) – \$400
- Second page of cover (200×290 mm) – \$400
- Third page of cover (200×290 mm) – \$400
- Fourth page of cover (200×290 mm) – \$400

Internal insert:

- Fully-colored (200×290 mm) – \$340
- Fully-colored (double page A3) (400×290 mm) – \$570
- Fully-colored (200×145 mm) – \$170

- Article in the form of advertising is 50 % of the cost of advertising area
- When the sum of advertising contracts exceeds \$1000, a flexible system of discounts is envisaged

Technical requirement for the advertising materials:

- Size of journal after cutting is 200×290 mm
- In advertising layouts, the texts, logotypes and other elements should be located 5 mm from the module edge to prevent the loss of a part of information

All files in format IBM PC:

- Corell Draw, version up to 10.0
- Adobe Photoshop, version up to 7.0
- Quark, version up to 5.0
- Representations in format TIFF, color model CMYK, resolution 300 dpi
- Files should be added with a printed copy (makeups in WORD for are not accepted)